AD-A212 940

ENDOCHRONICS

AFOSR-TR. 89-1212

ENDIC-007-AFOSR-1989

A THEORY OF DAMAGE IN BRITTLE AND CEMENTITIOUS MATERIALS

Final Report

K. C. Valanis
Endochronics, Inc.
8605 Lakecrest Court
Vancouver, WA 98665

Prepared for

July, 1989

89

REPORT DOCUMENTATION PAGE

Form Approved
OMB No. 0704-0188

1a. REPORT SECURITY CLASSIFICATION Unclassified	1b. RESTRICTIVE MARKINGS
2a. SECURITY CLASSIFICATION AUTHORITY	3. DISTRIBUTION/AVAILABILITY OF REPORT
2b. DECLASSIFICATION/DOWNGRADING SCHEDULE	Approved for public release; distribution is unlimited
4. PERFORMING ORGANIZATION REPORT NUMBER(S)	5. MONITORING ORGANIZATION REPORT NUMBER(S) AFOSR-TR. 89-1212

6a. NAME OF PERFORMING ORGANIZATION ENDOCHRONICS INC	6b. OFFICE SYMBOL (If applicable)	7a. NAME OF MONITORING ORGANIZATION AFOSR/NA
6c. ADDRESS (City, State, and ZIP Code) 8605 Lakecrest Court Vancouver, WA 98665		7b. ADDRESS (City, State, and ZIP Code) Bolling AFB Washington, DC 20332-6448

8a. NAME OF FUNDING/SPONSORING ORGANIZATION AFOSR	8b. OFFICE SYMBOL (If applicable) NA	9. PROCUREMENT INSTRUMENT IDENTIFICATION NUMBER F49620-88-C-0038

8c. ADDRESS (City, State, and ZIP Code) Bolling Air Force Base Washington, DC 20332-6448	10. SOURCE OF FUNDING NUMBERS			

PROGRAM ELEMENT NO.	PROJECT NO.	TASK NO.	WORK UNIT ACCESSION NO.
61102F	2302	C2	

11. TITLE (Include Security Classification)

A Theory of Damage in Brittle and Cementitious Materials.

12. PERSONAL AUTHOR(S)
K.C. Valanis

13a. TYPE OF REPORT Final	13b. TIME COVERED FROM 1/15/88 TO 5/15/89	14. DATE OF REPORT (Year, Month, Day) 7/17/89	15. PAGE COUNT 137

16. SUPPLEMENTARY NOTATION

Contributing Author: Dr. Khalid Khan, University of Portland

17. COSATI CODES			18. SUBJECT TERMS (Continue on reverse if necessary and identify by block number)
FIELD	GROUP	SUB-GROUP	Damage Theory, Brittle Fracture, Micromechanics, Softening, Concrete, Cast Iron.

19. ABSTRACT (Continue on reverse if necessary and identify by block number)

The purpose of the present study was to develop a local three-dimensional continuum theory of damage. Two materials were investigated: grey cast iron and plane concrete. The basic concepts (such as the form of the free energy in the presence of damage) were tested on cast iron, which is a brittle substantiallly elastic material. This approach was very fruitful. The free energy representation proved correct in view of the excellent agreement between the calculated and experimental results in elastic domains with a sharp geometric discontinuity (a crack). Since in endochronic plasticity the free energy is the basis for the derivation of the constitutive equation, this result was instrumental in the development of a damage sensitive constitutive theory for concrete where the interaction between plasticity and damage posed complex questions. Within the scope of the experiments performed the theory proved effective in depicting the observed response for both cast iron and concrete.

20. DISTRIBUTION/AVAILABILITY OF ABSTRACT ☑ UNCLASSIFIED/UNLIMITED ☐ SAME AS RPT. ☐ DTIC USERS	21. ABSTRACT SECURITY CLASSIFICATION Unclassified
22a. NAME OF RESPONSIBLE INDIVIDUAL Spencer T Wu	22b. TELEPHONE (Include Area Code) (202) 767-6962	22c. OFFICE SYMBOL AFOSR/NA

DD Form 1473, JUN 86 — Previous editions are obsolete.

SECURITY CLASSIFICATION OF THIS PAGE

ENDOCHRONICS

ENDIC-007-AFOSR-1989

A THEORY OF DAMAGE IN BRITTLE AND CEMENTITIOUS MATERIALS

Final Report

K. C. Valanis
Endochronics, Inc.
8605 Lakecrest Court
Vancouver, WA 98665

Prepared for

AFOSR
BOLLING AIRFORCE BASE
WASHINGTON, DC 20332-6448
CONTRACT NO. F49620-88-C-0038

July, 1989

ENDIC-007-AFOSR-1989

A THEORY OF DAMAGE
IN BRITTLE MATERIALS

Final Report - Part I

K. C. Valanis
Endochronics, Inc.
8605 Lakecrest Court
Vancouver, WA 98665

TABLE OF CONTENTS

QUALITY
INSPECTED
4

i

FOREWORD

The present study was undertaken with the purpose of developing a local continuum theory of fracture of sufficient breadth to encompass the constitutive response of degrading materials in the presence of three-dimensional stress and strain histories. Two specific materials were investigated: grey cast iron and plane concrete of low to intermediate strength.

Because *continuum damage theory* is a new and emerging field and because a great deal of what can be done with such an approach is still unknown, it was thought wise to test the fundamental concepts (specifically the form of the free energy in the presence of damage) on a brittle material, in our case cast iron, whose constitutive equation may be considered, quite adequately, elastic. The lessons learned from this first study would then be useful in the more complicated task of developing such a theory for a plastic material such as concrete where the interaction between plasticity and damage was expected to be much more complex.

This approach proved very fruitful. The work on cast iron showed that the free energy representation was indeed proper, in view of the excellent agreement between the calculated and experimental results in elastic domains with a sharp geometric discontinuity (a crack). *Since in the endochronic theory of plasticity* the free energy is the basis for the derivation of the constitutive equation, this result was instrumental in the development of the damage sensitive constitutive theory for concrete.

Within the limited scope of the experiments performed the theory proved effective in depicting the observed response for both cast iron and concrete. Of course this is only a beginning and many questions remain. These are discussed in somewhat greater detail in the sections on accomplished objectives and recommended further work.

ii

SUMMARY OF ACCOMPLISHED OBJECTIVES

• A continuum theory of damage first developed by the author in 1987 -- in terms of a damage coordinate and an integrity tensor -- has been refined and extended to apply to the constitutive response of brittle materials in the presence of evolving damage consisting of <u>sharp</u> cracks. The theory has been tested by experiments on grey cast iron thin plates with a central crack normal and at various angles to the direction of pull. Calculated and measured fracture stresses were found to <u>be in close agreement generally</u>, and in reasonably good agreement for angles of inclination less than 30 degrees to the direction of pull. A finite element program has been developed for the purpose of performing the calculations.

• Of great significance is the fact that a conceptual boundary has been established between the present damage theory and Linear Elastic Fracture Mechanics, in the sense that both theories give rise to the same result under Mode I conditions, when the damage coordinate is the crack length.

• A central key to the success of the theory is the evolution equation derived from irreversible thermodynamics. Despite its continuum nature it predicts damage that is very localized and is confined to the immediate neighborhood of the crack tip in agreement with observation.

• A micromechanical connection has been established between the integrity tensor and the crack length under Mode I conditions. The elements exist for the extension of this relation to more general cases.

• A constitutive theory of damage in plane concrete was developed leading to two different constitutive formulations -- Theories I and II -- depending on the underlying specific physical and geometric hypotheses. Theory II was used to depict the behavior of concrete in the course of axial compression. Calculated results in terms of the axial stress-strain relation and lateral expansion were compared with their experimental counterparts. Close agreement was demonstrated between theory and experiment.

• The study yielded insights into the physics of degradation with strong evidence that:

   (a)   Substantial damage does not occur until the material has reached
         its fully plastic state.

(b)   The rate of degradation is a strong increasing function of the initial
        elastic modulus.   This phenomenon becomes particularly pronounced
        in the softening region of the axial stress-strain curve.

Finding (b) has ramifications in regard to the design of concrete structures intended to survive damage.   The inference is that high strength concrete will degrade much faster in the softening region following the onset of maximum stress.   This point is worth pondering.

•   An earlier damage evolution equation (Valanis, 1987) proved very effective in describing the experimental findings in plane concrete.

INDICATED FUTURE RESEARCH

•   <u>Directionality of Damage.</u>

We highly recommend the continuation of an analytical-cum-experimental research program on the constitutive theory of damage of plane concrete, under spatially <u>heterogeneous</u> stress (and strain_ conditions.   It is important that we test further the predictive capability of the evolution equation in regard to the directionality of damage in spatially heterogeneous strain fields.

•   <u>The Constitutive Representation of Damage in Situ.</u>

The question of representation of observed damage by a constitutive damage measure is still an open question.   In our research we have been able to establish such a relation in the case of a single crack.   However how a crack configuration, even in two dimensions, is to represented by a damage measure, be it an integrity or a damage tensor, is still an open question.   Much research is needed in this area.

•   <u>Absorption of Transient Energy in Concrete.</u>

The finding that the rate of degradation is a strong increasing function of the initial modulus -- and by implication, the strength -- raises interesting questions regarding the absorption of energy in concrete due to impact.   If impact energy can move away from degrading regions prior to their disintegration then the absorption capability of the medium will be enhanced.   The interplay between the speed of

propagation and the rate of degradation merits investigation. Experimental (weight drop) and analytical studies on beams would be a propos projects for investigating this phenomenon.

- ### The Ill-posed Boundary and Initial Value Problem.

Spatial ellipticity and temporal hyperbolicity of the equations of the boundary and initial value problem respectively is a fundamental issue in constitutive theory. It is well known that continuum (local) damage theories without scale sensitive material functions (or constants) give rise to ill-posed boundary and initial value problems. This question can be addressed by the development of a non-local damage theory, which under homogeneous conditions will give rise to degenerate forms with size sensitive material parameters and functions. Such a theory would lend an underlying unity to the present research efforts in damage theories.

- ### Damage Theory of Composite Materials.

This is an indicated extension of the present damage theory of plane concrete to deal with reinforced concrete using the theory of mixtures. Certain inroads have been made in this area.[*]

GENERAL DISCUSSION ON THE QUESTION OF DAMAGE REPRESENTATION.

In recent years a great deal of effort has been devoted to the question of continuum representation of discreet damage consisting of configurations of cracks and voids. While this effort will contribute to the understanding of damage there are questions regarding the role of such a representation in a predictive theory. The following discussion is an expression of our views on this matter.

Let us assume (as a matter of hypothesis) that a relation between a damage pattern and a damage tensor has been found, without using the equation of evolution of damage. In this event the following situation would exist in our case.

---

[*] Valanis, K. C., "Thermomechanical Behavior of Anisotropic Inelastic Composites. A Micromechanical Theory," *J. Eng. Mat. and Techn.*, To be published.
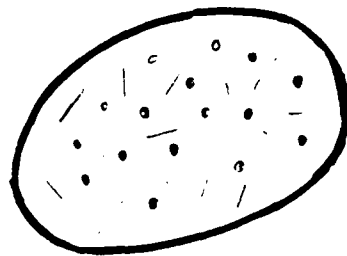
$\rightarrow \quad \phi \qquad\qquad\qquad (i)$

Visual Image of Damage Pattern

where ϕ is the integrity tensor -- the damage measure used in this work. Thus given a visual image of damage in a region,** the damage tensor in that region would be calculated from an analytical formula.

Consider now the case where the surface of the domain has been subjected to a displacement and/or traction history. Then at different points along the history the domain can be dissected and examined visually and ϕ can be determined as a function of the path.

If the resulting strain field is heterogeneous then a sufficient number of sub-domains must be dissected and visually examined to determine the damage field in the domain of interest.

To use this information in a predictive manner, given a strain history of the entire domain -- we omit the difficulties of determining the strain field in the interior of a domain -- one needs a constitutive equation that describes the material response in the presence of ϕ. We write such an equation symbolically as follows:

** A "region" by definition will denote a small sub-domain of a large domain.

$$\sigma = F[\epsilon; \phi] \qquad (ii)$$

where $F[.]$ is a function of the history of strain and ϕ. Since both ϕ and ϵ are known at every step then σ can be calculated as a function of the strain path.

If one does not wish to dissect and examine visually a large number of subdomains of a material domain and perform the necessary experiments to determine the strain field one must solve the initial or boundary value problem, as the case may be. For this an evolution equation for damage is necessary. This could be of an incremental or of functional type, but symbolically it may be written in the form:

$$\phi = G[\epsilon; \phi] \qquad (iii)$$

where G is a function of the history of ϵ and ϕ.

It is apparent that in the absence of copious experimentation and dissection, the Equivalence Relation (i) is of little value as a predictive tool though it may serve as a proof test for the evolution equation (iii) by giving values of ϕ (along the strain path) which can be compared with those calculated from relation (i). However we point out that the constitutive equation may also be used as a (more indirect) proof test by comparing the calculated and measured stress response.

Still one can argue that the relation (i) may be useful in determining an incremental form of the evolution equation. For instance one may write:

$$d\phi = G(\phi, \epsilon) \qquad (iv)$$

Knowing $d\phi$ along a strain path as well as $d\epsilon$, finding G would appear to be a plausible task. We explored such an approach in the case of cast iron but the physics of the problem was not co-operative. Very little observable damage was present until failure. There was no transient crack extension that could be measurable and thus be of value in the above approach. Of course our tests were monotonic. Cyclic tests would be more conducive to crack growth but much less so in brittle materials.

In ductile materials the situation is different. Cracks do propagate under cyclic strain histories. Authors have attempted to determine a relation between a damage measure and crack length, in Mode I conditions, in terms of the fracture toughness

parameter K_{Ic}. Yet as is well known and implicit in the Paris equation for cyclic crack growth in metals, the rate of crack growth is independent of K_{Ic} except for values of K_I nearly equal to K_{Ic}. Thus the evolution of damage in metals, in the course of a cyclic history, bears no relation to the damage measure determined from monotonic loading conditions involving K_{Ic}.

Another instance where relation (i) would appear to be of value is the case of concrete. Here damage does evolve in a manner that is visible -- though this does not appear to be the case under conditions of purely hydrostatic pressure where reduction in strength has been found in the absence of <u>visible</u> damage. A study by Valanis and Read (1989) and Valanis (reported in a proposal to AFOSR) of the experiments by Gopalaratnam and Shah (referenced in this report) and our own experiments reported here shows that the agent of damage is not the total strain but the plastic strain. This must be calculated (in three dimensions) in the presence of degrading elastic moduli and stress softening. Thus the calculation calls for knowledge of Eqs. (ii) and (iii). Thus the problem is coupled in the sense that one cannot use the equivalence relation (i) to determine the evolution equation in concrete without a priori knowledge of this equation.

It seems that if one accepts the position that the state of damage is one of geometry rather than physics, and wishes to determine a continuum representation of damage, then the approach indicated is to start with a well-defined damage pattern in an elastic domain and do tests to determine the "continuum" average elastic response of the region in terms of the integrity tensor ϕ, using Eq. (2.1c) of Report I. Or one may use a finite element analysis. This is the approach proposed to AFOSR. One may thus establish a relation between ϕ and the parameters of a specific pattern.

This would be a means of resolving the important question of <u>initial</u> damage. If a domain is initially damaged, the value of ϕ_o must be known before the initial or boundary value problem can be solved.

The Question of Element Size.

This question has been discussed in the literature a great deal in the last decade. What is often left unsaid, or not realized, is that <u>there are two questions</u> of

size. One involves the effect of the size of the domain on the representation of damage. Obviously such an effect exists and the only question is how to calculate it. The effect will depend on the damage pattern. Thus if damage is uniformly distributed, the effect will be small. On the other hand if it is concentrated, the effect will be large. The damage pattern is a material property and will vary from one material to the other given the same strain history. Thus the size effect is a geometric as well as a constitutive property.

The other size effect concerns the computation of the material response by means of a finite element method in the presence of damage-induced softening. The numerical solution of the associated initial or boundary value problem is sensitive to the size of the mesh. Local continuum damage theories are susceptible to this effect and give rise to ill-posed boundary or initial value problems.

Thus accounting for the effect of the size of the domain in the continuum representation of damage does not eliminate the effect of mesh size in a finite element analysis if the damage theory is of "local" character. In other words local damage theories apply only to situations where the overall stress and strain fields are spatially uniform. However, local theories are very useful in understanding material behavior. They are in fact special (degenerate) cases of the constitutive response, when the stress and stain fields are spatial uniform.

In conclusion it is our position that what is called for is a non-local evolution equation. Such an equation would have the effect of eliminating difficulties associated with the size of the mesh in finite element calculations and would resolve the question of the ill-posedness of the initial and boundary value problems. It is our suspicion that such an equation will also resolve, in passing, the question of the size of the domain on the continuum representation of damage.

We are working on such an approach right now and plan to make this the focus of our future work on damage theory. Our initial results are very encouraging.

A THEORY OF DAMAGE IN BRITTLE MATERIALS

ABSTRACT

The present paper addresses the geometric representation of damage in brittle solids, its equation of evolution and its incorporation in the constitutive equation. The concept of a damage coordinate is introduced and a thermodynamic derivation of the evolution equation follows. A <u>continuum</u> damage theory ensues. The theory is applied to the case of a thin plate with a <u>central crack</u>. Two cases are treated.

In Case (a) the tensile load is in a direction normal to the plane of the crack. The fracture stress is calculated numerically using a finite element code for various crack lengths and a comparison is made with its observed values. Excellent agreement between the two is obtained with the aid of only one damage parameter, the damage propensity constant. A congruence between the theory and linear fracture mechanics in Mode I is then shown when the damage coordinate is the crack length.

In Case (b) the crack length is constant but the angle of inclination of the crack to the direction of pull is varied. The fracture stress is calculated as above for various angles and comparison is made with observed values. While overall agreement is reasonable, excellent agreement is found when the angle is greater than 45°.

1. INTRODUCTION

Damage plays an essential role in the constitutive behavior of materials Its nature, in terms of its measurement and mathematical representation is complex. It can vary from a well defined crack to randomly distributed damage that can be thought of as a "damage field". It is important to understand under what initial damage conditions, stress history and material properties, one type will prevail over the other, or when the two types will co-exist.

Constitutive theories in the context of <u>continuum damage</u> have been proposed by Dragon and Mroz [1], Lemaitre and Mazars [2], Chaboche [3], Krajcinovic and Fouseka [4] and Fouseka and Krajcinovic [5] and Krajcinovic [6]. In this regard see also a recent paper by Chaboche [7].

Since, however, failure often occurs by the extension of one dominant crack, at times in the presence of distributed damage, a comprehensive theory must be able to deal with both types, and their mixture, simultaneously. Specifically a continuum theory should be able to deal with damage due to well-defined sharp cracks. The theory in this study is being pursued with this goal in mind. The state of directional damage (in the form of oriented cracks) is represented by an integrity tensor ϕ, and *randomly distributed scalar damage* by a scalar function Ω, both of which may co-exist.

While both types of damage were dealt with in a previous work Valanis [8], in this study, which is reported in Part I of this Report, we concentrate on damage in · brittle solids, which is <u>directed</u>, and begin with the case of a well-defined crack. The reason for this is born out of the foregoing discussion. In addition, however, there is the question of Linear Fracture Mechanics (LEFM) which has been successful in dealing with fracture due to sharp cracks in brittle materials and in Mode I conditions. In developing the theory we feel that we must establish a conceptual boundary with LEFM.

To this end we use the continuum damage theory developed herein, to solve the problem of a plate under tension with a central crack. Two case are considered.

Case (a).

In this case the crack is normal to the direction of pull. The fracture stress is determined as a function of the crack length. Its values are then compared with

those obtained by experiment on grey cast iron, and from the analytical linear elastic fracture mechanics solution. The agreement between the damage theory and experiment is excellent. The fracture mechanics solution disagrees with the experiment for values of the crack length that are small but is otherwise in close agreement also.

Case (b).

In this case the crack is of fixed length but its angle of inclination to the direction of pull is varied. The agreement between the damage theory and experiment is good for angles of inclination that exceed 45 degrees. A numerical solution could not be obtained for angles smaller than 30 degrees because of slow convergence of the iterative algorithm. Since the solution for an angle of zero degrees is known, this being the solution for the plate without a crack, an approximate analytic solution for angles less than 30 degrees has been obtained by interpolation. A deviation between theory and experiment, however, is already apparent for values of inclination between 45 and 30 degrees. While the reason for this is discussed at greater length in Section 7 we feel that the primary cause is the finiteness of the crack width and the non-zero value of the radius of the crack tip. This could not be avoided as the crack was made with best available technology. See Appendix B.

In addition to these overall results, the theoretical study has brought forth two central findings which are the following:

(i) The evolution equation -- with a firm basis in thermodynamics in the sense that it abides by the law that the rate of change of a thermodynamic variable is proportional to the dual thermodynamic force -- gives, in the course of increasing tension, a damage field which is very localized and is confined essentially to the vicinity of the crack root, in accord with observations on brittle fracture and our own experiments on grey cast iron. Visual examination of the material with a microscope -- magnification 400 -- in the neighborhood of the crack root, after fracture, revealed no visible changes in material structure, except very close -- within a millimeter or so -- of the crack root.

(ii)   The Proposed damage theory and linear fracture mechanics in Mode I are brought into correspondence in the context of the thermodynamic theory, when the damage coordinate is the crack length.

We have therefore a conceptual as well as a quantitative confluence among (a) the continuum theory, (b) Linear Elastic Fracture Mechanics and (c) experimental observation in Mode I conditions. We also have good agreement between the damage theory and experiment in the case of inclined cracks for angles of inclination greater than 45 degrees. The conclusion on smaller angles must await further developments.

2. DAMAGE THEORY.

We begin by setting out the fundamentals of a theory for incorporating directly the effects of damage in the constitutive equation of a linear elastic material. A work which addresses the behavior of elastic-fracturing and plastic-fracturing solids has appeared in two unpublished reports by Valanis [8] and Valanis and Read [9]. Here we shall be concerned only with directed damage. The question of scalar damage in the presence of directed damage was dealt with previously by Valanis [8].

The fundamental premise of the theory is that directed damage may be represented by a tensor valued function ϕ, "the integrity tensor", which appears explicitly in the equation for the free energy and the constitutive equation. Thermodynamically, ϕ is an internal variable. In the case of elastic-fracturing solids the free energy density is given by Eq. (2.1a) and the constitutive relation by Eq. (2.1c). Specifically [8],

$$\psi = (\lambda/2)\phi_{ij}\phi_{k\ell}\epsilon_{ij}\epsilon_{k\ell} + \mu\phi_{ik}\phi_{j\ell}\epsilon_{ij}\epsilon_{k\ell} \tag{2.1a}$$

where λ and μ are the Lamé constants. Thus, since

$$\sigma = \frac{\partial\psi}{\partial\epsilon} \tag{2.1b}$$

it follows that:

$$\sigma_{ij} = \lambda\phi_{ij}\phi_{k\ell}\epsilon_{k\ell} + 2\mu\phi_{ik}\phi_{j\ell}\epsilon_{k\ell} \tag{2.1c}$$

Equation (2.1a) is a statement to the fact that

$$\psi = \frac{1}{2} C_{ijk\ell} \epsilon_{ij} \epsilon_{k\ell} \tag{2.2}$$

where C, the stiffness tensor, is homogeneous and quadratic in ϕ.

There are two fundamental questions regarding the tensor ϕ:

(i)   What is its geometric nature? More specifically, how is it related to the actual material damage at some <u>microscale</u> -- i.e., a scale smaller than the one that underlies the macroscopic constitutive behavior of the material?

5

(ii)   How does $\underset{\sim}{\phi}$ evolve with the history of deformation?

In regard to question (i), it was previously shown Valanis [8], that if in a material element a principal value of $\underset{\sim}{\phi}$, say ϕ_r, is zero, and $\vec{N}_r$ is the eigenvector of ϕ_r, then the traction on a surface normal to $\vec{N}_r$ is zero. That is, the element cannot support shear or direct stress on that surface. Thus, ϕ_r represents <u>damage</u> on a plane normal to $\vec{N}_r$, and as such it is a measure of the effective area in the presence of microcrack(s) in that plane. Thus when $\phi_r = 0$, an <u>effective</u> plane crack has developed across the entire element on a plane normal to $\underset{\sim}{N}_r$. Conversely if $\phi_r = 1$ no damage has occurred on that plane.

With regard to question (ii), i.e., the evolution of $\underset{\sim}{\phi}$, the following equation was proposed as a basis for the description of damage due to mechanisms of brittle (or semi-brittle) fracture:

$$d\phi^\alpha = - \left(Q_n^\alpha\right)^m d\xi^\alpha \qquad (2.3)$$

The notation in Eq. (2.3) is the following: $d\phi^\alpha$ is the change in principal component ϕ^α of $\underset{\sim}{\phi}$ due to a strain increment $d\underset{\sim}{\epsilon}$ and n_i^α are the eigenvectors of $d\underset{\sim}{\epsilon}$. Also, ξ^α is a damage coordinate and Q_n^α a "damage force" in the direction $\vec{n}^\alpha$, i.e.,

$$Q_n^\alpha = n_i^\alpha n_j^\alpha Q_{ij} \qquad \text{(r not summed)} \qquad (2.4)$$

The power index m in Eq. (2.3) is a material constant.

The damage coordinate ξ^α is given by Eq (2.5) i.e.,

$$d\xi^\alpha = \begin{cases} kd\epsilon^\alpha \ ; \ d\epsilon_n^\alpha > 0, \ \epsilon_n^\alpha \geq 0, \ Q_n^\alpha > 0 \\ \\ 0 \ , \quad \text{otherwise} \end{cases} \qquad (2.5)$$

where $\epsilon_n^\alpha = \epsilon_{ij} n_i^\alpha n_j^\alpha$ (α, not summed) and k is a positive scalar. A complete discussion of these equations when $\underset{\sim}{Q} = \underset{\sim}{\phi}$ is given by Valanis [8].

Further Discussion of Eq. (2.2).

The appropriate "driving force" is of central importance to the evolution equation. In Ref. 8, $\underset{\sim}{Q}$ was set equal to $\underset{\sim}{\phi}$ because the resulting relation was of a

6

type that governs annihilation of species and, therefore, degradation. In brittle materials such as grey case iron, however, and in the case where damage is due to a well-defined crack, we found that this equation overestimates the damage in zones of low strain intensity [8]. This result is contrary to the behavior of brittle materials and our own observations on grey cast iron.

The Physical Fracturing Process.

The process of fracture of brittle and semi-brittle materials, such as grey cast iron which exhibits a small amount of plasticity but fractures at very low strain (~ 0.5%), shows two essential characteristics which are always consistently and clearly observable:

(i)   The damage is at first very minimal, but then increases suddenly becoming catastrophic.

(ii)   In the case of a single crack, material regions away from the crack remain essentially damage-free during the deformation process while damage, which leads to catastrophic failure, remains confined to the tip of the crack.

The above characteristics must be depicted quantitatively by the damage evolution equation whose suitability or otherwise, will be determined, in part, by its capability to describe the essential physics of the damage process.

A Thermodynamic Approach.

To arrive at a suitable evolution equation we appeal directly to thermodynamics. We recall that since ϕ is an internal thermodynamic variable, the thermodynamic force Q that drives the damage process is given by the relation

$$Q = -\frac{\partial \psi}{\partial \phi} \tag{2.6}$$

Also the direction of the damage increment - $d\phi$ is dictated by the eigendirections $\vec{n}^\alpha$ of the increment of strain $d\xi$ In view of the above observations we make the following two fundamental stipulations:

(i) $d\phi$ and $d\xi$ are coaxial.

7

(ii)   The operative force driving the damage process in the direction $\vec{n}^\alpha$ is Q_n^α, which is Q projected in direction $\vec{n}^a$ in accordance with Eq. (2.3). Using then the basic linear thermodynamic law "that the rate of change of a thermodynamic variable is proportional to the conjugate thermodynamic force," we obtain the relation:

$$\frac{d\phi^\alpha}{d\xi^\alpha} = bQ_n^\alpha \tag{2.7}$$

where b is a material scalar and

$$d\xi^\alpha = \begin{cases} kd\epsilon^\alpha \\ 0 \end{cases} \quad , \quad d\xi^\alpha \geq 0 \quad . \tag{2.8}$$

k having the significance of a damage propensity parameter. As before, $d\epsilon^\alpha$ are the eigenvalues of $d\underset{\sim}{\epsilon}$.

Previously, when Eq. (2.2) was used, Valanis [8], the following were the conditions that $d\xi^\alpha$ be non zero:

$$d\epsilon^\alpha > 0 \ , \ \epsilon_n^\alpha = \epsilon_{ij} n_i^\alpha n_j^\alpha \geq 0 \tag{2.9}$$

Otherwise, $d\xi^\alpha = 0$. However in the present case the explicit appearance of the thermodynamic force in the evolution equation brings the Clausius-Duhem dissipation inequality, i.e.,

$$-\frac{\partial\psi}{\partial\underset{\sim}{\phi}} \cdot d\underset{\sim}{\phi} > 0 \quad , \quad ||d\underset{\sim}{\phi}|| \neq 0 \tag{2.10}$$

into play directly. Thus in view of Eqs. (2.6) and (2.7) and the fact that

$$d\phi_{ij} = \sum_\alpha d\phi^\alpha n_i^\alpha n_j^\alpha \tag{2.11}$$

$\vec{n}^\alpha$ being the eigenvectors of $d\underset{\sim}{\phi}$, it follows that

$$-\frac{\partial\psi}{\partial\underset{\sim}{\phi}} \cdot d\underset{\sim}{\phi} = - \sum_\alpha d\phi^\alpha \frac{\partial\psi}{\partial\psi_{ij}} n_i^\alpha n_j^\alpha > 0 \tag{2.12}$$

8

Since ineq. (2.12) must be true for each α individually, i.e., for each independent fracture mechanism, then the following inequality must be satisfied for all α:

$$- d\phi^\alpha \frac{\partial \psi}{\partial \phi_{ij}} n_i^\alpha n_j^\alpha > 0 \qquad (2.13)$$

Furthermore, since $d\phi^\alpha$ is always negative whenever it is nonzero, then

$$\frac{\partial \psi}{\partial \phi_{ij}} n_i^\alpha n_j^\alpha > 0 \qquad (2.14)$$

for all α, whenever $|d\phi^\alpha| \neq 0$.

We have thus obtained the full set of conditions that govern the evolution of the damage coordinate $d\xi^\alpha$. Thus:

$$d\xi^\alpha = k d\epsilon^\alpha \qquad (2.15)$$

whenever:

$$d\epsilon^\alpha > 0 \;, \; \epsilon_n^\alpha \geq 0 \;, \; \frac{\partial \psi}{\partial \phi_{ij}} n_i^\alpha n_j^\alpha > 0 \qquad (2.16)$$

but $d\xi^\alpha = 0$ otherwise.

We recall that the search for a new evolution equation was motivated by the fact Eq. (2.2) overestimated the rate of growth of damage in regions of low strain intensity. To see that Eq. (2.7) is superior to Eq. (2.3) in this respect we write it in its explicit form given below:

$$d\phi^\alpha = - bd\xi^\alpha \left\{ \lambda \epsilon_{ij} \left(\phi_{k\ell} \epsilon_{k\ell} \right) + 2\mu \phi_{k\ell} \epsilon_{ik} \epsilon_j \right\} n_i^\alpha n_j^\alpha \qquad (2.17)$$

Note that the righthand side of Eq. (2.17) is now of order $\|\underset{\sim}{\epsilon}\|^2$ -- whereas previously it was of order $\|\underset{\sim}{\epsilon}\|^0$. Other things being equal the rate of diminution of ϕ^α will, therefore, be expected to be substantially higher in regions of high strain intensity such as the root of an existing crack.

Material Parameters and Their Experimental Determination.

It may be seen from Eq. (2.7) and (2.8) that b and k merge into a constant bk so that without loss of generality we take b to be equal to unity. There are,

9

therefore, three constants to be determined: k, the fracture susceptibility, and the two elastic constants λ and μ. In a uniaxial test Young's modulus E was determined, while ν, the Poisson ratio, was taken equal to 0.3. The elastic constants λ and μ were then calculated and were found to be 15×10^3 and 10×10^3 ksi, respectively.

The constant k is determined from a simple tension test on an uncracked specimen. Under these conditions

$$\sigma_1 = E\epsilon_1\phi_1^2 \tag{2.18}$$

and using Eqs. (2.17) and (2.18)

$$d\phi_1 = kE\epsilon_1^2\phi d\epsilon_1 \tag{2.19}$$

Equation (2.19) ma be integrated to give:

$$\phi_1 = e^{-(kE/3)\epsilon_1^3} \tag{2.20}$$

Thus, in view of Eqs. (2.18) and (2.20)

$$\sigma_1 = E\epsilon_1 \exp\left[(2k/3)E\epsilon_1^3\right] \tag{2.21}$$

Fracture will take place when σ_1 reaches a maximum value. The condition is

$$\frac{d\sigma_1}{d\epsilon_1} = 0 \tag{2.22}$$

which, in conjunction with Eq. (2.21) gives the relation:

$$\epsilon_{1\ max} = (1/2kE)^{1/3} \tag{2.23}$$

$$\sigma_{1\ max} = E(1/2keE)^{1/3} \tag{2.24}$$

where e in Eq. (2.24) is the base of the natural logarithm.

Two different batches of specimens were used in the experiments, one from ingot (a) for Case (a) and one from ingot (b) for Case (b).

Case (a).

In a series of experiments grey cast iron specimens from ingot (a) were tested in axial tension and the fracture stress $\sigma_{1\ max}$ was found to lie within the limits

$$32 \times 10^3 < \sigma_{1\ max} < 38 \times 10^3 \text{ psi}$$

while an upper bound for E was found to be 26.6×10^6 psi. Thus, choosing k to be equal to 2000 in units of $(ksi)^{-1}$, $\sigma_{1\ max}$ was found to be 40.2 ksi which is close to the upper bound of the experimentally determined value.

Case (b).

From tensile experiments on specimens from ingot (b), E was found to be 17×10^6 psi while values of the fracture stress clustered close to a value of 30×10^3 psi. Thus k was found to be equal to 2×10^3 $(ksi)^{-1}$ in this case as well. Values of λ and μ were then calculated for both cases by setting $\nu = 1/3$.

COMPUTATIONAL STUDY

As discussed in the Introduction, the computational study consisted of:

(a)   Developing a Finite Element Analysis Program, in the presence of the damage evolution equation, for the computation of the deformation, stress and damage fields in a flat plate in the presence of a central crack.

(b)   Computing these quantities for central cracks of various lengths in Case (a) and for a crack of constant length and varying angle of inclination to the direction of pull in Case. (b).

(c)   Developing a numerical Algorithm for the above purpose.

Case (a).

The numerical experiment performed was one of the longitudinal displacement control (in the presence of free transverse displacement) on the outer boundary. All other boundaries were stress-free. An incremental displacement of 2.5×10^{-3} units

was imposed at each stage. The computations were carried out for a square grid of fixed size. For reasons relating to the geometry of the specimen, 3/64" was designated as a unit of length. Half-domains were used in the computations utilizing the longitudinal axis of symmetry.

To test the effect of specimen length on the fracture stress two such domains were used. The first had a width of eight units and a height of eleven units of length. The second had the same width as the first, but a height of twenty-one units. Stress, strain and damage fields were obtained in both cases. For the domains tested the length effect was negligible. Fracture was considered to have occurred when the displacement field was such that two halves of the plate (symmetrically located relative to the crack line) began to move relative to each other as rigid bodies.

Case (b).

In this case the boundary conditions were the same as in Case (a). When the crack was inclined, however, there was no reflective axis of symmetry. For this reason the entire plate (width 16 units, length 32 units) was used in the calculations. In Figure 9 we show the geometry of the right half of the plate and the "idealized" set of cracks used in the computation -- in the sense that some of the cracks were slightly longer than the ones used in the experiments. The resulting advantage was that in the idealized configuration all elements affected by the presence of a crack has the same initial value of $\pmb{\ell}_0$, i.e.,

$$\pmb{\ell}_0 = \begin{bmatrix} c^2 & cs & 0 \\ cs & s^2 & 0 \\ 0 & 0 & 1 \end{bmatrix} \tag{2.24a}$$

where $c = \cos\theta$, $s = \sin\theta$ and $\theta = \pi/2 - \alpha$, where α is the inclination of the crack to the direction of pull. In this case failure was considered to have occurred when the axial stress in the element adjacent to the crack reached a maximum value, since following this event the displacement field became prohibitively large and erratic and while convergence of the iterative process failed.

12

Brief Description of the Numerical Algorithm.

The boundary value problem for a brittle material in the presence of initiation and evolution of damage is non-linear, and there are strong coupling effects between the elastic stiffness and the state of damage. The coupling is manifested through the constitutive matrix $[k_\phi]$ which is directly dependent on the integrity tensor ϕ. Specifically the constitutive response in plane stress is given by Eq. (2.25) where

$$
\begin{Bmatrix} \sigma_{11} \\ \sigma_{22} \\ \sigma_{12} \end{Bmatrix} = \begin{bmatrix} k_\phi \end{bmatrix} \begin{Bmatrix} \epsilon_{11} \\ \epsilon_{22} \\ \gamma_{12} \end{Bmatrix}
\tag{2.25}
$$

where γ_{12} is the engineering shear strain and

$$
[k_\phi] = \begin{bmatrix} \phi_{11}^2(\lambda + 2\mu) & \left(\lambda\phi_{11}\phi_{22} + 2\mu\phi_{12}^2\right) & \phi_{11}\phi_{22}(\lambda + 2\mu) \\ \left(\lambda\phi_1\phi_2 + 2\mu\phi_{21}^2\right) & \phi_{22}^2(\lambda + 2\mu) & \phi_{22}\phi_{12}(\lambda + 2\mu) \\ \phi_{11}\phi_{12}(\lambda + 2\mu) & \phi_{12}\phi_{22}(\lambda + 2\mu) & (\lambda + \mu)\sigma_{12}^2 + \mu\phi_1\phi_1 \end{bmatrix}
\tag{2.26}
$$

On the other hand the evolution equation for the integrity tensor ϕ involves both the state of damage (given by ϕ) the state of strain ϵ as well as the increment of strain $d\epsilon$ which determines the damage coordinate. increments $d\xi^\alpha$ ($\alpha = 1,2,3$). Specifically:

$$
d\phi^\alpha = Q_n^\alpha d\xi^\alpha \quad (\alpha \text{ not summed})
\tag{2.27}
$$

$$
Q_n^\alpha = Q_{ij} n_i^\alpha n_j^\alpha
\tag{2.28}
$$

$$
Q_{ij} = \lambda\epsilon_{ij}(\phi \cdot \epsilon) + 2\mu\phi_{k\ell}\epsilon_{ik}\epsilon_{j\ell}
\tag{2.29}
$$

The algorithm adopted here was one of incremental application of boundary displacements in conjunction with the Newton-Raphson method of iteration. In the equilibrium configuration each node is in equilibrium. Loads applied externally plus loads applied by the elements must sum to zero. If this sum if $[\Delta R]$ instead of the null vector, the load imbalance $[\Delta R]$ will produce a displacement difference vector $[\Delta u]$ which is computed by solving the equation

13

$$[K_0][\Delta u] = [\Delta R] \tag{2.30}$$

where $[K_0]$ is the stiffness matrix of the structure in <u>absence</u> of damage. In iterative notation:

$$[u]_n^{k+1} - [u]_n^k = [K_0^k]^{-1}[\Delta R]_n^k \tag{2.31}$$

where k denotes the iteration number, n the incremental loading step and

$$[\Delta R]_n^k = [K_\phi]_n[\Delta u]_n^k \tag{2.32}$$

i.e., $[\Delta R]_n^k$ is calculated using the current secant stiffness matrix $[K_\phi]$ and the current iterated displacement u_n^k.

The imbalance "node force" ΔR and the displacement difference between two iterations will decrease during the iteration process. Computation is stopped when a tolerance is reached, i.e., when

$$|u_n^{k+1} - u_n^k| < e \, |u_n^k| \tag{2.33}$$

where e is a small number. In this study, e was set equal to 10^{-6}.

As discussed previously, in Case (a) the plate was considered as having fractured when the difference in the displacements of any two nodes in either the top or bottom part of the plate relative to crack line, was less than 10^{-6}, while in Case (b) fracture was considered to have occurred when the stress in the element adjacent to the crack reached a maximum value. The numerical computations were conducted on a VAX 750.

Discussion of Results.

Figure 1 shows the calculated curve of fracture stress versus crack length, based on the damage theory. Also shown, are the experimentally determined values of fracture stress. The comparison shows excellent agreement between calculated and experimental data. Figure 1a shows the calculated fracture curve when linear elastic fracture mechanics is used. It is apparent that LEFM gives good agreement with the data for larger values of crack length, as expected.
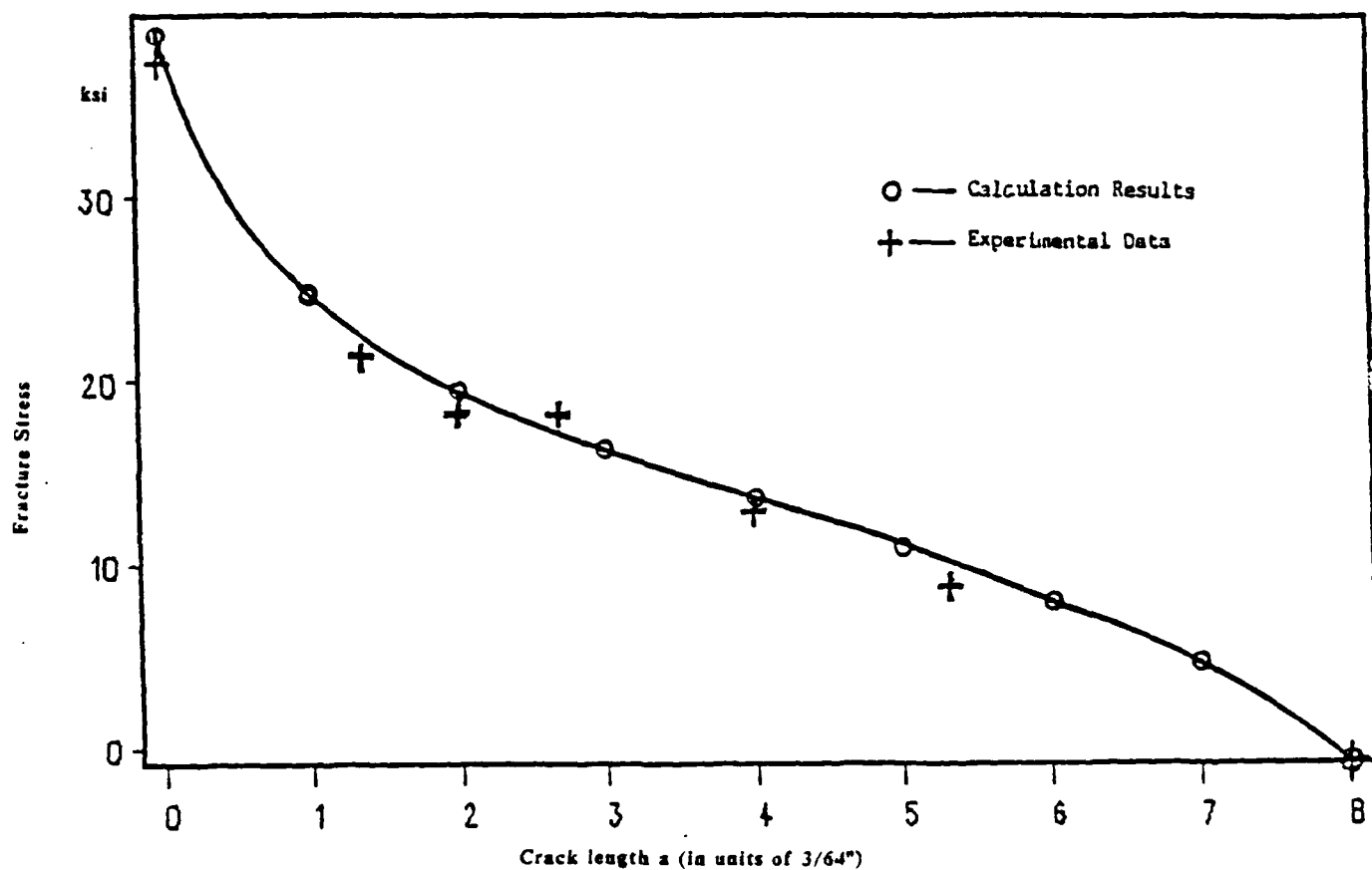
14

Figure 1.   Calculated versus observed fracture stress using the damage theory.

15

$$\sigma_c = \frac{K_{Ic}}{\sqrt{\pi a}} \, F(a/b)$$

$$\sigma_c = \frac{K_{Ic}}{\sqrt{\pi a}}$$

$K_{Ic} = 13.2$ ksi-in $^{1/2}$

...... Experimental Points
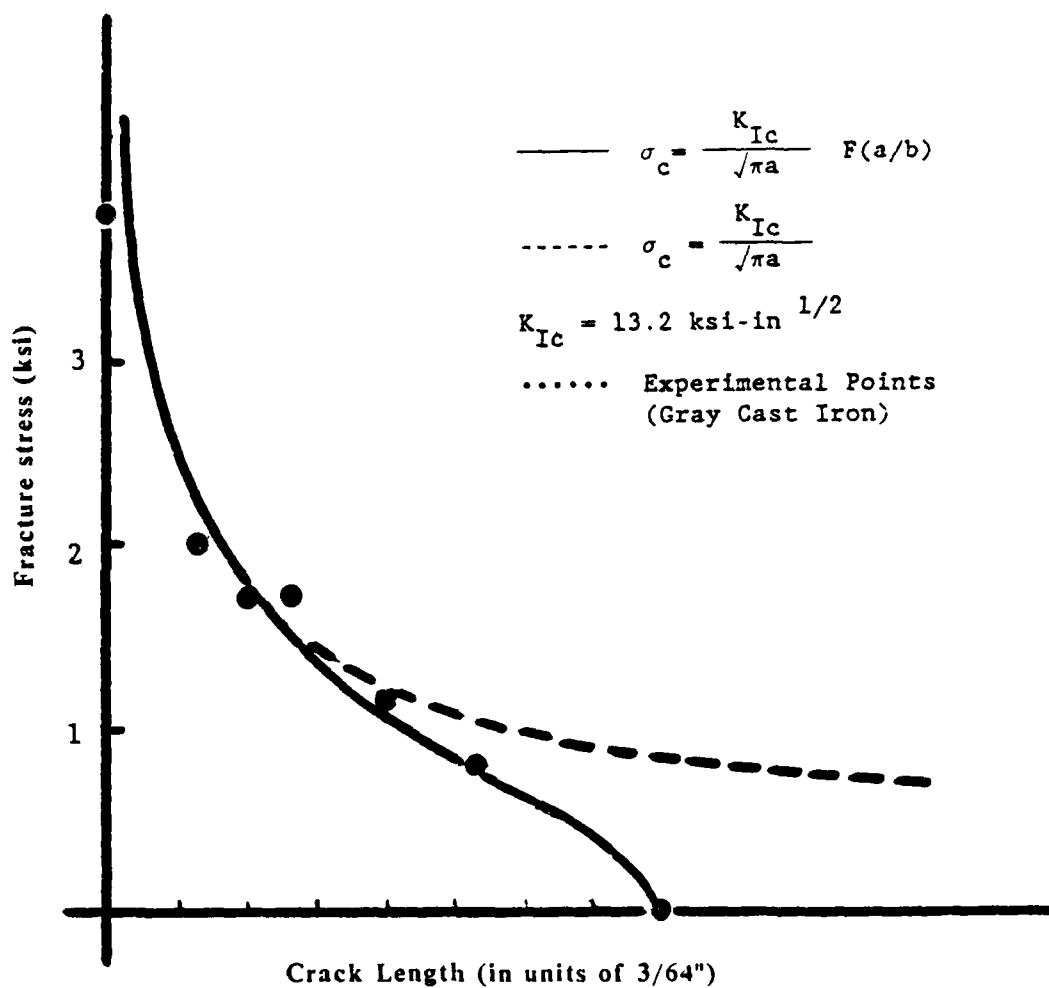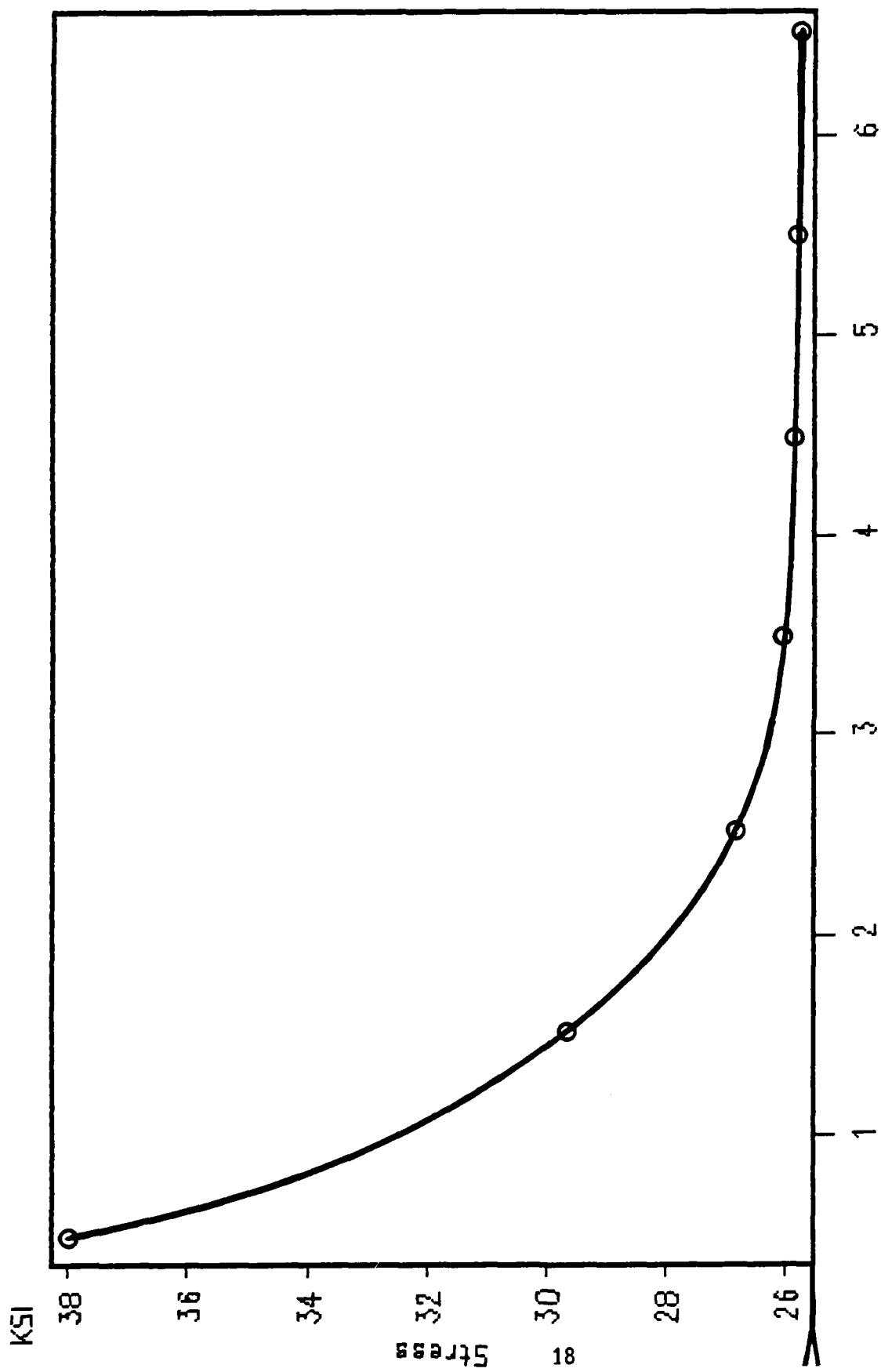(Gray Cast Iron)

Figure 1a.   Comparison of LEFM prediction with experimental observation.

Figures 2, 3, and 4a show, respectively, the stress, strain and damage distribution along the crack line when the half-crack is one unit long. Also shown in Figure 4a is the damage distribution along the elements just below the crack line -- again when the half-crack length is one unit. It may be seen that the calculated damage away from the crack is indeed negligible. In Figure 4b we show the damage distribution along the crack line when the half-crack is one unit long and three units long -- for comparison.

Figure 5 shows the stress-strain curve for the element adjacent to the tip of the crack when its half length is three units. Material softening is clearly visible leading to failure when the stress reaches a maximum value. Figure 6 shows a similar type of behavior, when the stress of the element adjacent to the crack tip is plotted versus boundary displacement -- for a crack whose half-length is again 3 units.

The attenuating effect of damage on the stress concentration is shown clearly in Figure 7, while Figure 8 shows the evolution of damage in the element adjacent to the crack tip versus boundary displacement. It may be seen that damage proceeds at a slow rate in the range of small strains, accelerating rapidly to a catastrophic rate as the strain increases. The half length of the crack was again three units.

In Figure 9 we show a comparison between the experimental and calculated values of the fracture stress for various angles of inclination α of the crack to the direction of pull. Agreement between theory and experiment is very good for values of α greater than 45 degrees. We believe that the discrepancy for values of α smaller than 45 degrees is due to the finiteness of the crack width and root radius. This conjecture was arrived at by observing that the crack extension did not originate at the root of the crack but at a point where a vertical line made tangential contact with the crack contour. This question needs further investigation.
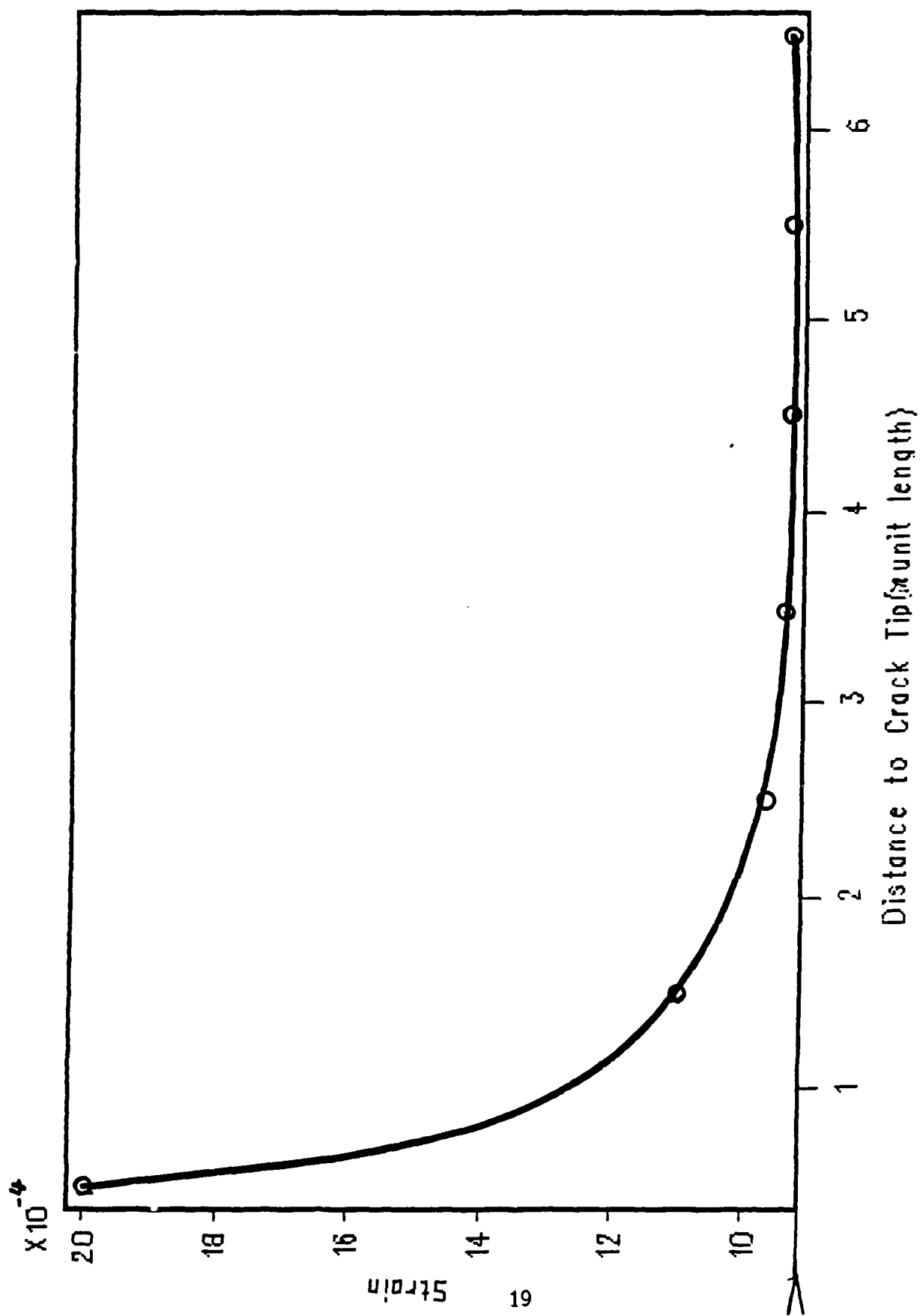
17

Figure 2. Stress distribution along crack line.

Distance to Crack Tip{x:unit length}

Figure 3. Strain distribution along crack line.

Strain

$\times 10^{-4}$

19
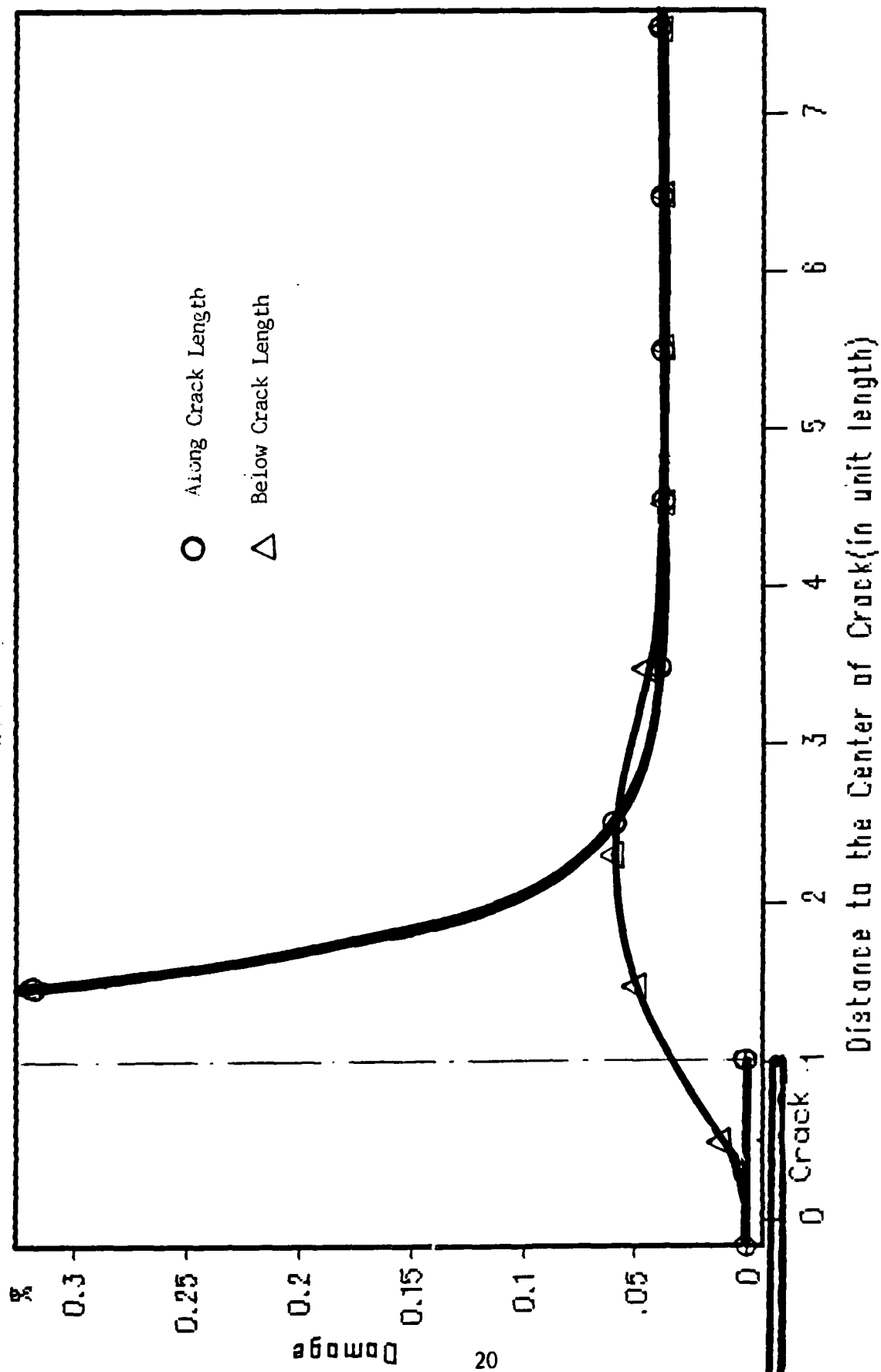
Figure 4. Damage distribution along and below crack line.
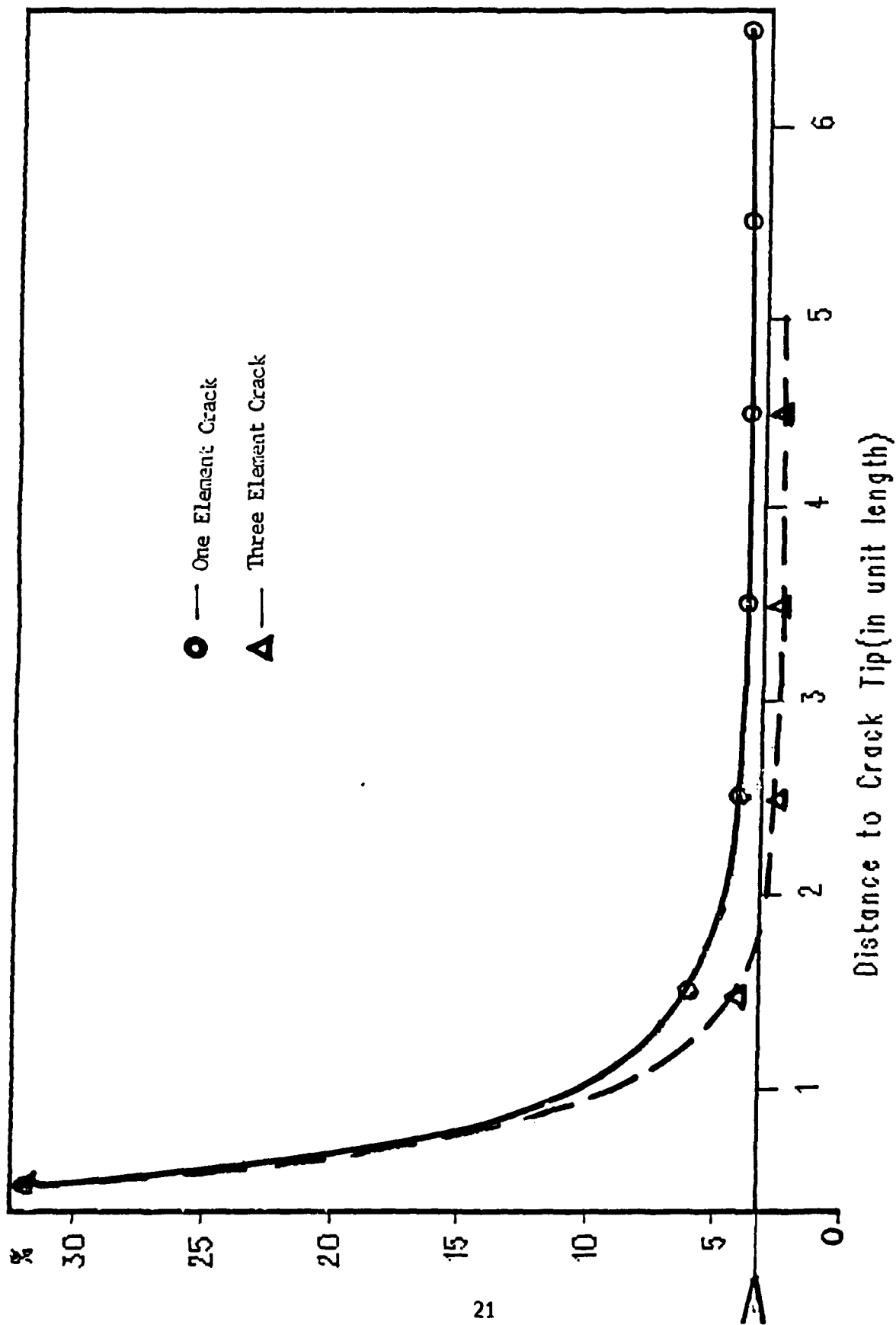
Distance to Crack Tip(in unit length)

Figure 4b. Damage distribution along crack line.
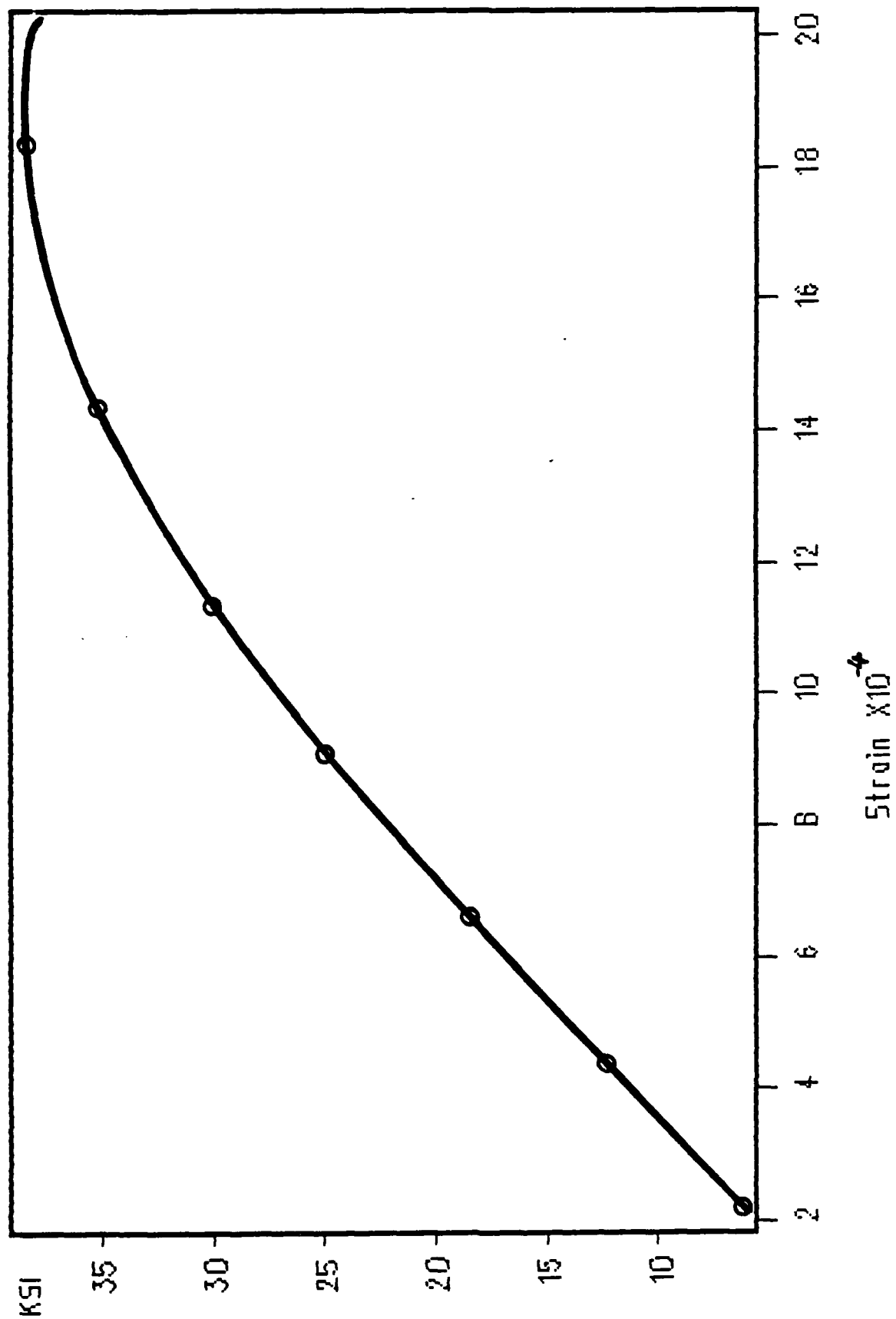
Figure 5. Stress-strain curve for the tip of crack.
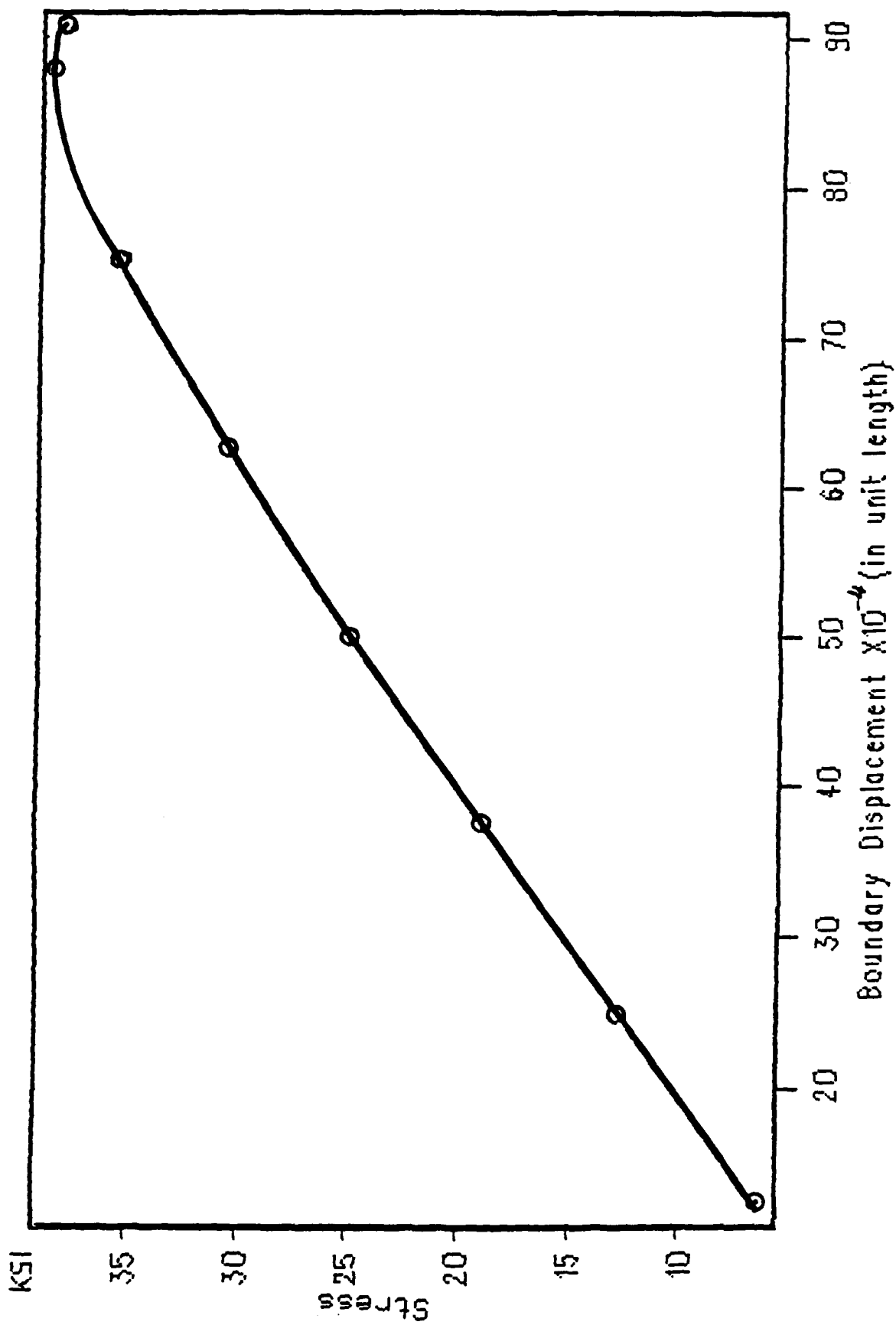
22

Boundary Displacement $\times 10^{-4}$ (in unit length)

Figure 6. Stress versus boundary displacement.

23
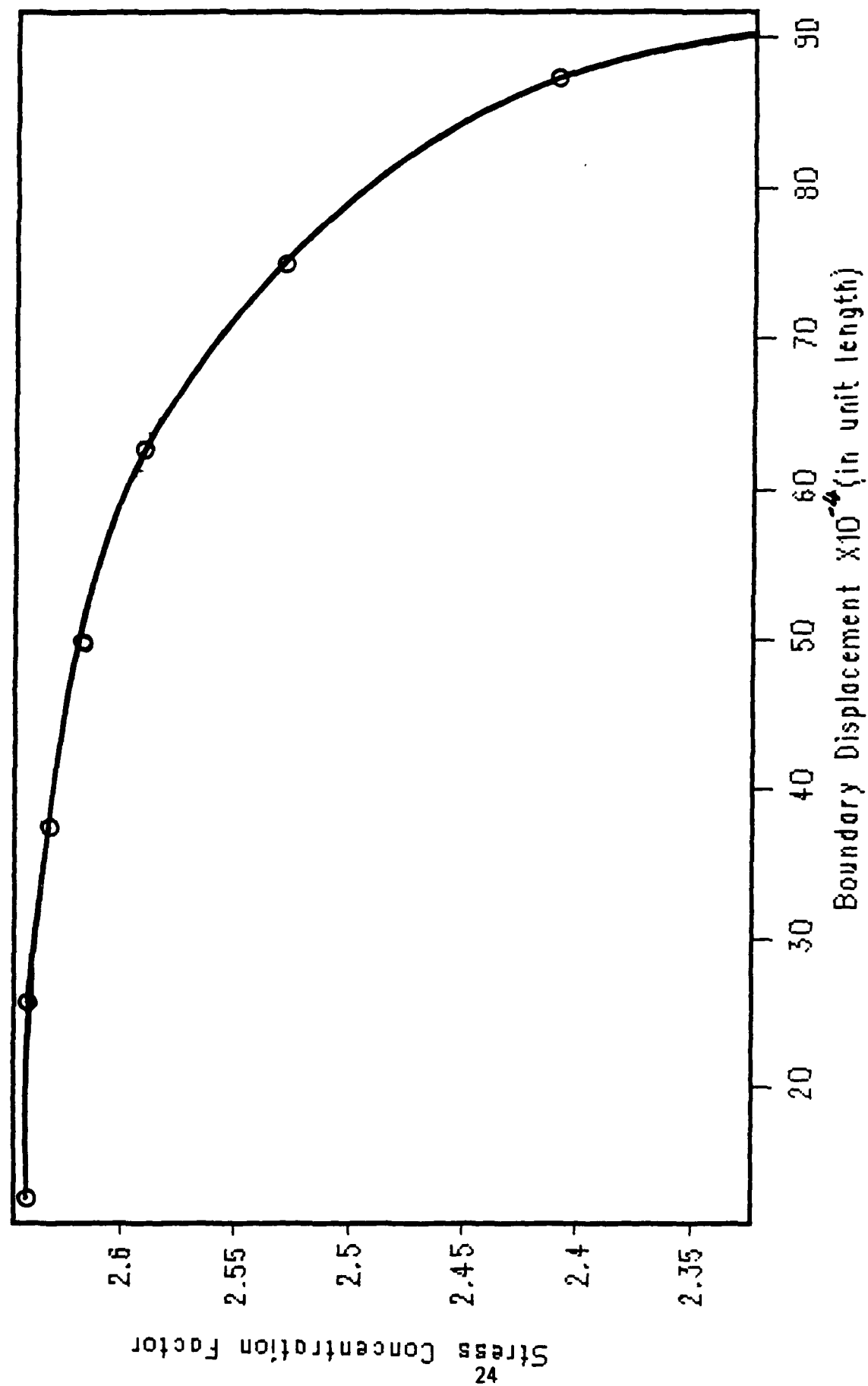
Figure 7. Stress concentration factor versus boundary displacement.

Boundary Displacement X10^{-4} (in unit length)

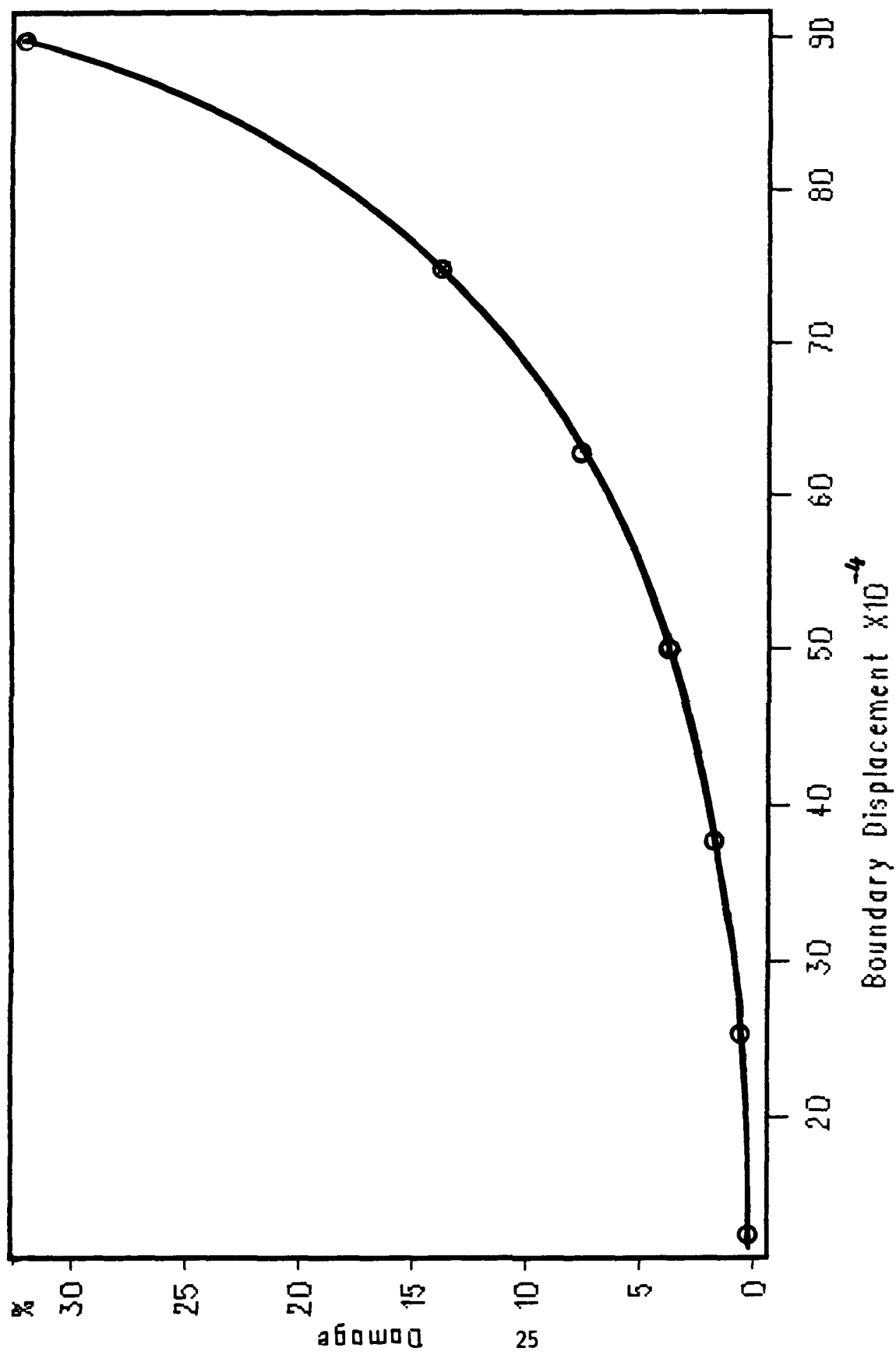Stress Concentration Factor

24

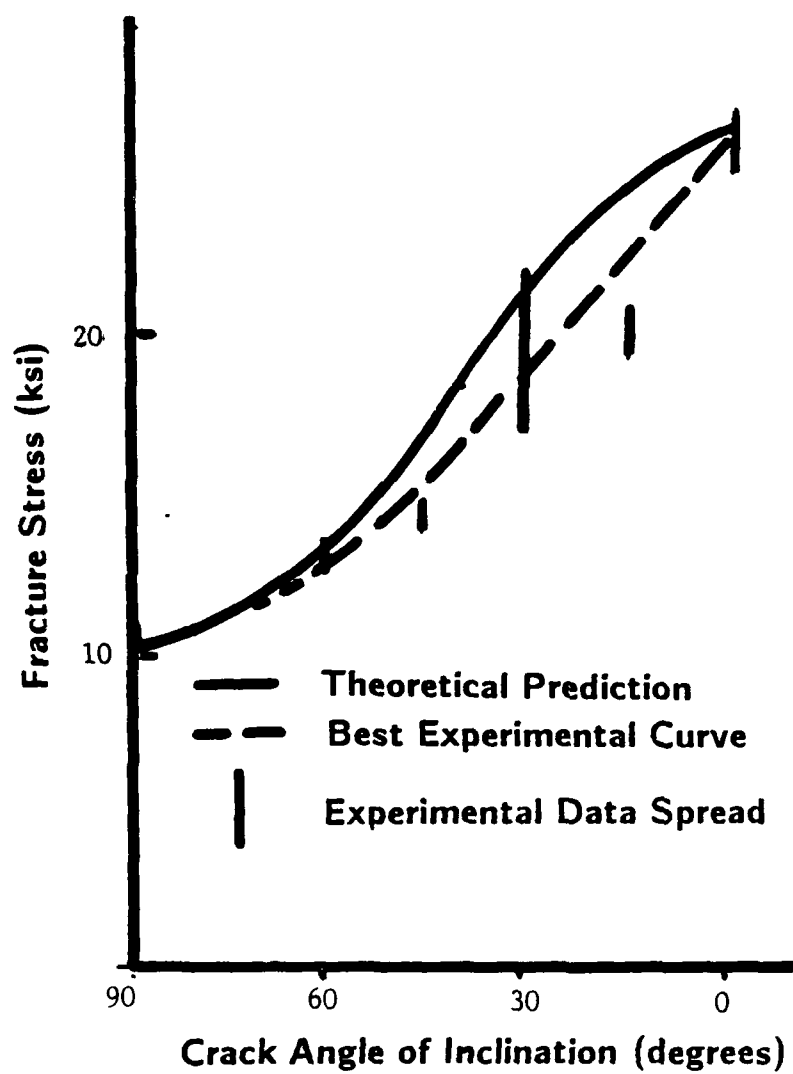Figure 8.   Damage evolution versus boundary displacement.
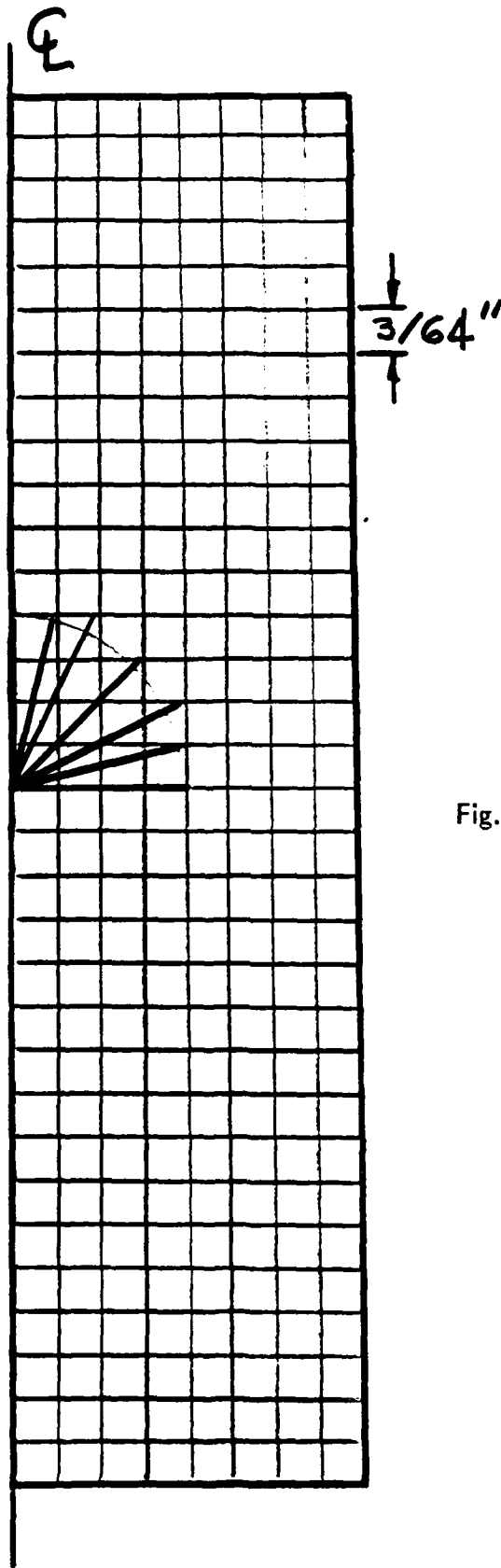
Figure 9. Fracture stress versus angle of crack.

Fig. 10   Right half of plate
with crack at various
angles of inclination.

3. DAMAGE THEORY IN THE CONTEXT OF FRACTURE MECHANICS IN MODE I.

As pointed out in the Introduction our purpose in this study is two-fold. We wish to examine the proposed theory in the light of experimental data, as well as in the context of linear fracture mechanics and thereby give perspective to the equations of the theory. Moreover we are also aiming at determining how ϕ depends quantitatively on the microdamage when this consists of a well-defined crack of a certain extent and direction relative to a material microelement. Of course a sub-part of our micromechanical aim is to determine the effective crack "extent" when the damage is not mathematically well defined. However, this last part must await the findings of the first phase of this work.

We begin by considering a thin sheet of "large" extent (and unit thickness) under axial stress in the presence of a through crack normal to the direction of stress. Also within the sheet, is a circular region whose center is at the midpoint of the crack and whose radius is R. The strain energy of the circular region in the absence of the crack is Ψ_o where

$$\Psi_o = \frac{1}{2} \frac{\sigma^2}{E} \pi R^2 \tag{3.1}$$

According to the Griffith calculation [10], in the limit of very large R, or vanishingly small "a", the reduction $\Delta\Psi$ in strain energy due to the onset of the crack at fixed strain ϵ is given by Eq. (3.2).

$$\Delta\Psi = \frac{1}{2} \frac{\sigma^2}{E} \pi a^2 \tag{3.2}$$

Hence, the free energy of the circular region in the presence of the crack is:

$$\Psi = \Psi_o - \Delta\Psi = \frac{1}{2} \frac{\sigma^2}{E} \pi \left(R^2 - a^2 \right) \tag{3.3}$$

or

$$\Psi = \frac{1}{2} \frac{\sigma^2}{E} \left[1 - (a/R)^2 \right] \pi R^2 \tag{3.4}$$

28

or

$$\Psi = \frac{1}{2} E \epsilon^2 \left[1 - (a/R)^2 \right] \pi R^2 \qquad (3.5)$$

since the far field axial stress is related to the far field axial strain by the relation: $\sigma = E \epsilon$.

In the Griffith fracture theory the "energy release rate" at fracture is equal to the rate of creation of surface energy, i.e.,

$$- \frac{\partial \Psi}{\partial a} = 2\gamma \qquad (3.6)$$

since for an increment of crack length "da" the surface energy created is 2γ da. Thus using Eqs. (3.5) and (3.6) in the limit of $R \to \infty$,

$$\frac{\sigma^2 \pi a}{E} = 2\gamma \qquad (3.7)$$

which is the Griffith equation for the critical stress, i.e.,

$$\sigma_c = \sqrt{\frac{2E\gamma}{\pi a}} \quad . \qquad (3.8)$$

The Present Theory.

It is easily shown that in the case of a thin plate under axial stress conditions $(\phi_{ij} = 0, i \neq j, \phi_{22} = \phi_{33} = 1)$ Eq. (2.1a) gives:

$$\psi = \frac{1}{2} E\epsilon^2 \phi_1^2 \qquad (3.9)$$

Thus Ψ which is the energy of a region with radius R becomes

$$\Psi = \pi R^2 \psi = \frac{1}{2} E\epsilon^2 \phi_1^2 \pi R^2 \qquad (3.10)$$

comparison of Eq. (3.10) with Eq. (3.4) shows that in the limit of a vanishingly small crack length

29

$$\phi = \sqrt{1 - (a/R)^2} \tag{3.11}$$

This is a highly interesting result which though precisely valid only for small values of "a", it nonetheless satisfies, for circular regions, the condition $\phi_1 = 0$ for $a = R$. Thus, when the crack has spread across the entire circular region $\sigma_1 = 0$ as expected. This suggests that in a strip of finite width b and height h

$$\phi_1 = f\left(1 - (a/b)^2, \; h/b\right) \tag{3.12}$$

where the form of the function f is to be determined from an exact elastic solution of the problem.

We now return to the Griffith crack criterion i.e., Eq. (3.6). Regarding the entire circular region as a thermodynamic system, ϕ_1 is an internal variable of the system and since ϕ_1 depends on "a", then so is "a". We proceed to define a generalized strain $\bar{\epsilon}$ where

$$\epsilon = \bar{\epsilon} R \sqrt{\pi} \tag{3.13}$$

and a generalized stress $\bar{\sigma}$ where

$$\sigma = \bar{\sigma} R \sqrt{\pi} \tag{3.14}$$

then

$$\bar{\sigma} = \partial \Psi / \partial \bar{\epsilon} = E \bar{\epsilon} \phi_1^2 \tag{3.15}$$

recovering the relation

$$\sigma = E \epsilon \phi_1^2 \tag{3.16}$$

It also follows from the usual thermodynamic considerations that $-\partial \Psi / \partial a$ is the internal force operating on the fracture mechanism, i.e., the "driving thermodynamic force" that is the cause of crack growth. In view of Eqs. (3.10), (3.11), (3.13) (3.14), and (3.15):

30

$$-\frac{\partial \Psi}{\partial a} = \frac{\partial \pi}{\left[1 - (a/R)^2\right]^2} \frac{\sigma^2}{E} \qquad (3.17)$$

Now if we use linear thermodynamics of internal variables, the classical equation of evolution for "a" is

$$\partial \Psi / \partial a + \eta \, da/d\xi = 0 \qquad (3.18)$$

where η is the resistance to cracking and $d\xi$ is an <u>intrinsic</u> time measure and η is the resistance coefficient of the internal fracture mechanism. In our case ξ is the <u>damage</u> coordinate. If, therefore, we set

$$d\xi = da \qquad (3.19)$$

Eq. (3.18) becomes

$$- \partial \Psi / \partial a = \eta \qquad (3.20)$$

Thus Eqs (3.6) and (3.18) are completely reconciled if $\eta = 2\gamma$. Therefore, using Eq. (3.20)

$$\sigma_c = \sqrt{\frac{2E\gamma}{\pi a}} \left[1 - (a/R)^2\right] \qquad (3.21)$$

which in the limit of vanishingly small "a" agrees with the Griffith crack criterion, but is also <u>qualitatively</u> true for finite regions of width R in the range $0 \leq a \leq 1$, as will be shown.

We have thus demonstrated that the griffith fracture theory is totally consistent with the damage theory proposed here, in the context of irreversible thermodynamics put forth above, for the choice of damage co-ordinate given in Eq. (3.19). It also provides a means for determining the dependence of ϕ on the crack extent in Mode I, for crack lengths that are small in relation to the size of the size of the overall thermodynamic system.

31

4. GENERALIZATION TO OTHER DOMAINS.

We wish to extend the above ideas to other domains. To this end we begin with a strip of finite width b and height h. Our purpose here is to use linear fracture mechanics as a basis from which to view the damage theory. Thus we are looking for a paradigm, an example of convergence of the two theories, when the material is an elastic solid that fractures in an ideally brittle manner.

In accordance with Eq. (3.9) the free energy of the plate (width 2b, height 2h) is given by the expression

$$\Psi = \frac{1}{2}E\epsilon^2\Phi\left(\left[1 - \left(\frac{a}{b}\right)^2\right], \frac{b}{h}\right)bh \tag{4.1}$$

where

$$\Phi = \phi_1^2 \tag{4.2}$$

ϕ_1 being the first principal component of the integrity tensor ϕ. Again we define a generalized stress $\bar{\sigma}$ and strain $\bar{\epsilon}$ such that

$$\sigma = \bar{\sigma}\sqrt{bh}, \quad e = \bar{e}\sqrt{bh} \tag{4.2a,b}$$

Thus the thermodynamic relation

$$\bar{\sigma} = \partial\Psi/\partial\bar{\epsilon} \tag{4.4}$$

gives rise to the expected constitutive relation:

$$\sigma = E\epsilon\Phi \tag{4.5}$$

Equation (4.5) provides the first limiting condition on Φ in the sense that

$$\lim_{h\to\infty} \Phi = 1 \tag{4.6}$$

since in the limit of $h\to\infty$, $\sigma = E\epsilon$.

From the theory of fracture mechanics:

$$-\partial\psi/\partial a = K_I^2/E \tag{4.7}$$

32

This, in view of Eq. (3.18) damage theory and fracture mechanics are brought into correspondence if

$$\eta = K_1^2 / E \tag{4.8}$$

and $da = d\zeta$ in accordance with Eq. (3.19).

Using Eqs. (4.7) and (4.1):

$$E \epsilon^2 \left(a \cdot b^2 \right) \hat{\phi} = K_1^2 / E \tag{4.9}$$

where $\hat{\phi} = \partial \phi / \partial (1 - a^2/b^2)$ at constant h/b. At this point, using Eq. (4.5) we find that,

$$K_I^2 = \sigma^2 a \left(\hat{\phi} / \phi^2 \right) \left(\frac{h}{b} \right) \tag{4.10}$$

In the notation of fracture mechanics [11]

$$K_I = \sigma \sqrt{\pi a} \, F \left(\frac{a}{b} \, , \, \frac{h}{b} \right) \tag{4.10a}$$

Thus

$$\frac{\hat{\phi}}{\phi^2} = \pi \frac{b}{h} \, F^2 \left(\frac{a}{b} \, , \, \frac{h}{b} \right) \tag{4.10b}$$

Since F is known from an elastic analysis, we have, therefore, established an exact connection between the damage tensor and the crack length "a" under Mode I conditions and the stipulation that the damage co-ordinate ζ is a linear function of the crack length.

More specifically if we write $1 - a^2/b^2 = x$, $h/b = y$, Eq. (4.10b) becomes

$$- \frac{\partial}{\partial x} \left(\frac{1}{\phi} \right) = \frac{\pi}{y} \, F^2 (x,y) \tag{4.10c}$$

Thus

$$\phi = \frac{h/b}{c - \pi \int F^2 dx} \tag{4.10d}$$

where c is a constant of integration to be determined from the condition

$$\phi\big|_{a/b = 1} = 0 \tag{4.10e}$$

Equation (4.9) provides another limiting condition on ϕ. Fracture mechanics requires that [11], in the limit of $h \to \infty$

$$K_I^2 = \sigma^2 \pi a F^2(b/a) \tag{4.11}$$

and since under these conditions $\sigma = E\epsilon$, it follows from Eq. (3.9) that

$$\lim_{h \to \infty} \left(\frac{h}{b}\right)\hat{\phi} = \phi^*\left(\frac{a}{b}\right) \tag{4.12}$$

where the function ϕ^* is a function of (a/b) only.

Now if we use limiting conditions (4.6) and (4.12), and in view of Eq. (4.10), we find that:

$$K_I = \sigma\sqrt{\pi a} \sqrt{\phi^*} \tag{4.13}$$

thus providing a relation between the damage function and the fracture toughness coefficient in Mode I, for a strip of finite width. Note if a_r is the effective area representation of the damage on a plane normal to $\vec{N}_r$ then $\phi_r(a_r)$ must satisfy the end conditions $\phi(0) = 1$; $\phi(1) = 0$.

A Specific Example.

To illustrate the ideas involved in the section we consider a form of ϕ given in Eq. (4.14), whish satisfies the limiting conditions $\phi = 1$ at $a = 0$ and $\phi = 1$ at $h = \infty$. Thus in the limit of $h \to \infty$ we set:

$$\phi = \left[1 - \left(\frac{a}{b}\right)^2\right]^{\frac{\pi b}{h}} \tag{4.14}$$

and explore the extent to which K_I derived from this form, agrees with the one derived from the principles of fracture mechanics.

34

Use of Eq. (4.10b) gives the result

$$F\left(\frac{a}{b}, \frac{b}{h}\right) = \frac{1}{\left[1 - \left(\frac{a}{b}\right)^2\right]^{1/2}(1+\pi b/h)}$$ (4.15)

In the specific case of the infinite strip ($h = \infty$)

$$F = \frac{1}{\left[1 - \left(\frac{a}{b}\right)^2\right]^{1/2}}$$ (4.16)

In Table 1 we compare the exact solution for F as given in [10] with that of Eq. (4.16). One can see that the agreement is reasonably close for a trial solution such as the one given by Eq. (4.14)

Table 1. Comparison of the Exact Values of F with Those of Eq. (4.16)

a/b	0	0.1	0.2	0.3	0.4	0.5	0.6	0.7	0.8	0.9	1.0
1/F(a/b)	1	.994	.976	.945	.901	.843	.767	.672	.551	.388	0
$[1-(a/b)^2]^{1/2}$	1	.995	.980	.954	.916	.866	.800	.714	.599	.435	0

Equation (4.14), however, does not lead to a good representation of F for finite values of h. Other simple forms of Φ will be explored in the future.

5. MORE ON THE RATE EQUATION (3.18).

In the previous sections we showed a precise correspondence between the integrity tensor and the stress intensity factor in the context of linear fracture mechanics. The key to this correspondence is the evolution equation (3.18) in the specific instance when the fracture coordinate ζ is such that

$$d\zeta = da \tag{5.1}$$

One disadvantage of linear fracture mechanics is that the evolution law for the crack length degenerates into an instability statement in the sense that when the stress is below a critical stress level the rate of growth of zero, whereas at the critical stress level the crack grows in an unstable-fashion.

Previously, we proposed an evolution law of damage given by Eq. (2.2), where the damage coordinate ξ is such that when $d\xi > 0$, then

$$d\xi = kd\epsilon \ , \ d\epsilon > 0 \tag{5.2}$$

It is therefore of interest to explore the effect of Eq. (5.2) on the evolution Eq. (3.18). In this specific case we find that the Griffith crack theory is used, in the limit of $R\to\infty$, but in the context of Eq. (5.2):

$$a\pi\epsilon^2 E = (\eta/k)(da/d\epsilon) \tag{5.3}$$

This equation may be integrated to give the relation

$$a = a_o e^{\frac{kE\pi}{3\eta}\epsilon^3} \tag{5.4}$$

where a_o is the <u>initial</u> crack length. Note that in this approach that a crack will not grow unless an initial crack length is assumed. While this result is physically unrealistic, (in the sense that Eq. (5.4) does not account for crack initiation), it agrees with linear fracture mechanics precepts whereby a specimen with a zero crack length cannot fail. Note, however, the rapid growth of "a" with ϵ^3.

Other Forms of $d\xi$.

The question of coupling between "a" and ϵ, just inevitably arise in so far as the definition of the damage coordinate ξ is concerned. In keeping with our previous

36

ideas on the concept of intrinsic time we set $d\xi$ equal to the righthand side of Eq. (5.5)

$$d\xi = \left(k^2 d\epsilon^2 + da^2\right)^{1/2} \tag{5.5}$$

where k is a material constant that has the dimension of length. Thus in view of Eq. (3.17), (3.18) and (5.5) and in the limit of $R \to \infty$, one finds that

$$\frac{da}{d\epsilon} = \frac{kE\pi a\epsilon^2}{\left(\eta^2 - E^2 a^2 \pi^2 \epsilon^4\right)^{1/2}} \tag{5.6}$$

Evidently, unstable crack growth occurs when $da/d\epsilon = \infty$, i.e., where

$$\eta = Ea\pi\epsilon^2 = a\pi\sigma^2/E \tag{5.7}$$

or at

$$\sigma_{cr} = \sqrt{\frac{\eta E}{a\pi}} \tag{5.8}$$

thus recovering the Griffith crack condition. However, Eq. (5.6) is now a crack growth equation which describes the rate of crack growth prior to instability. In view of Eq. (5.6), for low values of ϵ

$$da/d\epsilon \sim kE\pi a\epsilon^2/\eta \tag{5.9}$$

and thus Eq. (5.4) applies. The crack grows continuously until fracture takes place, when the denominator of the righthand side of Eq. (5.6) becomes zero, in accordance with the Griffith condition. Thus the evolution Eq. (3.18) in conjunction with the definition of damage coordinate given by Eq. (5.5) gives an ultimate Griffith crack conditions, but also, a crack growth law prior to instability.

These ideas will prove useful in the future for developing a comprehensive damage theory for brittle or semi-brittle solids.

6. EFFECT OF SIZE ON SPECIMEN STRENGTH.

In Eq. (3.18) the driving force on the fracture process is the rate of change of the _entire_ energy of the specimen with respect to the crack length (actually crack area of unit width). In the case of a strip, height h and width b, the fracture stress is given by Eq. (4.10a). Thus, given two different geometrically similar specimens so that a/b and h/b are the same in both specimens, but different in size, the larger specimen will have a smaller fracture stress σ_c (K_I being a material property), since

$$\sigma_c \sim 1\sqrt{a} \tag{5.10}$$

all other factors being equal. This rule is not satisfied precisely since the inverse square law is satisfied only approximately and only so for larger values of a.

The question of size on fracture strength is basically an unresolved problem which could be investigated in the future. The effect can be accounted for, however, in a formalistic manner by stipulating that η (the damage resistance coefficient) is a function of the geometry in some sense which is not quantized at this stage. Thus, we denote the geometry by G and we proceed to set

$$\eta = \eta(G) \tag{5.11}$$

This formalism allows one to treat the rate equation in terms of the average density ψ of the free energy of the specimen.

REFERENCES

[1]   Dragon, A., and Mroz, Z., "A Continuum Model for Plastic-Brittle Behavior of Rock and Concrete.. *Int. J. Eng. Sci.*, 17, 121-137 (1979).

[2]   Lemaitre, J., and Lazars, J., "Application de la Theories de L'Endommagament au Comportement Nonlineaire et la Rupture du Beton de Structure," *Annales de l'ITBTP*, 41 (1982).

[3]   Chaboche, J. L., "The Concept of Effective Stress Applied to Elasticity and to Viscoelasticity in the Presence of Anisotropic Damage," Royal Aircraft Est., ONERA Report No. 1979-77, Farnborough (1979).

[4]   Krajcinovic, D., and Fouseka, "The Continuous Damage Theory of Brittle Materials, Part I.," *J. App. Mech.*, 48, 809, (1981).

[5]   Fouseka, G. U., and Krajcinovic, D., "The Continuous Damage Theory of Brittle Materials, Part II," *J. App. Mech.*, 48, 816, (1981).

[6]   Krajcinovic, D., and Fanella, D., "A Micromechanical Damage Model for Concrete," *Eng. Fract. Mech.*, 25, 386-396, (1986).

[7]   Caboche, J. L., "Continuum Damage Mechanics, Part I - General Concepts; Part II Damage Growth, Crack Initiation and Crack Growth," *J. App. Mech.*, 55, 59-72, (1988).

[8]   Hegemier, G. A., Read, H. E., Valanis, K. C., and Murakami, H., "Development of Advanced Constitutive Models for Plain and Reinforced Concrete," S-CUBED Report SSS-R-87-8454 (1987).

[9]   Valanis, K. C., "A Theory of Damage in Brittle and Semi-Brittle Materials," ENDOCHRONICS Report Endic-005-AFOSR-1988, (1988).

[10]   Knott, J. F., "Fundamentals of Fracture Mechanics," Butterworths, London, (1973).

[11]   Tada, H., Paris, P., and Irwin, G., "The Stress Analysis of Cracks Handbook," DEL Corporation, Hellertown, PA, USA, (1973).

ENDIC-007-AFOSR-1989

A THEORY OF DAMAGE IN PLANE CONCRETE

Final Report - Part II

K. C. Valanis
Endochronics, Inc.
8605 Lakecrest Court
Vancouver, WA 98665

Prepared for

AFOSR
BOLLING AIRFORCE BASE
WASHINGTON, DC 20332-6448
CONTRACT NO. F49620-88-C-0038

JULY, 1989

TABLE OF CONTENTS

A THEORY OF DAMAGE IN CONCRETE

ABSTRACT

A constitutive theory of damage in plane concrete was developed leading to two different constitutive formulations -- Theories I and II -- depending on the underlying specific physical and geometric hypotheses. Theory II was used to depict the behavior of concrete in the course of axial compression. Calculated results in terms of the axial stress-strain relation were compared with their experimental counterparts. Close agreement was demonstrated between theory and experiment.

The study yielded insights into the physics of degradation with strong evidence that:

(a)   Substantial damage does not occur until the material has reached its fully plastic state.

(b)   The rate of degradation is a strong increasing function of the initial elastic modulus. This phenomenon becomes particularly pronounced in the softening region of the axial stress-strain curve.

Finding (b) has ramifications in regard to the design of concrete structures intended to survive damage. The inference is that high strength concrete will degrade much faster in the softening region following the onset of maximum stress.

A earlier damage evolution equation (Valanis, 1987) proved very effective in describing the experimental findings in plane concrete.

1. INTRODUCTION.

The effects of damage on the constitutive behavior of concrete pose difficult questions that cannot be treated in a trivial manner. In the first place, the physics of damage in this material is very much a function of the prevailing hydrostatic stress. At low pressures a substantial amount of microcracking occurs in a brittle manner in preferred directions leading to induced material anisotropy.

Higher pressures inhibit brittle microcracking and the macroscopic deformation is the result of material "flow" in a ductile manner. At these high pressures isotropic damage is present but experimental techniques to separate damage from purely plastic constitutive behavior are not always explicit. In fact purely constitutive theories of concrete either ignore the presence of isotropic damage at these pressures, or, by implication, treat its effects in a manner pertaining to plastic deformation.

The nature of damage notwithstanding, the underlying constitutive behavior of concrete is very complex in the sense that history dependence and strain path effects are significant.

Such observations are reported by Scavuzzo *et al.* (1983), on the basis of extensive experiments on medium strength plain concrete. Specifically Scavuzzo recorded the strain response to various complex non-proportional stress paths that brought into focus the underlying influences of the stress history.

Recently Valanis and Read (1986) used the framework of the endochronic theory to develop an advanced non-linear constitutive equation for concrete, that describes correctly the strain response to the paths investigated by Scavuzzo, in the absence of damage.

In this work constitutive questions concerning the representation of damage and the incorporation of its effects in the constitutive equation of concrete are addressed. In this context, the equation of evolution of damage is of central importance. We point out at this juncture that a constitutive theory of concrete in the presence of damage (which in this work we call Theory I) has been applied to concrete under conditions of axial tension (Valanis and Read, 1989). This theory proved too complex for application to three-dimensional problems. In this work, therefore, we have

2

developed an alternative approach which is much more physically transparent and more easily applicable to three-dimensional geometries.

Damage in Concrete.

In the theoretical treatment that follows, we maintain the position in our previous work, Valanis (1988, 1989a,b) to the effect that the representation of damage and its evolution are two separate issues. The former is of geometric character and is independent of the constitutive properties of the material at hand. The evolution of damage on the other hand, is very much a function of material physics and is, therefore, a constitutive problem. This question is taken up in greater detail in Section 2.

A substantial part of the damage in concrete at low hydrostatic stress occurs in a "brittle" manner. The work "brittle" is not used idly but is meant to signify damage consisting of microcracks caused by <u>increasing tensile strain</u>. Damage increments take place in preferential directions dictated by the eigen-directions of the <u>tensile</u> principal components of the strain increment tensor. Thus the directions of microcracking are dictated by the eigen-vectors of the <u>tensile</u> principal components of the strain increment tensor.

The proposition regarding directionality is consistent with the observations that: (a) damage in tension is in terms of cracks whose plane is <u>normal</u> to the direction of the axial stress; (b) in compression crack planes are <u>tangential</u> to the direction of the axial stress; (c) oblique cracks in a tensile stress field extend in planes <u>normal</u> to the direction of the axial stress. This we have found in our work of the extension of oblique cracks in grey cast iron. See Part I of this Final Report.

The above discussion on the physics of damage in concrete will serve as the basis for the development of a constitutive theory of damage in conjunction with a constitutive relation which accounts explicitly for the effect of damage on the mechanical response of this material.

3

2. A THEORETICAL FRAMEWORK FOR DIRECTED-CUM-ISOTROPIC DAMAGE IN CONCRETE

THEORY I.

The conceptual foundations of the present theory of damage were laid in an earlier work by Valanis as a separate contribution in the work of Hegemier, Read, Valanis and Murakami (1987) (see Appendix A). As a result of that work the problem was resolved into two separate parts one of damage representation and one of damage evolution. The former is a geometric problem while the latter involves the physics of damage and is influenced by the material constitution.

In multiphase media such as concrete damage in the form of directed cracks is accompanied by the presence of small randomly oriented microcracks which, in the mean, constitute isotropic damage (Diamond and Bentur, 1984). In Reference 1 directed damage was represented by an integrity tensor value of field, $\underset{\sim}{\Phi}(x_i)$, symmetric and of second order. When $\underset{\sim}{\Phi}$ is null, at some x^i, the material has fully failed in the neighborhood of x_i and cannot support stress in any direction, while if $\underset{\sim}{\Phi}$ is unity, then the corresponding damage is zero. Other values of $\underset{\sim}{\Phi}$ represent intermediate levels of damage.

To account for the simultaneous presence of isotropic and directed damage a tensor field $\underset{\sim}{\phi}(x_i)$ is introduced, which is a measure of directed damage, and a scalar field $w(x_i)$, which represents isotropic damage. Thus,

$$\underset{\sim}{\Phi} = \underset{\sim}{\Phi}(w, \underset{\sim}{\phi}) \tag{2.1}$$

subject to the conditions:

$$\underset{\sim}{\Phi}(1, \underset{\sim}{\phi}) = \underset{\sim}{\phi} \tag{2.2a}$$

$$\underset{\sim}{\Phi}(0, \underset{\sim}{\phi}) = \underset{\sim}{0} \tag{2.2b}$$

To satisfy conditions (2.2a,b) a representation of the multiplicative type is adopted whereby

$$\underset{\sim}{\Phi} = w\underset{\sim}{\phi} \; ; \quad w(o) = 1 \tag{2.3}$$

4

The effect of damage on the constitutive behavior is introduced by appealing to the thermodynamics of internal variables. In the manner adopted in Part I of this work on damage in brittle, elastic solids, the free energy density of concrete is a function of $\underset{\sim}{\phi}$. However, because concrete is not elastic the problem has to be treated differently.

It has been shown recently (Valanis, 1989c) that the elastoplastic process is the result of two series processes, plastic and elastic. Each process is accompanied by a change in the free energy density (relative to the reference configuration) -- ψ_p for the plastic process and ψ_e for the elastic counterpart. The total change in the free energy, ψ, is the sum of the two so that

$$\psi = \psi_e + \psi_p \tag{2.4}$$

The essence of a series process is that the same stress $\underset{\sim}{\sigma}$ is the causal agent for both processes while the corresponding strains are additive. Thus it follows from thermodynamics that

$$\underset{\sim}{\sigma} = \frac{\partial \psi_e}{\partial \epsilon^e} = \frac{\partial \psi_p}{\partial \underset{\sim}{\epsilon}^p} \tag{2.5}$$

while

$$\underset{\sim}{\epsilon} = \underset{\sim}{\epsilon}^e + \underset{\sim}{\epsilon}^p \tag{2.6}$$

When the reference state is a "natural" state devoid of initial internal stresses then, in small deformation theory, the free energy is a homogeneous quadratic function of its arguments. Therefore,

$$\psi_e = \frac{1}{2} A^o_{ijk\ell} \epsilon^e_{ij} \epsilon^e_{k\ell} \tag{2.7}$$

$$\psi_p = \frac{1}{2} \sum_{r=1}^{n} A^r_{ijk\ell} \left(\epsilon^p_{ij} - q^r_{ij} \right) \left(\epsilon^p_{k\ell} - q^r_{k\ell} \right) \tag{2.8}$$

5

The effect of damage in the constitutive response is introduced by letting the "elastic moduli" $\underset{\approx}{A}^r$, $(r = 0, \ldots n)$, be quadratic functions of $\underset{\sim}{\phi}$. In the event that in the undamaged state $\underset{\approx}{A}^r$ are constant isotropic tensors depicting a material which is initially isotropic then it is shown (Valanis, 1987) that

$$A^r_{ijk\ell} = A^r_1 \phi_{ij}\phi_{i\ell} + A^r_2 \phi_{ik}\phi_{j\ell} \tag{2.9}$$

where A^r_1 and A^r_2 are the elastic constants in the undamaged state. In fact, since in that state $\underset{\sim}{\phi} = \underset{\sim}{\delta}$, then the undamaged form of $\underset{\approx}{A}^r$ is given by Eq. (2.9a)

$$\hat{A}^r_{ijk\ell} = A^r_1 \delta_{ij}\delta_{k\ell} + A^r_2 \delta_{ik}\delta_{j\ell} \tag{2.9a}$$

Damage During the Plastic Process.

It follows from Eq. (2.5) that

$$\sigma_{ij} = \sum_{r=1}^{n} A^r_{ijk\ell}\left(\epsilon^p_{k\ell} - q^r_{k\ell}\right) \tag{2.10}$$

Thus, upon substitution of Eqs. (2.3) and (2.9) in Eq. (2.10) one finds that

$$\sigma_{ij} = \omega^2 \left[\sum_{r=1}^{n} A^r_1 \phi_{ij}\phi_{i\ell}\left(\epsilon^p_{k\ell} - q^r_{k\ell}\right) + A^r_2 \phi_{ik}\phi_{j\ell}\left(\epsilon^p_{k\ell} - q^r_{k\ell}\right) \right] \tag{2.11}$$

Though $\underset{\sim}{\phi}$ is positive semidefinite in the sense that $\underset{\sim}{\phi} = 0$ in a fully damaged material, for analytical purposes we will regard $\underset{\sim}{\phi}$ as positive definite in the sense that we can make it approach zero to any required degree of accuracy without making it exactly zero. Let

$$\underset{\sim}{A} = \underset{\sim}{\phi}^{1/2} \tag{2.12}$$

$$A_{ij} = \sum_{\alpha=1}^{3} n^\alpha_i n^\alpha_j \, \phi^{1/2}_\alpha \tag{2.13}$$

6

where n_j^{α} are the eigenvectors of ϕ and ϕ_{α} its eigenvalues, always non-negative. Hence $\phi_{\alpha}^{1/2}$ always exist, for all α. Following now the work by Valanis and Read (1989), we introduce the transformed quantities $\hat{\sigma}$, $\hat{\epsilon}^P$ and $\hat{q}^r$ such that

$$\hat{\epsilon}^P = \underset{\sim}{A} \cdot \underset{\sim}{\epsilon}^P \cdot \underset{\sim}{A}^T \quad , \quad \hat{a}_r = \underset{\sim}{A} \cdot \underset{\sim}{g}^r \underset{\sim}{A} \tag{2.14a}$$

$$\underset{\sim}{\sigma} = \underset{\sim}{A} \hat{\sigma} \underset{\sim}{A}^T \tag{2.14b}$$

where
$$A^T = A \tag{2.14c}$$

Note that the matrix $\underset{\sim}{A}$ used by Valanis and Read (1989) differs from the present by an orthogonal transformation. However both give rise to Eq. (2.16).

Use of Eqs. (2.14a,b) in Eq.(2.11) gives the following relation between stress and strain in the transformed state:

$$\hat{\sigma}_{ij} = \omega^2 \left\{ \sum_r A_1^r \delta_{ij} \left(\hat{\epsilon}_{kk}^P - \hat{q}_{kk} \right) + A_2^r \left(\hat{\epsilon}_{ij}^P - \hat{q}_{ij}^r \right) \right\} \tag{2.15}$$

Also use of Eq. (2.8) gives the following expression for the free energy:

$$\psi_p = \omega^2 \sum_{r=1}^{n} \left\{ \frac{1}{2} A_1^r \left[tr \left(\hat{\epsilon}^P - \hat{g}^r \right) \right]^2 + \frac{1}{2} A_2^r \left| \left| \hat{\epsilon}^P - \hat{g}^r \right| \right|^2 \right\} \tag{2.16}$$

Since Eq. (16) can be reached by setting $\phi = \underset{\sim}{\delta}$ in Eq. (2.8) we conclude that the transformed state is one where only isotropic damage has taken place.

Equation (2.16) provides a convenient vehicle for determining the material plastic response in the presence of directed damage. The evolution Equation for $\underset{\sim}{q}^r$ is Eq. (2.17):

$$\frac{\partial \psi_p}{\partial \hat{q}_r} + \underset{\sim}{b}^r \frac{d\hat{g}_r}{dz} = 0 \tag{2.17}$$

7

The resistance tensors $\underset{\sim}{b}^r$ must decrease with volumetric damage and must got to zero as $\omega \to 0$. Thus we set

$$\underset{\sim}{b}^r = \omega^2 \underset{\sim}{\hat{b}}^r \tag{2.18}$$

Equation (2.18) in conjunction with Eq. (2.17) gives the evolution equation for g^r in the absence of damage, directed or volumetric. Specifically,

$$-\left\{ A_1^r \, \mathrm{tr}\left[\hat{\varepsilon}^P - \hat{g}^r\right]\underset{\sim}{\delta} + A_2^r\left(\hat{\varepsilon}^P - \hat{g}^r\right)\right\} + \underset{\sim}{\hat{b}}^r \cdot \frac{d\hat{q}^r}{dz} = 0 \tag{2.19}$$

where

$$\hat{b}^r_{ijk\ell} = b_1^r \delta_{ij}\delta_{k\ell} + b_2^r \delta_{ik}\delta_{j\ell} \tag{2.20}$$

note that the resistance tensors $\underset{\approx}{b}^r$ in the current configuration are given by the transformation:

$$b^r_{ijk\ell} = A_{ir}A_{js}A_{kt}A_{\ell n}\hat{b}_{rstn} \tag{2.20a}$$

so that

$$b^r_{ijk\ell} = \phi_{ij}\phi_{k\ell}b_1^r + \phi_{ik}\phi_{j\ell}b_2^r \tag{2.20b}$$

In the work on the constitutive response of concrete Valanis and Read (1986) we set

$$b_0^r = b_1^r + \frac{1}{3}\, b_2^r = b_{oo}' F_H \tag{2.21}$$

$$b_2^r = b_{20}^r F_D \tag{2.22}$$

where F_H and F_D are hydrostatic and deviatoric hardening functions respectively.

Solving Eq. (2.19) for $\hat{g}^r$ in the light of Eqs. (2.20), (2.21) and (2.22) and substituting in Eq. (2.5) the following constitutive relation is obtained for $\hat{\sigma}$:

8

$$\frac{1}{\omega^2}\,\hat{\mathcal{Q}} = \int_0^{Z_D} \rho(z_D - z')\,\frac{d\hat{e}^p}{dz'} + \oint_0^{Z_H} K(z_H - z')\frac{d\hat{\epsilon}^p_{kk}}{dz'}\,d\epsilon' \tag{2.23}$$

where, as shown previously (Valanis and Read, 1986):

$$\rho(z_D) = \sum A_2^r\, e^{-\alpha_r z_D} \tag{2.23a}$$

$$K(z_H) = \sum K_r\, e^{-\beta_r z_H} \tag{2.23b}$$

$$\alpha_r = \frac{A_2^r}{b_2^r} \tag{2.23c}$$

$$\beta_r = \left(3A_1^r + A_2^r\right)\Big/\left(3b_1^r + b_2^r\right) \tag{2.23d}$$

$$K_r = A_1^r + \frac{1}{3}A_2^r \tag{2.23e}$$

However recent work by Valanis and Peters (1989) points strongly to the possibility that

$$F_D = F_H = F \tag{2.24}$$

We shall adopt this view in this work in which case Eq. (2.23) becomes

$$\frac{1}{\omega^2}\,\hat{\mathcal{Q}} = \int_0^z \rho(z - z')\frac{d\hat{\underset{\sim}{\epsilon}}^p}{dz'}\,dz' + \oint_0^z K(z - z')d\,\frac{\hat{\epsilon}_{kk}}{dz'}\,dz' \tag{2.25}$$

where

$$dz = \frac{dz}{F} \tag{2.26}$$

At this point we recast Eq. (2.25) in the original configuration to obtain the following constitutive relation in the presence of directed <u>and</u> isotropic damage:

9

$$\frac{1}{\omega^2} \sigma_{rs} = A_{ri}A_{sj} \int_0^z \rho(z - z') \frac{d}{dz'} \left[A_{ik}A_{j\ell}\epsilon_{k\ell}^p \right]$$

$$+ \phi_{rs} \int_0^z K(z - z') \frac{d}{dz'} \left[\phi_{k\ell}\epsilon_{k\ell}^p \right] \ell z' \qquad (2.27)$$

Special Forms of Eq. (2.27).

Of particular interest is the case where shear stress and strains are absent. In this event $\underset{\sim}{\sigma}$, $\underset{\sim}{\epsilon}^p$ and $\underset{\sim}{\phi}$ (and $\underset{\sim}{A}$) are diagonal tensors whose elements are denoted by σ_i, ϵ_i^p and ϕ_i and A_i) respectively. In this case Eq. (2.25) takes the following form:

$$\frac{1}{\omega^2} \sigma_i = \phi_i \int_0^z \rho(z - z') \frac{d}{dz'} \left[\phi_i \ \epsilon_i^p \right] dz'$$

$$+ \phi_i \int_0^z K(z - z') \frac{d}{dz'} \left[\sum_{R=1}^3 \phi_r \epsilon_r^p \right] dz' \quad \text{(i not summed)} \qquad (2.28)$$

The Case of Axial Stress.

The experiments by Gopalaratnam and Shah (1985) and Valanis and Khan (1989) were performed under axial stress conditions, i.e.,

$$\sigma_1 \neq 0, \ \sigma_2 = \sigma_3 = 0, \ \epsilon_1 \neq 0 \ , \ \epsilon_2 = \epsilon_2 \neq 0.$$

In this instance Eq. (2.28) gives rise to the following result:

$$\frac{1}{\omega^2} \sigma_1 = \phi_1 \int_0^z E(z - z') \frac{d\left[\phi_1 \epsilon_1^p \right]}{dz'} dz' \qquad (2.29)$$

$$\phi_2\epsilon_1 = - \int_0^z \nu(z - z') \frac{d}{dz'} \left[\phi_1 \epsilon_1^p \right] dz' \qquad (2.30)$$

10

where $E(z)$ and $\nu(z)$ are related to the functions $\rho(z)$ and $K(z)$ in the Laplace Transform plane by the following equations:

$$\bar{\rho}(p) = \frac{\bar{E}(p)}{1 + p\bar{\nu}(p)} \tag{2.31a}$$

$$\bar{K}(p) = \frac{\bar{E}}{3(1 - 2p\bar{\nu}(p))} \tag{2.31b}$$

where a bar over a quantity denotes its Laplace Transform. Note that scalar damage has no effect on the relation between ϵ_2^p and ϵ_1^p.

We note that Eqs. (2.29) and (2.30) may also be written in the transformed configuration where they have the following form:

$$\hat{\sigma}_1 = \omega^2 \int_0^z E(z - z') \frac{d\hat{\epsilon}_1^p}{dz'} \, dz' \tag{2.32}$$

$$\hat{\epsilon}_2 = - \int_0^z \nu(z - z') \frac{d\hat{\epsilon}_1^p}{dz'} \, dz' \tag{2.33}$$

The Intrinsic Time Scale z.

Since the purely plastic behavior is formulated in the undeformed configuration where damage effects are absent, the intrinsic time z should also be defined in the same configuration. In keeping, therefore, with the concepts of endochronic plasticity,

$$d\varsigma^2 = d\hat{\epsilon}_{ij}^p d\hat{\epsilon}_{ij}^p + \kappa^2 \left| d\hat{\epsilon}_{kk}^p \right|^2 \tag{2.34a}$$

where the Greek letter κ is a material parameter. Use may now be made of Eq. (2.14a) to express dz in the present configuration. As a result,

$$d\varsigma^2 = \phi_{ri}\phi_{sj} \, \epsilon_{ij}^p \epsilon_{rs}^p + \kappa^2 \left| \phi_{k\ell}\epsilon_{k\ell}^p \right|^2 \tag{2.34b}$$

11

THEORY II.

Theory II is motivated by a desire to provide an alternative physical premise to the mechanism of the plastic process and to arrive at an analytically simpler damage-sensitive constitutive equation without sacrificing the rigor of derivation on the physical properties of damage adopted in Theory I.

As previously, the point of departure is the free energy ψ_p given by Eq. (2.8) with the damage-sensitive stiffness tensors $\underset{\approx}{A}^r$ given by Eq. (2.9). Equations (2.10) and (2.11) follow so that Eqs. (2.8) - (2.11) are common to both theories. However, the resistance tensors $\underset{\approx}{b}^r$ are <u>not</u> the same in both theories. In Theory II $\underset{\approx}{b}^r$ are not given by Eq. (2.21,b) as other, additional conditions, apply.

The basic difference lies in the equation of evolution of the internal variables in the damaged state. In Theory II this has the form

$$\frac{\partial \psi_p}{\partial g^r} + \underset{\sim}{b}^r \cdot \frac{dq_r}{dz} = 0 \tag{2.35}$$

i.e., it is expressed in the present state rather than the transformed state. The premise that the effect of damage is geometric and does not affect the physics of the plastic process is also maintained in Theory II. The constraint of this premise on Eq. (2.35) is discussed below.

In view of Eq. (2.8), Eq. (2.35) becomes

$$- \underset{\approx}{A}^r \cdot \left(\underset{\sim}{\epsilon}^p - \underset{\sim}{g}^r \right) + \underset{\sim}{b}^r \cdot \frac{dq_r}{dz} = 0 \tag{2.36}$$

Since $\underset{\approx}{b}^r$ is positive definite it has a unique inverse. We form the "relaxation tensor" $\underset{\approx}{\Lambda}^r$ as in Eq. (2.37), where

$$\underset{\sim}{\Lambda}^r = \left(\underset{\approx}{b}^r \right)^{-1} \underset{\approx}{A}^r \tag{2.37}$$

The underlying physical justification for the term: "relaxation tensor" will become clear in what follows.

12

In the undamaged isotropic state Λ^r has the form

$$\Lambda^r_{ijk\ell} = \Lambda^r_1 \delta_{ij}\delta_{k\ell} + \Lambda^r_2 \delta_{ik}\delta_{j\ell} \qquad (2.38)$$

In fact, with reference to Eqs. (2.23c,d)

$$\alpha_r = \Lambda^r_2,$$

$$\beta_r = 3\Lambda^r_1 + \Lambda^r_2 \qquad (2.39a,b)$$

Thus Λ^r_1 and Λ^r_2 are the determining constants of how fast the material relaxes, or how its memory fades, with respect to the intrinsic time.

The premise that the physics of the plastic process is unaffected by damage leads to the conclusion that the relaxation tensors Λ^r remain constant during damage.

Equation (2.37) then provides the key on how the resistance tensor b^r are affected by damage, since a rearrangement of this equation gives the result:

$$\underset{\sim}{b}^r = \underset{\sim}{\Lambda}^r \cdot \left(\underset{\sim}{\Lambda}^r\right)^{-1} \qquad (2.40)$$

Analysis.

Use of Eqs. (2.36) and (2.37) gives the following evolution equation for the internal variables:

$$- \Lambda^r_1 \delta_{ij}\left(\epsilon^p_{kk} - q^r_{kk}\right) - \Lambda^r_2\left(\epsilon^p_{ij} - q^r_{ij}\right) + \frac{dq^r_{ij}}{dz} = 0 \qquad (2.41)$$

At this point we introduce the variable $\underset{\sim}{\rho}^r$ defined by Eq. (2.42):

$$\underset{\sim}{\rho}^r = \underset{\sim}{\epsilon}^p - \underset{\sim}{g}^r \qquad (2.42)$$

13

Equations (2.41) and (2.42) combine to give the following evolution equation for $\underline{p}^r$:

$$\Lambda_1 \delta_{ij} p_{kk}^r + \Lambda_2 p_{ij}^r + \frac{dp_{ij}^r}{dz} = \frac{d\epsilon_{ij}^p}{dz} \tag{2.43}$$

This equation is solved in the normal fashion by taking its deviatoric and hydrostatic parts in which event:

$$p_{ij}^r = \frac{1}{3}\,\delta_{ij} \int_0^z e^{-\beta_r(z-z')}\,\frac{d\epsilon_{kk}^p}{dz'}\,dz' + \int_0^z e^{-\alpha_r(z-z')}\,\frac{de_{ij}^p}{dz'}\,dz' \tag{2.44}$$

where

$$dz = \frac{d\varsigma}{F} \tag{2.45}$$

$$e_{ij}^p = \epsilon_{ij}^p - \frac{1}{3}\,\epsilon_{kk}^p\,\delta_{ij} \tag{2.46}$$

and F is the hardening function of the plastic proc'ess.

At this point we use Eqs. (2.9) and (2.10) in conjunction with Eq. (2.42) to determine the stress in terms of the variables $\underline{p}^r$. Hence:

$$\sigma_{ij} = \sum \left\{ A_1^r \psi_{ij} \phi_{k\ell} + A_2^r \phi_{kk} i\ell \right\} p_{\kappa\ell}^r \tag{2.47}$$

where $\underline{p}^r$ are given by Eq. (2.22). This completes the formulation of the constitutive equation in the presence of damage.

A Simplified Form of Eq. (2.44).

The Poisson ratio in undamaged materials -- or more correctly, materials in their undamaged state -- remains substantially constant during an axial test. Furthermore, the Poisson ratio of concrete is small (about 0.10, or less) as we have found in the course of our own axial compression tests reported here in a later section. Thus small deviations in the Poisson's ratio are not likely to be of significance in the prediction of the constitutive response of concrete.

14

An analysis of Eq. (2.44), the details of which are omitted here, shows that a constant Poisson ratio, requires as a necessary (but not sufficient) condition:

$$\beta_r = \alpha_r \tag{2.48}$$

and hence, in view of Eq. (2.39a,b)

$$\Lambda_1^r = 0 \ . \tag{2.49}$$

Equation (2.49) reduces Eq. (2.44) to the much simpler form:

$$\varrho^r = \int_0^z e^{-\alpha_r(z-z')} \frac{d\varepsilon^p}{dz'} \ dz' \tag{2.50}$$

which, in conjunction with Eq. (2.48) gives rise to the following plastic constitutive equation in the presence of damage:

$$\sigma_{ij} = \Phi_{ij}\Phi_{\kappa\ell}\int_0^z A_1(z-z') \frac{d\varepsilon_{\kappa\ell}^p}{dz'} \ dz' + \Phi_{ik}\Phi_{i\ell}\int_0^z A_2(z-z') \frac{d\varepsilon_{k\ell}^p}{dz'} \ dz' \tag{2.51}$$

where

$$A_1(z) = \sum A_1^r e^{-\alpha_r z} \tag{2.52a}$$

$$A_2(z) = \sum A_2^r e^{-\alpha_r z} \tag{2.52b}$$

The sufficiency condition for a constant Poisson ratio is that $A_1(z)$ also be proportional to $A_2(z)$.

At this point we may use Eq. (2.3) to write Eq. (2.51) in terms of the isotropic damage ω and the directed damage ϕ. Thus:

$$\frac{1}{\omega^2} \sigma_{ij} = \phi_{ij}\phi_{k\ell}\int_0^z A_1(z-z') \frac{d\varepsilon_{k\ell}^p}{dz'} \ dz' + \phi_{ik}\phi_{1\ell}\int_0^z A_2(z-z') \frac{d\varepsilon_{k\ell}}{\Lambda z} \ dz' \tag{2.53}$$

15

This equation has an elegance and simplicity which is preferable to its counterpart, Eq. (2.27), of Theory I. It also appears to be easier to deal with numerically. Also as in Theory I the intrinsic time scale is given by Eq. (2.59)

$$dz^2 = \kappa^2 \left(\phi_{\kappa\ell} \epsilon^p_{\kappa\ell} \right)^2 + \phi_{ir} \phi_{js} d\epsilon^p_{ij} d\epsilon^p_{rs} \ . \tag{2.54}$$

Equation (2.53) will be used in Section 4 in the analysis of experimental data on concrete in axial tension and axial compression.

The Constitutive Equation (2.53) Under Axial Stress Conditions.

A straightforward analysis of Eq. (2.53) under conditions of homogeneous axial stress ($\sigma_1 \neq 0$, $0_s = \sigma_3 = 0$, $\epsilon_1 \neq 0$, $\epsilon_s = \epsilon_3 \neq 0$) yields the following result:

$$\frac{1}{\omega^2} \sigma_1 = \phi_1^2 \int_0^z E(z - z') \frac{d\epsilon^p_1}{dz'} dz' \tag{2.55}$$

$$\phi_2 \epsilon^p_2 = - \nu \phi_1 \epsilon^p_1 \tag{2.56}$$

where

$$E = \frac{A_2 \left(3A_1 + A_2 \right)}{2A_1 + A_2} \tag{2.57}$$

$$\nu = \frac{A_1}{2A_1 - A_2} \tag{2.58}$$

Evidently, since A_1 is proportional to A_2, it follows that $\nu(z)$ is indeed a constant function.

16

3. THE DAMAGE EVOLUTION EQUATION.

The task of determining the form of the damage evolution equation in the plastic state is difficult. If we follow the approach taken in the case of the elastic-fracturing solid then the driving thermodynamic force that causes damage is Q^ϕ in the case of directed damage and Q^ω in the case of isotropic damage, where

$$Q^\phi = -\frac{\partial \psi}{\partial \phi} \quad , \quad Q^\omega = -\frac{\partial \psi}{\partial \omega} \tag{3.1a,b}$$

noting that in the case of plastic materials

$$\psi = \psi_e + \psi_p \tag{3.2}$$

Insofar as directed damage is concerned the evolution equation would be

$$d\phi_r = k_1 \left(Q_\phi^r \right)^m d\xi^r \tag{3.3a}$$

while in the case of isotropic damage

$$d\omega = k_o \left(Q^\omega \right)^n d\Omega \tag{3.3b}$$

where $d\phi_r$ is an eigenvalue of $d\phi$, Q_ϕ^r is Q^ϕ projected normally on the eigenvector $\vec{n}^r$ and ξ^r is a damage coordinate in the direction of $\vec{n}^r$. Also Ω is a damage coordinate for the isotropic damage process. The parameters k_o, k_1, m and n are material constants.

This approach leads to enormously complex evolution equations involving both the elastic and plastic parts of the free energy. Furthermore since ψ_p depends on both ϕ and ω Eqs. (3.3a) and (3.3b) are explicitly coupled. Thus while the above approach is conceptually appealing, it is analytically unwieldy.

A Useful Approximation.

There are certain physically motivated approximations which lead to substantially simplified forms of the damage evolution equations that can be of practical value in the development of a useful model. The first stems from the fact that the Poisson

17

ratio of concrete in the undamaged state is small (less than 0.1) and its contribution to the free energy may be ignorable. Perusal of Eq. (2.58) shows that for this to be so the memory function $A_1(z)$ must be zero.

Also an examination of the experimental data by Gopalaratnam and Shah (1985) and Valanis and Khan (1989) shows that significant damage does not occur until plastic effects approach a saturated state, i.e., at a value of the plastic strain at which the axial stress would be close to a saturated value had damage not taken place.

Since during the saturated undamaged state the stress remains constant it follows that the elastic strain also remains constant. Thus, under uniaxial conditions the physics is such that damage -- to a very good approximation -- takes place at constant elastic strain. Furthermore a close analysis of the experimental data of Gopalaratnam and Shah shows that this in fact is the case. The obvious immediate generalization of this observation in three dimensions would be that (a) the elastic free energy ψ_e remains constant during damage and thus $\partial \psi_e / \partial \phi = 0$, $\partial \psi_e / \partial \omega = 0$, and (b) the agent of damage is essentially the <u>plastic</u> strain tensor $\underset{\sim}{\epsilon}^p$.

Direction Damage.

Addressing the case of directed damage first, it follows that

$$Q_{rs}^\phi = - \frac{\partial \psi_p}{\partial \phi_{rs}} = A_2 p_{ri} p_{sj} \phi_{ij} \tag{3.4}$$

The fact that significant damage begins to occur at the onset of the saturated plastic state, means that $\underset{\sim}{p}^r$ would be near saturation where the condition of $dp^r/dz = 0$ would be satisfied closely, if not exactly.

The result of that idealization, in conjunction with Eq. (2.48) and the fact that $\Lambda_1 = 0$, is that during damage,

$$\Lambda_2 p_{ij}^r = d\epsilon_{ij}^p / dz \tag{3.4a}$$

Insertion of this equation in Eq. (3.1) gives the relation:

$$Q^{\phi}_{rs} = A_2 \frac{d\epsilon^{p}_{ri}}{dz} \frac{d\epsilon^{p}_{sj}}{dz} \phi_{ij} \tag{3.4b}$$

The actual evolution equation is Eq. (3.3a), i.e.,

$$d\phi_r = - k \left[Q^{(r)}_{\phi} \right]^m d\xi^r \tag{3.5}$$

where

$$Q^{(r)}_{\phi} = Q^{\phi}_{ij} n^{(r)}_i n^{(r)}_j \tag{3.5a}$$

If we now make use of Eq. (3.3) in Eq. (3.5),

$$Q^{(r)}_{\phi} = A_2 \frac{d\epsilon^{p}_{ki}}{dz} \frac{d\epsilon^{p}_{\ell j}}{dz} \phi_{k\ell} \, n^{(r)}_i n^{(r)}_j \tag{3.6}$$

At this point we note that $n^{(r)}_i$ are the eigenvectors (orthogonal) of $d\underset{\sim}{\epsilon}^p$. This fact reduces Eq. (3.6) to the form:

$$Q^{(r)}_{\phi} = \frac{d\epsilon^r_p}{dz} \frac{d\epsilon^r_p}{dz} \, n^r_\kappa n^r_\ell \phi_{\kappa\ell} \qquad \text{(r not summed)} \tag{3.7}$$

At this point we note that, whenever Eq. (3.5) applies, i.e., condition (2.39) is satisfied,

$$d\epsilon^r_p \approx d\xi^r \tag{3.8}$$

and

$$\phi^{(r)}_n = \phi_{\kappa\ell} n^{(r)}_\kappa n^{(r)}_\ell \tag{3.9}$$

i.e., $\phi^{(r)}_n$ is the normal projection of $\underset{\sim}{\phi}$ in the direction $\vec{n}^{(r)}$. Hence if we let

$$k_r = k \left(\frac{d\xi^r}{dz} \right) \quad , \tag{3.10}$$

19

then evolution Eq. (3.4) becomes, simply,

$$d\phi_r = -k_r \left[Q_n^{(r)} \right]^m d\xi^r \qquad \text{(r not summed)} \qquad (3.11)$$

Isotropic Damage.

In a similar manner, since ψ_e is constant during damage:

$$Q^\omega = -\frac{\partial \psi_p}{\partial \omega} \qquad (3.12)$$

Terms in Eq. (3.3b) are now defined except for still the explicit coupling between $\underset{\sim}{Q}^\phi$ and $\underset{\sim}{Q}^\omega$ persists leading to complicated forms which are difficult to handle at this stage of theoretical and experimental development. For this reason we develop uncoupled equations from an idealization to the effect that $\underset{\sim}{\phi}$ is oblivious of ω and vice-versa, i.e., $\underset{\sim}{\phi} = \underset{\sim}{\delta}$. Hence $\underset{\sim}{Q}^\phi$ and $\underset{\sim}{Q}^\omega$ are now derived from the relations:

$$\underset{\sim}{Q}^\phi = -\left. \frac{\partial \psi_p}{\partial \underset{\sim}{\phi}} \right|_{\omega=1} \qquad (3.12a)$$

$$Q^\omega = -\left. \frac{\partial \psi_p}{\partial \omega} \right|_{\underset{\sim}{\phi}=\underset{\sim}{\delta}} \qquad (3.12b)$$

The isotropic damage coordinate Ω.

Since to a good approximation the agent of damage (both $\underset{\sim}{\phi}$ and $\underset{\sim}{\omega}$) is the plastic strain tensor $\underset{\sim}{\epsilon}^P$, it follows that $d\Omega$ must be an isotropic function of the increment in plastic strain $d\underset{\sim}{\epsilon}^P$. The physically most appealing such function is the quadratic function. But such a function is the intrinsic line dz. Hence we set

$$d\Omega^2 = d\epsilon_{ij}^P d\epsilon_{ij}^P + a^2 \left(d\epsilon_{ii}^P \right)^2 \qquad (3.13)$$

Thus $d\Omega$ is a plastic path increment in the plastic strain space of the damage material.

This form of the theory of evolution of damage is now complete. We summarize below the relevant equations.

SUMMARY OF EQUATIONS

Directed Damage.

$$d\phi_2 = k_r \left(Q_\phi^r\right)^m d\xi^r \tag{3.14}$$

$$Q_\phi^r = n_i^r n_j^r Q_{ij}^\phi \qquad \text{(r not summed)} \tag{3.15}$$

$$d\xi^r = \begin{cases} d\epsilon_p^r; d\underset{\sim}{\epsilon}_o^{rp} > 0, \ \epsilon_p^r > 0, \ Q_\phi^r > 0 \\ 0; \ \text{otherwise} \end{cases} \tag{3.16}$$

$$\epsilon_n^{rp} = n_i^r n_j^r \ \epsilon_{ij}^p \qquad \text{(r not summed)} \tag{3.17}$$

$$d\phi_r = \text{eigenvalues of } d\underset{\sim}{\phi}$$

$$d\epsilon_p^r = \text{eigenvalues of } d\underset{\sim}{\epsilon}^p$$

$$n_i^r = \text{eigenvectors of } d\underset{\sim}{\epsilon}^p$$

$$k_r = k_1 \left(\frac{d\xi^r}{dz}\right) \tag{3.18}$$

$$\underset{\sim}{Q}^\phi = - \left.\frac{\partial \psi_p}{\partial \underset{\sim}{\phi}}\right|_{\omega=1} \tag{3.19}$$

Isotropic Damage.

$$d\omega = k_o \left(Q^\omega\right)^n dz \quad , \quad Q^\omega > 0 \tag{3.18}$$

$$Q^\omega = - \left.\frac{\partial \psi_p}{\partial \omega}\right|_{\underset{\sim}{\phi}=\delta} \tag{3.19}$$

21

Discussion.

The foregoing work on damage evolution was developed quite late in the life of the present project and therefore could not play a role in the theoretical treatment of the experiments. A simpler theory of damage evolution developed previously by Valanis (1987) was actually used. We felt, however, that, for completeness, the above theory is of sufficient moment and depth to merit inclusion in the report. Moreover, its inclusion invites two points of discussion:

(i)   It demonstrated that the equation of evolution of damage is not a trivial matter and a significant amount of experimentation is necessary for its full understanding -- particularly in the presence of complex strain paths.

(ii)   It points to possible directions for future research in the theory of evolution of damage.

A Simpler Theory of Damage Evolution.

A simpler evolution equation for both directed and scalar (isotropic) damage was developed earlier by Valanis (1987) and was used in applications to elastic materials. Though the results showed the right qualitative trends the lack of experimental data prevented any precise conclusions as to its suitability. The experimental data reported in Part I of this report showed that the proposed form was inclined to overestimate damage in regions of low strain intensity. For this reason a more suitable equation was developed. The earlier work on the simpler theory is appended to the report. See Appendix A.

The case in plastic materials, however, is different in the sense that damage is more widely distributed around areas of geometric discontinuities. Thus we expect that the simpler theory may be better suited for concrete as opposed to brittle solids such as cast iron or glass. Here we shall be dealing with the simpler theory in the *uncoupled form*.

The Case of Directed Damage.

The evolution equation is the following:

22

$$d\phi_r = \begin{cases} -k\left(\phi_r\right)^m d\xi_r; & d\epsilon_r^n > 0, \ \epsilon_1 > 0 \\ \\ 0; & \text{otherwise} \end{cases} \qquad (3.20)$$

$$d\xi_r = \left|d\epsilon_r\right| \qquad (3.21)$$

$$\phi_r^n = \phi_{ij} n_i^r n_j^r \quad \text{(r not summed)} \qquad (3.22)$$

$$\epsilon_r^n = \epsilon_{ij} n_i^r n_j^r \qquad \text{(r not summed)} \qquad (3.23)$$

k_1, m : material constants

The Case of Isotropic Damage.

$$d\omega = -k_\omega \omega^n \ d\Omega \qquad (3.24)$$

where Ω is the isotropic damage coordinate and k_ω and n are material constants. The nature and definition of Ω are discussed in Section 4.

4. THE CONSTITUTIVE RESPONSE UNDER AXIAL COMPRESSION.

The Lateral Strain Response.

The lateral expansion of plane concrete of low strength ($\sim 2 \times 10^3$ psi) was measured in the course of an axial compression test as described in APPENDIX B on the experimental program. Low strength concrete brought the tests within the capacity of the testing machine and obviated the danger of sudden and catastrophic splintering of the specimens associated with highly brittle fracture. This was of concern to the personnel making the lateral strain measurements.

We begin with a descriptive account of the nature of the lateral expansion of concrete under axial compression. During the beginning stages of the test when the compressive stress was small, the observed lateral expansion was negligible and hardly measurable with a displacement gauge of sensitivity of $1'' \times 10^{-4}$. During this stage of the test damage was minimal (non-observable) i . . s of visible microcracks on the specimen surface. The Poisson ratio could not be measured accurately at this stage but appeared to be of the order of 0.05.

As the axial stress was increased visible damage in terms of small micro-cracks began to appear in the specimen surface while simultaneously the lateral strain began to increase and eventually became of the same order as the axial strain. This coincided with an attainment of maximum compressive stress on the axial stress strain diagram.

Further increase in the compressive strain beyond the point of maximum stress began to cause substantial damage in the form of long vertical cracks running along the length of the specimen. This coincided with a substantial drop in the compressive stress. This region of strain is known in the literature as the "softening" region. As the axial strain was increased further into the softening region the lateral strain increased dramatically and became large, of the order of three to four times that of the axial strain.

> Thus excessive lateral expansion in the course of axial compression
> is directly related to the occurrence of substantial of damage.

The test was terminated when damage was so severe that, with further damage, the specimen could no longer be regarded as a continuous medium.

To proceed with the theoretical prediction of the observed lateral strain we first note that the elastic response in the presence of damage is given by Eqs. (4.1) and (4.2) which parallel equations (2.55) and (2.56) and can be obtained from these by setting $E(z) = $ constant. Thus

$$\frac{1}{\phi^2} \sigma_1 = \phi_1^2 E_e \epsilon_1^e \tag{4.1}$$

$$\phi_2 \epsilon_2^e = - \nu \phi_1 \epsilon_1^e \tag{4.2}$$

where ν is a constant in both the elastic and plastic response as discussed previously. In view of Eqs. (2.56) and (4.2)

$$\phi_2 \epsilon_2 = - \nu \phi_1 \epsilon_1 \tag{4.3}$$

Because the axial strain ϵ_1 is compressive $\phi_1 = 1$. Thus the relation of the lateral to the axial strain is given by Eq. (4.4):

$$\phi_2 \epsilon_2 = - \nu \, \epsilon_1 \tag{4.4}$$

For the purpose of probing the micromechanical implications of the integrity tensor ϕ (in this case ϕ_2) a series of tests was carried out whereby specimens with a square cross-section were tested in axial compression -- with different initial plane "through" cracks (or slots) of rectangular area each parallel to one longitudinal side of the specimen. Three different cracks were used each of length of 1 in., 2 in., and 3 in., respectively. See Appendix B for details.

The question that we posed is whether the presence of these cracks constitutes damage in which case ϕ_2 would be different from unity at the beginning of the test. If that were the case then the relation between ϵ_1 and ϵ_2 would be different in each case and would be <u>correlated</u> with the initial length of the corresponding crack.

Figure 4.1 shows that no such correlation exists. One of two possibilities presents itself: either the cracks do not constitute damage for the stress history in question, or the material constants are such that the effect of the initial cracks is concealed. Of course both the above are possible.
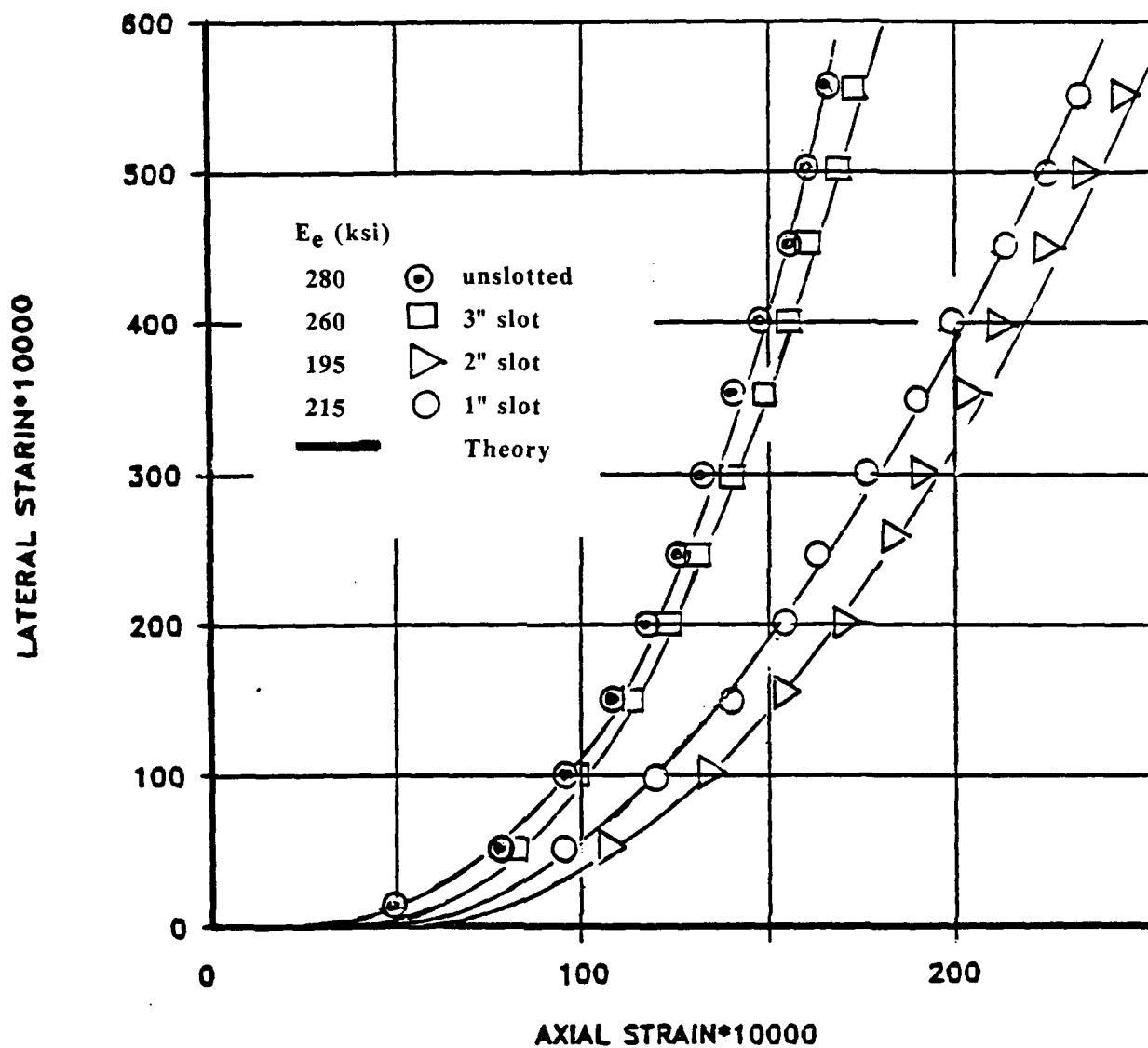
25

Figure 4.1. Lateral response of concrete in axial compression.

On the other hand there is an <u>excellent</u> correlation between the initial elastic modulus of the specimens and the lateral strain attained in the course of the experiment, assuming that the initial cracks have no effect. Specifically "stiffer" specimens expanded laterally faster than their less stiff counterparts. Thus there is an excellent correlation between the value of the initial elastic modulus and the extent of the lateral expansion in the course of damage. This observation is consistent with the degree of damage observed -- in terms of the loss of strength following the attainment of maximum stress during compression. The rate of softening --- i.e., degradation -- was faster for the stiffer specimens.

Thus we conclude that the damage rate constant k_ϕ is a monotonically increasing function of the initial elastic modulus. In fact we found the relation

$$k_\phi = k_o \left(sinh\beta E_e \right)^{m-2}$$
(4.5)

where k is the damage constant in the damage evolution Eq. (4.6) and k_o, β and m are material parameters.

The Damage Evolution Equation.

For reasons which were discussed earlier in Section 3, we chose the damage evolution equation (4.6) which was originally proposed by Valanis (1986). Thus

$$d\phi_2 = - k_\phi \phi^m_2 d\epsilon_2$$
(4.6)

where k_ϕ and m are material parameters. Since ϵ_2 is a monotonically increasing function of ϵ_1, the parameter m must satisfy the inequality m > 1 as can be seen directly from Eq. (4.7) (see Valanis (1986), Appendix A). Integration of Eq. (4.6) in the light of an initial value ϕ_{20} gives the result:

$$\phi_2 = \left\{ \phi^{1-m}_{20} + k_\phi (m - 1) |\epsilon_2| \right\}^{- \frac{1}{m-1}}$$
(4.7)

We propose this equation as the basis for the prediction of the observed results shown in Fig. 6.1, where axial and lateral strains are shown in units of 10^{-4}. As previously we shall use 10^{-4} as the unit of strain. We note that since ϵ_2 does not correlate with ϕ_{20} then k must be a large number, if ϕ_{20} is of order of unity. This turned out to be the case. Equation (4.7) then reduces to the form:

$$\phi_2 = \left\{ k_\phi (m - 1) |\epsilon_2| \right\}^{-\frac{1}{m-1}} \qquad (4.8)$$

which is approximate but represents the real situation closely. Equation (4.8) in conjunction with Eq. (4.3) gives the following expression relating $\epsilon 2$ to ϵ_1:

$$|\epsilon_2| = [k_\phi (m - 1)]^{\frac{1}{m-2}} \; \nu^{\frac{m-1}{m-2}} \left(\epsilon_1\right)^{\frac{m-1}{m-2}} \qquad (4.9)$$

or,

$$|\epsilon_2| = c \; \epsilon_1^{m'} \qquad (4.10)$$

where

$$c = [k_\phi (m - 1)]^{\frac{1}{m-2}} \; \nu^{\frac{m-1}{m-2}} \qquad (4.10a)$$

$$m' = \frac{m - 1}{m - 2} \qquad (4.10b)$$

Equation (4.10) was found to describe the experimental data of Fig. 4.1 in excellent fashion and a relation between c and E_e was thereby found and shown in Figure 4.2. The analytical representation of this relation is given by Eq. (4.11):

$$c = c_o \sinh \beta \; E_e \qquad (4.11)$$

where $c_o = 2.2 \times 10^{-6}$ and $\beta = 1.310 \times 10^{-6}$.

Thus

$$k_\phi = k_o \left(\sinh \beta \, E_e \right)^{m-2} \tag{4.12}$$

where

$$k_o = \frac{1}{(m-1)\nu^{(m-1)}} \, c_o^{m-2} \tag{4.13a}$$

and

$$m = 2.36 \tag{4.13b}$$

Discussion And Conclusions.

The experiments on plane concrete in conjunction with the theory of damage developed herewith lead us to the following conclusions:

The damage induced by vertical cracks in concrete specimens in axial (vertical) compression:

(i)   Does not have an effect on the axial stress-strain relation in accordance with the predictions of the theory.

(ii)   Initial damage in the form of vertical cracks, is either negligible or the material constants are such that the lateral strain response is unaffected by its presence.

(iii)   The theory predicts the lateral strain response due to axial compression in excellent fashion and in so doing establishes an important relation between the initial elastic modulus and the rate of directed damage. Specifically the higher the initial modulus the higher the rate of damage. It is significant to note that in elastic-fracturing solids failure is immediate with an ideally infinite rate of damage.

The Axial Stress-Strain Response.

Commonly, the axial compression test is treated as a one-dimensional problem in terms of an axial stress-strain relation. However while the stress tensor has only one non-vanishing diagonal component the strain tensor has three such non-vanishing

29

components. In fact the lateral strain response is in itself a difficult constitutive problem when damage in present -- as we have seen in the first part of this section.

To treat the axial stress-strain response we recall Eq. (2.55). In the light of the fact that the axial strain is compressive, $\phi_1 = 1$, this equation becomes

$$\sigma_1 = \omega^2 \int_0^z E(z - z') \frac{\partial \epsilon_1^p}{dz'} dz' \qquad (4.14)$$

Since in this test the hydrostatic pressure is small and to keep analytical complications to a minimum, we set $F = 1$ in Eq. (2.45) so that

$$dz^2 = d\varsigma^2 = \kappa^2 \left(\phi_{\kappa\ell} d\epsilon_{k\ell}^p \right)^2 + \phi_{ir}\phi_{js} d\epsilon_{ij}^p d\epsilon_{rs}^p \qquad (4.15)$$

In the theory of endochronic plasticity the value of κ is important in shear-volumetric interactions relating to densification or dilatancy. Since no such effects are present here its effect is not critical and its value is therefore set equal to zero. Thus in the case of the axial test Eq. (4.15) becomes

$$dz = d\varsigma = \left(d\epsilon_1^p \right)^2 + 2 \left(\phi_2 d\epsilon_2^p \right)^2 \qquad (4.16)$$

again because $\phi_1 = 1$.

It may be seen from Eq. (4.16) that to calculate the axial stress response from Eq. (4.14) one must know ϕ_2 and ϵ_2^p as a function of ϵ_1^p. To find this functional relation we recall Eqs. (2.56) and (4.2) from which it follows that

$$\frac{\epsilon_2^p}{\epsilon_1^p} = \frac{\epsilon_2^e}{\epsilon_1^e} = \frac{\epsilon_2 - \epsilon_2^p}{\epsilon_1^e} \qquad (4.17)$$

Thus:

$$\epsilon_2^p = \frac{\epsilon_2\left(\dfrac{\epsilon_1^p}{\epsilon_1^e}\right)}{1 + \left(\dfrac{\epsilon_1^p}{\epsilon_1^e}\right)} \qquad (4.18)$$

We are interested in the stress response in the damage region in which ϵ_1^e is substantially constant and equal to its value at the peak stress. Thus ϵ_2^p can be found from the measured strains shown in Figure 4.1.

We suspect however that the term $\left(\phi_2 d\epsilon_2^p\right)^2$ is to be small relative to $\left(d\epsilon_1^p\right)^2$ or $\phi_2^2\left(d\epsilon_2^p/d\epsilon_1^p\right)^2$ to be small relative to unity and numerical computations proved that to be the case. Thus for our purposes, during the axial test

$$dz = d\zeta = \left|d\epsilon_1^p\right| \qquad (4.19)$$

which would have been the result had one regarded the axial test as a one-dimensional problem -- which it is not. Equation (4.14) now simplifies and becomes

$$\sigma_1 = \omega^2 M\left(\epsilon_1^p\right) \qquad (4.20)$$

where

$$M\left(\epsilon_1^p\right) = \int_0^{\epsilon_1^p} E(z)\,dz' \qquad (4.21)$$

Thus to find the experimentally measured stress-strain response in compression as depicted in Fig. 4.2 one needs the memory function $E(z)$ and the scalar damage function ω.

The Measured Axial Stress-Strain Response.

The measured stress-strain response during axial compression is shown in Figure 4.2. Damage in the course of the test was minimal prior to attainment of maximum stress and became visible in terms of small vertical cracks just prior
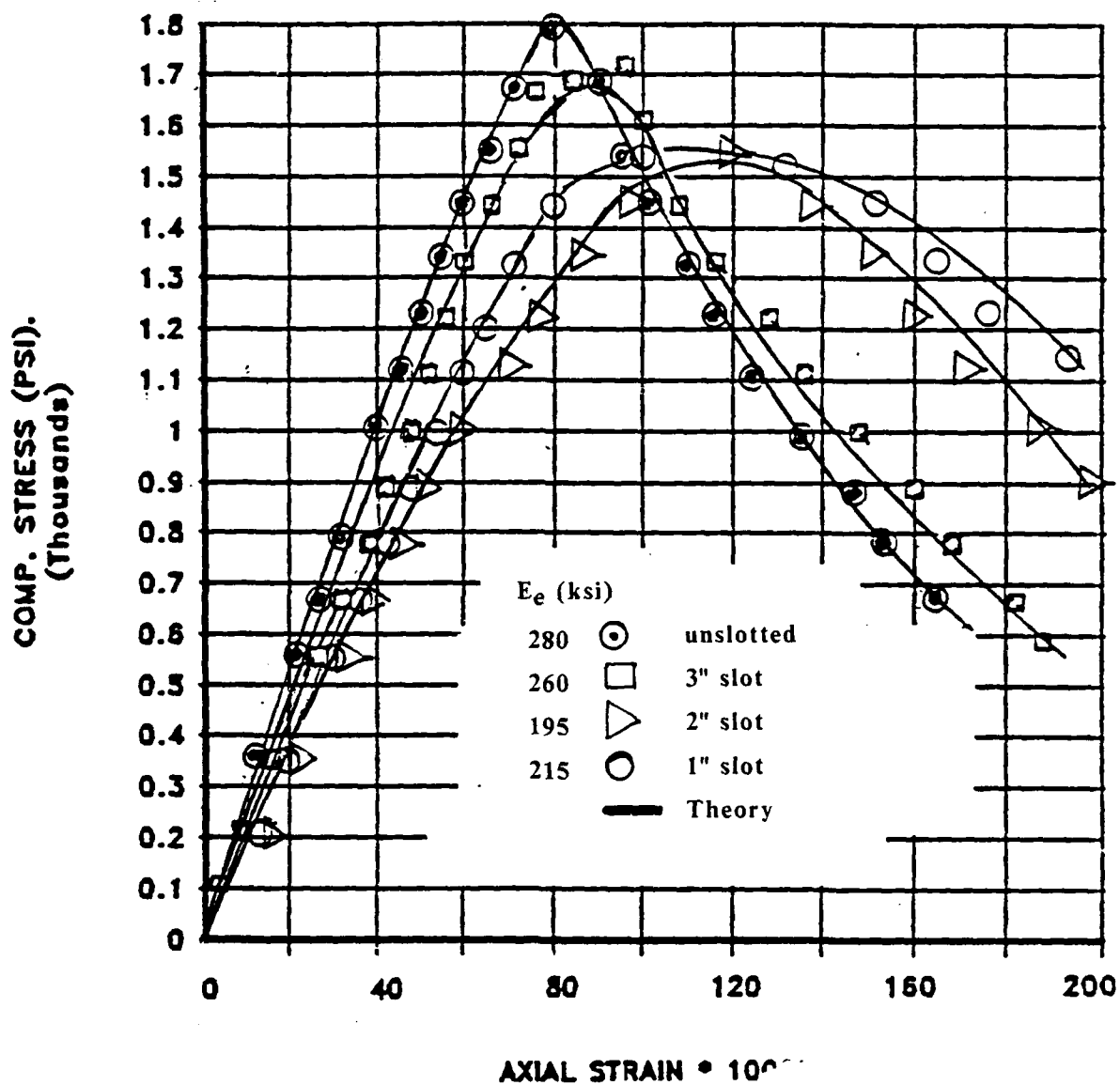
Figure 4.2   Axial stress-strain curve in concrete in axial compression.

32

to the appearance of the peak stress. Substantial damage in the form of visible vertical cracks began to appear following straining beyond the peak stress and into the softening region.

An important feature of the stress-strain curves of Figure 4.2 is the absence of any correlation between the initial and subsequent directional damage in terms of the vertical cracks, and the measured stress response. This is of course the prediction of the theory in accordance with Eqs. (4.10) and (4.20). Thus in this sense, the theory is upheld by experiment.

Furthermore, just as in the case of the lateral strain response, we see that the rate of damage -- in terms of stress diminution in the damage region -- is an increasing function of the initial elastic modulus. Thus the observed scatter is only apparent and can be explained on the basis of the dependence of the rate of damage on the initial elastic modulus.

Observed Response in the Context of the Damage Theory.

To put the observed data of Fig. 4.2 in an analytical context we took the following position:

(i) The plastic response of the undamaged state is the same for all specimens.

(ii) The rate of degradation (damage) is an increasing function of the initial elastic modulus. This was the case in the lateral strain response.

We note from Eq. (4.20) that $M(\epsilon_1^p)$ is $\sigma_1(\epsilon^p)|_{\omega=1}$, i.e., the stress response in the absence of scalar damage. For convenience, we take this to be the extrapolation of the stress-strain curve (prior to damage) of the specimen with the maximum initial elastic modulus. This is shown as the dotted curve in Fig. 4.3a. We adopt the endochronic representation of this curve by the functional relation

$$\sigma_1 = \sigma_0 \left(\epsilon_1^p \right)^{1-\alpha} \tag{4.22}$$

where α is close to unity. In this case the presumed plastic stress-strain curve of the undamaged state is given by Eq. (4.22) with $\alpha = 0.92$ and $\sigma_0 = 1.47$ ksi, where the unit of strain, as before, is 10^{-4}. The plastic response in the undamaged state is then calculated for the other specimens and is shown by dotted lines in same figure.
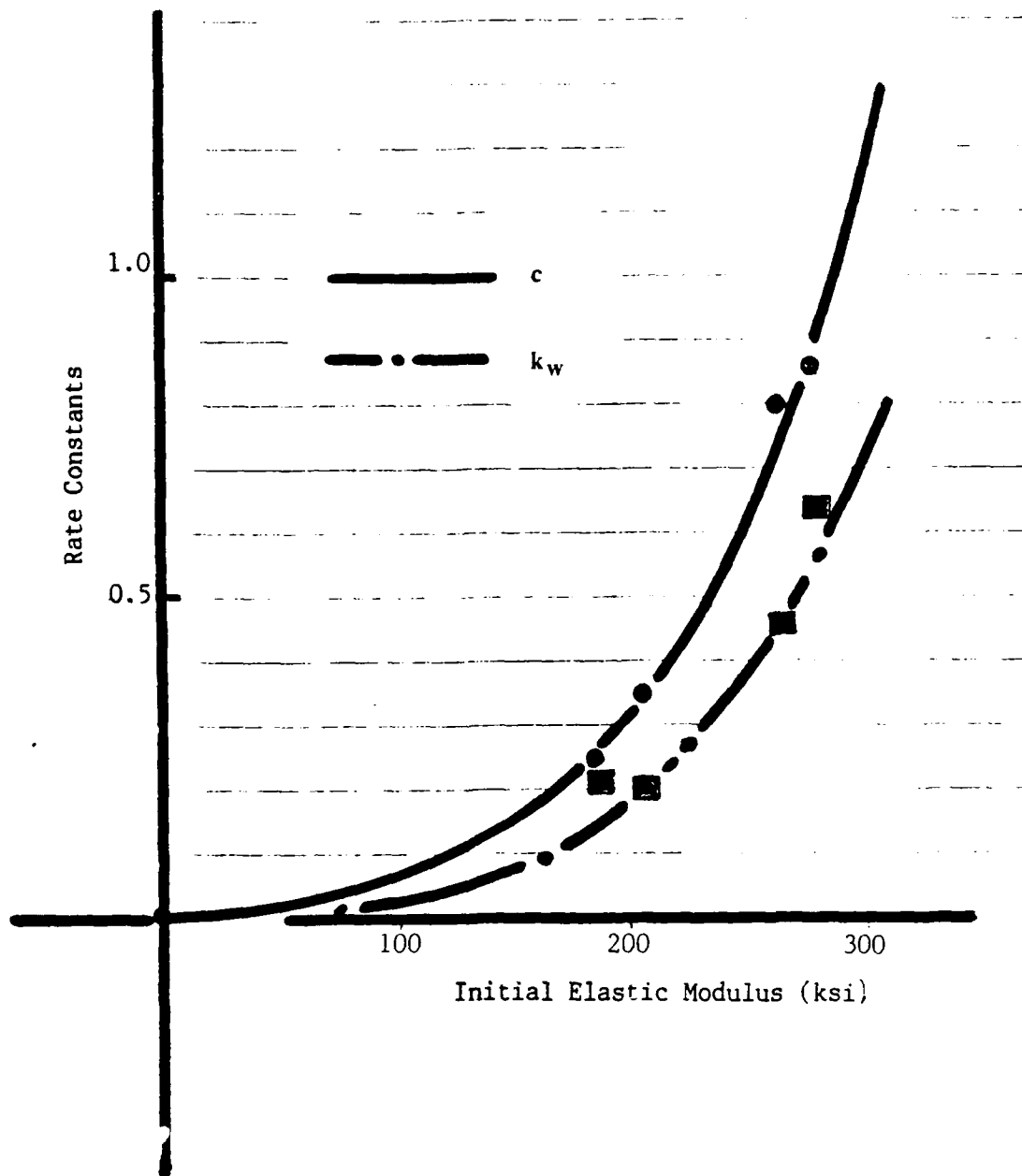
33

Figure 4.3   Effect of initial elastic modulus on the directional and isotropic damage rate constants.
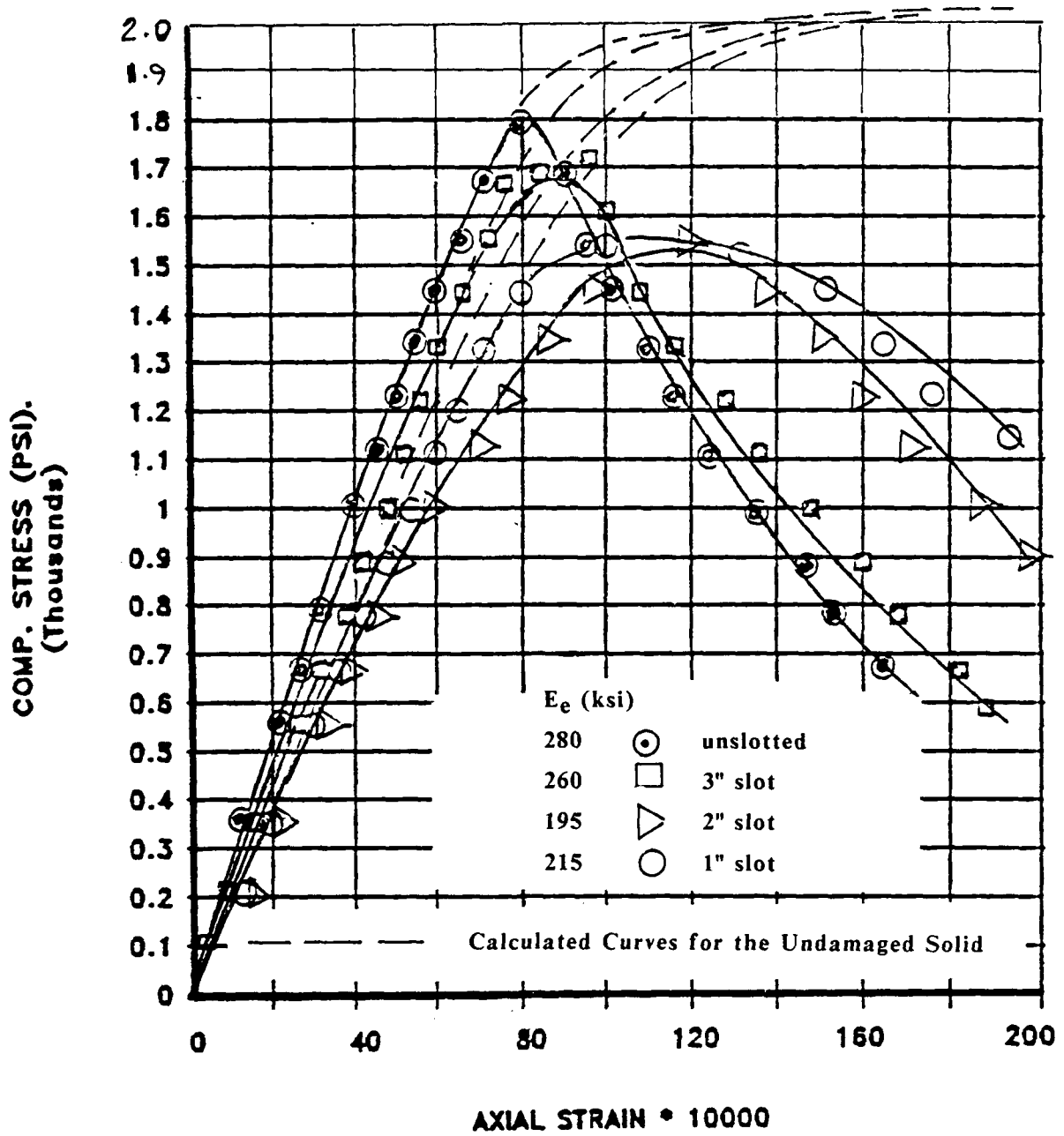
34

Figure 4.3a Calculated curves for undamaged solids.

35

The Evolution Equation of Isotropic Damage.

Just as in the case of directed damage where we follow the theory developed by Valanis (1987). Thus the isotropic damage evolution equation is given by Eq. (3.22):

$$dw = - k_w w^n \, d\Omega \tag{4.23}$$

where Ω is the isotropic damage coordinate. We point out a difference between the present notation and that used previously in the reference cited above. There, the isotropic damage coordinate was denoted by ς and the symbol Ω played a different role. We reason that since w has no directionality it is most likely to be be associated with the plastic state of a material in which case $d\Omega$ must be related to a "plastic" strain increment. After a great deal of search for the __right__ definition of the "plastic" strain as the agent of w we found that the plastic strain of the undamaged state was the most appropriate candidate. The physics of this conclusion is that the damage due to brittle fracture does not affect the evolution of isotropic damage. Thus we define $\underset{\sim}{\epsilon}^w$ as:

$$d\underset{\sim}{\epsilon}^w = d\underset{\sim}{\epsilon} - \underset{\sim}{\Lambda} \, d\underset{\sim}{\sigma}^U \tag{4.24}$$

where $d\underset{\sim}{\epsilon}^w$ is the "plastic" strain increment which is the cause of isotropic damage, Λ is the elastic compliance of the undamaged state, and $\underset{\sim}{\sigma}^U$ is obtained from Eq. (2.53) by setting $\underset{\sim}{\phi} = \underset{\sim}{\delta}$ and $w = 1$. Furthermore since we are dealing with isotropic damage, it is natural to set $d\Omega^2$ as a quadratic isotropic function of $d\epsilon_{ij}^w$. Thus:

$$d\Omega^2 = \kappa_w^2 \left(d\epsilon_{ii}^w \right)^2 + d\epsilon_{ij}^w \, d\epsilon_{ij}^w \tag{4.25}$$

where κ_w is a material parameter. In the case of simple compression which will be considered in Section 4, we set

$$d\epsilon^w = d\epsilon - \frac{d\sigma^U}{E_e} \tag{4.26}$$

$$d\Omega = \left| d\epsilon^w \right| \tag{4.27}$$

within an immaterial constant insofar as Eq. (4.27) is concerned.

36

Comparison of Theory with Experiment.

We found that Eq. (4.23) with n = 1 was appropriate for describing the isotropic damage of plane concrete under compression. The measured response shown in Fig. 4.2 was used to determine experimentally the relation between w and Ω using the definition of $d\Omega$ given by Eqs. (4.26) and (4.27). This is shown in Fig. 4.4. As pointed out above, the relations between w and Ω (for various values of the initial elastic modulus) satisfy Eq. (4.23), with n = 1. Integration of Eq. (4.23) in the light of the initial condition $w(0) = 1$, gives the relation

$$w = e^{-k_w \Omega} \tag{4.28}$$

It is quite apparent that the damage rate constant k_w is a function of the initial modulus E_e and the appropriate functional relationship is shown in Figure 4.3

On the basis of these findings the theoretically depicted response is shown in Fig. 4.2. As may be seen a good agreement between theory and experiment has been achieved. While the theoretical analysis is not totally predictive it does provide a consistent conceptual framework for the interpretation of the experimental findings.

Discussion and Conclusions.

A theoretical development in the form of Theory II in Part II of this report led to a constitutive formulation for concrete in the presence of damage -- in conjunction with two evolution equations each motivated by two different physical considerations: one relating to thermodynamics and the other to the physics of annihilation of species. In the analysis the second evolution equation was used because of its simplicity and the fact that it lends itself more easily to numerical computations.

The constitutive relation in question, i.e., Eq. (2.53) and specifically, its one-dimensional counterparts, Eqs. (2.55) and (2.56), were put to the test by comparison with experimental data on concrete under axial compression. The results of the comparison of the theory with experiment were the following:

(i)   <u>Both directional and isotropic damage are necessary to explain the behavior of concrete under compression.</u>
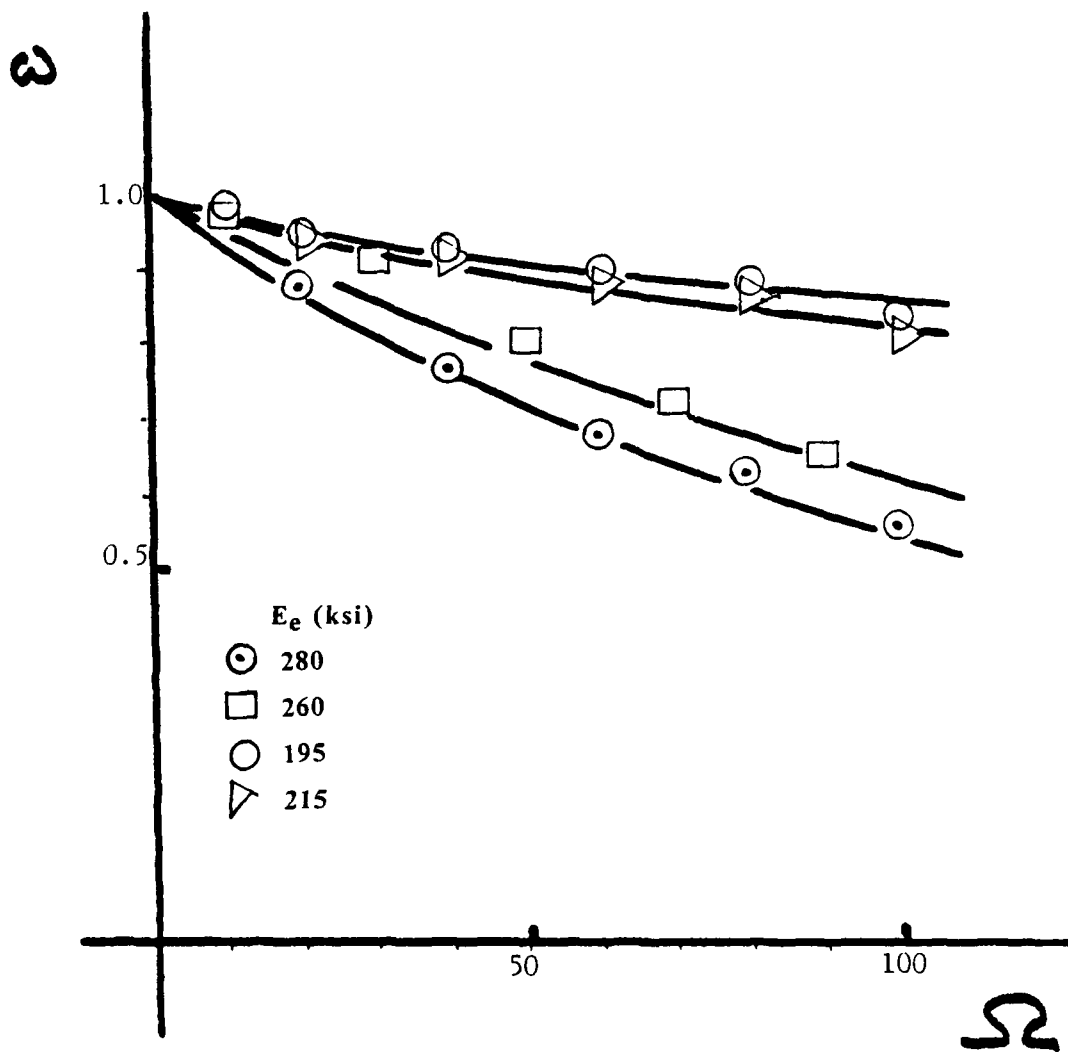
37

Figure 4.4   Effect of initial elastic modulus on rate of scalar degradation.

This is in contrast to the case of axial tension where isotropic damage is present, yet its inclusion in the constitutive behavior is not necessary to explain experimentally observed phenomena which can be modeled by directional damage alone (see Valanis and Read, 1989).

(ii)   The theoretical prediction, that the stress-strain response is unaffected by directional damage but depends significantly on isotropic damage, was upheld by the experiments.

(iii)   The parallel theoretical prediction that the lateral strain response -- with excessive lateral expansion developing progressively with damage -- does not depend on the isotropic damage but is governed by the directional damage is also upheld by experiment.

(iv)   The "simpler" form of the damage evolution equation, associated with species annihilation, gives good agreement with experiment but this result is limited to observations associated with macroscopically homogeneous deformation (and an axial loading history) and further experiments associated with strain gradient fields are necessary to verify its range of applicability.

(v)   The micromechanical experiments in terms of initial vertical cracks designed to determine ϕ in terms of crack geometry (by measuring the lateral response during axial compression) did not help in this instance to establish such a relation because the material damage rate constant was such that its magnitude concealed the effect of the initial cracks in the lateral strain response. Further experiments in this regard are indicated.

(vi)   The micromechanical question regarding the geometric relation between microdamage and ϕ as well as ω is still open. We believe that establishing such a relation will depend a great deal on the correct form of the damage evolution equation which must be corroborated by experiments with heterogeneous strain fields.

REFERENCES

Scavuzzo, R., T. Stankowski, J. H. Gerstle and H. Y. Ko, (1984), "Stress-strain Curves for Concrete under Multiaxial Load Histories," CEAE Dept., Un. of Colorado, Boulder.

Diamond, S., and A. Bentur, (1984), "On the Cracking in Concrete and Fiber-Reinforced Cements," in Application of Fracture Mechanics to Cementitious Composites, NATO Advanced Research Workshop, Ed., S. P. Shah, Northwestern University.

Gopalaratnam. V. S., and S. P. Shah, (1985), "Softening Response of Plane Concrete in Direct Tension," ACI Journal, May-June, 310.

Valanis, K. C., and H. E. Read, (1986), "An Endochronic Plasticity Theory for Concrete," Mech. of Materials, 5, 277-295.

Hegemier, G. A., H. E. Read, K. C. Valanis and H. Murakami, (1987), "Development of Advanced Constitutive Models for Plain and Reinforced Concrete," S-CUBED, La Jolla, CA., Final Report to AFOSR, SSS-R-87-8454.

Valanis, K. C., (1987), "A New Continuous Damage Model for Concrete," Appendix A in "Development of ADvanced Constitutive Models for Plane and Reinforced Concrete," Hegemier, G. A., et al., S-CUBED, La Jolla, CA., Report SSS-R-87-8454.

Valanis, K. C., "1988) "A Theory of Damage of Brittle and Semibrittle Materials," Endochronics, Inc.,/AFOSR Report ENDIC 005-AFOSR-1988.

Valanis, K. C., (1989a), "A Theory of Damage in Brittle Materials," Eng. Fracture Mech. (to appear).

Valanis, K. C., (1989b), "Continuum Modeling of Damage due to Sharp Cracks," Proceedings, PLASTICITY 89: The Second Symposium on Plasticity and Its Current Applications, Mie University, Tsu, Japan.

Valanis, K. C., (1989c), "Finite Plasticity in the Context of the Endochronic Theory," Proceedings, International Conference on Constitutive Laws for Engineering Materials, Congqing Univ., Congqing, China

Valanis, K. C., and J. Peters, (1989), "An Endochronic Plasticity Theory with Shear-Volumetric Coupling," *Int. J. For Num. and Anal. Meth. in Geomech.* (to appear).

Valanis, K. C., and H. E. Read, (1989), "An Internal Variable Theory for Plastic Fracturing Solids," *Intl. J. for Num. and Analyst. Meth. in Geomechanics* (Submitted).

APPENDIX A

NEW CONTINUOUS DAMAGE MODEL FOR CONCRETE

A.1 INTRODUCTION.

The purpose of this appendix is to describe, in detail, a damage-cracking model that has been developed under the present program. The model was formulated by Valanis (1985) and is presently under development. The discussion given below largely follows that given by Valanis (1985) but does not reflect various topics that are presently under study, which include (a) the addition of plasticity, (b) size effects and (c) strain rate dependence.

A.2 FORMULATION OF MODEL.

Consider a linearly elastic material which is isotropic in its virgin unstrained state and undergoes small deformation at isothermal conditions. As the deformation proceeds, damage gradually develops, which in turn reduces the material integrity. For sufficiently large deformation, the accumulated damage can lead to complete fracture, in which the material cannot support tensile stress in a direction normal to the damage. We shall formulate this damage-cracking process within the context of irreversible thermodynamics and, for this purpose, we introduce the free energy ψ per unit volume.* Since fracture leads to a reduction in material integrity, we introduce an integrity tensor ϕ which will be discussed at length later and which is symmetrical such that $\phi = \delta$ (the unit tensor), when the material is in its virgin (undamaged) state, and $\phi = 0$ when the material has fully failed, i.e., when the material cannot support stress in any direction. We thus set:

$$\psi = \psi(\varepsilon, \phi) \tag{A-1}$$

where ε denotes the strain tensor. In a thermodynamic sense, ϕ now plays the role of an internal variable, in which case we can write the following relations:

$$\sigma = \frac{\partial \psi}{\partial \varepsilon} \quad , \quad g = -\frac{\partial \psi}{\partial \phi} \tag{A-2}$$

---

* This nomenclature is preferred to free energy density, in view of the concept of "irreducible" material volume which must be introduced when dealing with heterogeneous multi-phase materials, such as plain concrete.

where σ is the stress tensor and g denotes the internal force, dual to ϕ which is driving the fracturing process.

In view of the definition of ϕ, the following relations must hold:

$$\psi(\xi, Q) = 0 \quad , \quad \psi(Q, \phi) = 0 \quad , \tag{A-3}$$

the first meaning that a fully failed material cannot contain free energy and the second that an unstrained material must have zero free energy: both conditions are relative to the reference state. Furthermore, the following conditions must also hold:

$$\sigma(\xi, Q) = Q \quad , \quad \sigma(Q, \phi) = Q \tag{A-4}$$

$$g(\xi, Q) = Q \tag{A-5}$$

Equations (A-4) require that the stress vanish in the fully failed material and that, since the material remains elastic in the damaged state, the stress will vanish at zero strain. Equation (3.5) stipulates that the internal fracture causing force g must vanish in the fully failed material.

If we now expand ψ in a Taylor series in ξ, retain terms no higher than the quadratic, and observe relations (3.3), we obtain the following form of ψ:

$$\psi = C_{ijk\ell} \epsilon_{ij} \epsilon_{k\ell} \tag{A-6}$$

where $C = C(\phi)$. It is further assumed that C depends upon ϕ in a purely quadratic manner. Since the material is assumed to be isotropic in its virgin state, C may be represented in terms of outer products of the unit tensor δ and ϕ. Furthermore, since C is purely quadratic in ϕ, it has no other representation than

$$C_{ijk\ell} = \lambda \, \phi_{ij}\phi_{k\ell} + 2\mu \, \phi_{ik}\phi_{j\ell}, \tag{A-7}$$

in view of the symmetries imposed upon it by the symmetry of ξ implied in Eq. (A-6). The constants λ and 2μ in Eq. (A-7) must indeed by the Lame constants of the virgin material, since

---

* This assumption has recently been verified by Valanis (1987), using a non-thermodynamic approach involving a mapping from undamaged to damaged material.

A-2

$$C_{ijk\ell} = \lambda\, \delta_{ij}\delta_{k\ell} + 2\mu\delta_{ik}\delta_{j\ell} \tag{A-8}$$

when $\phi = \delta$. Thus, we can write

$$\Psi = \frac{1}{2}\lambda(\phi_{ij}\epsilon_{ij})^2 + \mu\,\phi_{ik}\phi_{j\ell}\epsilon_{ij}\epsilon_{k\ell} \quad, \tag{A-9}$$

so that, in view of Eq. (A-2a), σ us given by the expression:

$$\sigma_{ij} = \lambda\,\phi_{ij}\phi_{k\ell}\epsilon_{k\ell} + 2\mu\,\phi_{ik}\phi_{j\ell}\epsilon_{k\ell} \tag{A-10}$$

This equation defines the constitutive response of an elastic fracturing material, once we establish how the integrity tensor ϕ is related to the fracturing process. In particular, an equation is needed which describes the manner in which ϕ evolves with accumulated damage, and this is considered below.

A.3 EVOLUTION EQUATION FOR ϕ(DIRECTED DAMAGE)·

When the material is not strain rate sensitive, an increment of tensile strain will produce an increment of damage. Specifically, given an increment in strain, $d\epsilon$, let $d\epsilon^\alpha$ be its eigenvalues and n_i^α its eigenvectors. If $d\epsilon$ and ϵ are coaxial, then $d\epsilon^\alpha$ will constitute an increase in tensile strain if $d\epsilon^\alpha > 0$ and $\epsilon^\alpha \geq 0$, where ϵ^α denote the eigenvalues of ϵ. In the more general case where $d\epsilon$ and ϵ are not co-axial, $d\epsilon^\alpha$ is said to be an increase in tensile strain if $d\epsilon^\alpha > 0$ and $\epsilon_{ij} n_i^\alpha n_j^\alpha \equiv \epsilon_\alpha^n \geq 0$ (α not summed). Now let $d\phi$ be the change in the integrity tensor ϕ due to the increment $d\epsilon$, and let n_ϕ^α be the eigenvectors of $d\phi$. We now specify that $d\phi$ and $d\epsilon$ are co-axial, so that

$$n_\phi^\alpha = n^\alpha \tag{A-11}$$

The physical significance of Eq. (A-11) is examined in the discussion following Eq. (A-14).

To completely characterize the evolution of ϕ, the relation between $d\phi^\alpha$ and $d\epsilon^\alpha$ needs to be specified. In this section, we consider a type of damage that is completely "directed", that is, it develops in a specific direction without being accompanied by non-directed (or isotropic) damage. This type of damage is the variety dealt with in linear elastic fracture mechanics (LEFM) and appears to typify that which occurs in single phase brittle materials. Later on in Section A.7, we shall consider the more general case in which the advancing damage consists of both

A-3

directed and non-directed (isotropic) components. Such damage is characteristic of multi-phase materials. such as plain concrete. as discussed by Diamond and Bentur (1984).

Restricting attention now to completely "directed" damage. we adopt the following expression relating $d\phi^\alpha$ and $d\epsilon^\alpha$:

$$d\phi^\alpha = - \left[\phi_n^\alpha\right]^m d\xi^\alpha \tag{A-12}$$

where

$$d\xi^\alpha = \begin{cases} kd\epsilon^\alpha \, , & \text{for } d\epsilon^\alpha > 0 \text{ and } \epsilon_n^\alpha \geq 0 \\ 0 \, , & \text{otherwise} \end{cases} \tag{A-13}$$

Here. k and m are positive constants. and $\phi_n^\alpha = \phi_{ij} n_i^\alpha n_j^\alpha$ (α not summed). The form of Eq. (A-12) has its basis in the physics of annihilation. but may be changed to provide a more realistic description of damage accumulation for a particular material.

In view of Eq. (A-11). we can therefore write

$$d\phi_{ij} = - \sum_\alpha \left[\phi_n^\alpha\right]^m n_i^\alpha n_j^\alpha \, d\xi_\alpha \tag{A-14}$$

With this evolution equation for ϕ. the constitutive description of the elastic fracturing solid is now complete. once the material parameters λ. μ. k and m have been specified.

Physical Interpretation of Equations

The physical meaning of the above equations. and their relation to the fracturing process. is best understood by reference to Eq. (A-10). which relates the stress tensor to the strain tensor. Let N^α be the eigenvectors of ϕ and let σ and ϵ be referred to a system of coordinates $\bar{X}_\alpha$. Then. the components of σ and ϵ on the $\bar{X}_\alpha$ coordinate system can be written as:

$$\bar{\sigma}_{rs} = \sigma_{ij} N_i^r N_j^s \tag{A-15}$$

$$\bar{\epsilon}_{rs} = \epsilon_{ij} N_i^r N_j^s \tag{A-16}$$

A-4

In this system of coordinates, ϕ is diagonal, i.e., $\bar{\phi}_{rs} = 0$ for $r \neq s$, and Eq. (A-10) takes the form:

$$\bar{\sigma}_{rs} = \lambda \, \bar{\phi}_{rs}\bar{\phi}_{mn}\bar{\epsilon}_{mn} + 2\mu \, \bar{\phi}_{rm}\bar{\phi}_{sn}\bar{\epsilon}_{mn} \tag{A-17}$$

Since $\bar{\phi}$ is diagonal, we can write:

$$\bar{\sigma}_{11} = \lambda \, \bar{\phi}_{11} \sum_{r=1}^{3}\phi_{rr}\epsilon_{rr} + \bar{\phi}_{11}^{2}\bar{\epsilon}_{11}$$

$$\bar{\sigma}_{21} = \bar{\sigma}_{12} = 2\mu \, \bar{\phi}_{11}\bar{\phi}_{22}\bar{\epsilon}_{12} \tag{A-18}$$

$$\bar{\sigma}_{31} = \bar{\sigma}_{13} = 2\mu \, \bar{\phi}_{11}\bar{\phi}_{22}\bar{\epsilon}_{13}$$

Let us now single out the eigenvector N^1 and examine what happens to the stress when the eigenvalue $\phi^1 (= \bar{\phi}_{11})$ vanishes. Note from Eqs. (A-18) that, if $\bar{\phi}_{11} = 0$, it follows that $\sigma_{11} = \bar{\sigma}_{12} = \sigma_{13} = 0$, that is, the solid cannot support stresses on a plane normal to N^1, on which $\phi^1 \equiv \bar{\phi}_{11} = 0$. The physical meaning of this is that the decrease of ϕ^1 represents damage __normal__ to the plane of N^1 and, as such, it is a measure of the plane microcracks that have developed normal to N^1 and/or the increase in the size of such cracks, so that when $\bar{\phi}_{11} = 0$, a plane crack in the accepted sense has formed across the material element on a plane with normal N^1, so that the element cannot support tensile or shear stresses on that plane.

On the basis of the above observations, the physical meaning of Eqs. (A-11), (A-12) and (A-13) now becomes clear. An increase in tensile strain $d\epsilon^\alpha$ on a plane with normal n^α causes planar damage $d\phi^\alpha$ on that plane, where $d\phi^\alpha$ is given by Eq. (A-12), in accordance with the observation that "planar microcracks form perpendicular to the direction of the principal tensile strain.

The constant k in Eq. (A-13) is a material parameter that reflects the fracture resistance or fracture toughness of the material. Eq. (A-12) is representative of processes involving annihilation of populations and catastrophic processes in systems where the increment of annihilation is proportional to the state of integrity, which is given here by the factor $(\phi_n^\alpha)^m$. This form is representative of such systems, even though any monotonically decreasing function $f(\phi_n^\alpha)$, such that $f(0) = 0$, will likely do as well. Finally, we note that the damage tensor D can be expressed in terms of ϕ as follows:

A-5

$$D_{ij} = \sum_{\alpha} \left[1 - \left(\phi^{\alpha} \right)^2 \right] N_i^{\alpha} N_j^{\alpha} \qquad \text{(A-19)}$$

The physical interpretation of the governing equations is now complete.

A.4 APPLICATION TO SOME SIMPLE CASES OF HOMOGENEOUS DEFORMATION.

In this section. analytic solutions. based upon the constitutive model described above. are presented for several simple cases of homogeneous deformation including simple tension. simple compression and simple shear. These solutions provide valuable insight into the characteristics of the model and reveal its remarkable predictive capabilities. despite the fact that it involves only four material parameters.

A.4.1 Homogeneous Triaxial Strain Fields.

As a preliminary development. consider the case in which the strain field is homogeneous and consists only of principal strains. i.e.. $\epsilon_{ij} = 0$ for $i \neq j$. Thus. $d\underset{\sim}{\epsilon}$ and $\underset{\sim}{\epsilon}$ are always coaxial and $\underset{\sim}{\phi}$ is coaxial with $\underset{\sim}{\epsilon}$ by virtue of Eq. (A-11). As a result. $\underset{\sim}{\phi}$ is diagonal. In view of Eq. (A-10). $\underset{\sim}{q}$ is also diagonal. The principal stresses are given below in terms of the principal strains and the principal values of $\underset{\sim}{\phi}$:

$$\sigma_1 = \lambda \, \phi_1 \sum_r \phi_r \epsilon_r + 2\mu \phi_1^2 \epsilon_1$$

$$\sigma_2 = \lambda \, \phi_2 \sum_r \phi_r \epsilon_r + 2\mu \, \phi_2^2 \epsilon_2 \qquad \text{(A-20)}$$

$$\sigma_3 = \lambda \, \phi_3 \sum_r \phi_r \epsilon_r + 2\mu \, \phi_3^2 \epsilon_3$$

The appropriate evolution equation for $\underset{\sim}{\phi}$ is obtained from Eq. (A-14) and is given in terms of the principal components of $\underset{\sim}{\phi}$ as follows:

$$d\phi_i = - \left(\phi_i \right)^m d\xi, \qquad \text{(A-21)}$$

A-6

where

$$d\xi_i = \begin{cases} k \, d\epsilon_i & , \text{ if } d\epsilon_i > 0 , \; \epsilon_i \geq 0 \\ 0 & , \text{ otherwise} \end{cases}$$

We now consider two special cases of the above equations. namely. simple tension and simple compression.

A.4.2 Simple Tension.

Consider the case of monotonically increasing simple tension. In this case. $\sigma_2 = \sigma_3 = 0$. and integration of Eqs. (A-21) with $\epsilon_2 = \epsilon_3$ and the initial conditions $\phi_2 = \phi_3 = 1$. shows that $\phi_2 = \phi_3$ always. Hence. we find that

$$\phi_2 \epsilon_2 = - \frac{\lambda}{2(\lambda+\mu)} \epsilon_1 \phi_1 = - \nu \phi_1 \epsilon_1 \tag{A-22}$$

and

$$\sigma_1 = E \phi_1^2 \epsilon_1 \tag{A-23}$$

where

$$E = \frac{(2\mu+3\lambda)\mu}{\lambda+\mu} \tag{A-24}$$

From Eq. (A-21a). the evolution equation for ϕ_1 is

$$d\xi_1 \phi_1^m + d\phi_1 = 0 \quad , \tag{A-25}$$

subject to the initial condition $\phi_1(0) = 1$. Thus. the solution is

$$\phi_1 = \begin{cases} e^{-k\epsilon_1} & , \text{ if } m = 1 \\ \left\{ 1 - (1-m)k\epsilon_1 \right\}^{\frac{1}{1-m}} & , \text{ if } m \neq 1 \end{cases} \tag{A-26}$$

Combining Eqs. (A-23) and (A-26). we obtain the expression:

$$\sigma_1 = \begin{cases} \overbrace{E\epsilon_1} \\ e^{-2k\epsilon_1}, & \text{if } m = 1 \\[2ex] E\,\epsilon_1\left\{1-(1-m)k\epsilon_1\right\}^{\frac{2}{1-m}}, & \text{if } m \neq 1 \end{cases} \tag{A-27}$$

Inspection of Eq. (A-27) reveals that, for $0 \leq m < 1$, σ_1 is not a monotonic function of ϵ_1, but reaches a maximum and then goes to zero for finite ϵ_1. For $1 \leq m < 3$, σ_1 again reaches a maximum and then decays monotonically to zero as $\epsilon_1 \to \infty$. For $m = 3$, σ_1 monotonically increases to an asymptotic constant value as $\epsilon_1 \to \infty$, while for $3 < m < \infty$, σ_1 increases monotonically with ϵ_1. The influence of m on the constitutive response is shown in Figure A.1a. Thus, in the range $0 \leq m < 3$, the model exhibits softening in tension in agreement with experimental data.

The model also unloads elasticity with an effective modulus of $E\phi_1^2$ which is diminished by the accumulated damage. Thus, the model has all of the characteristics of a fracturing elastic solid. It follows from Eq. (A-22) that $\epsilon_2 \leq 0$ and hence $\phi_2 = 1$, i.e., no damage is produced in the transverse direction due to the uniaxial tension loading.
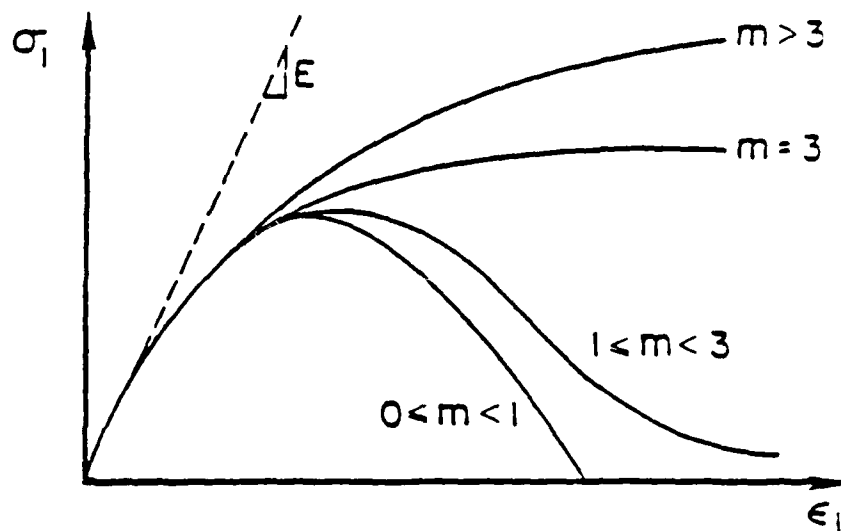
A.4.3 Simple Compression.

Consider now the case of monotonically increasing uniaxial compression. Here, $\sigma_2 = \sigma_3 = 0$, while σ_1 and ϵ_1 are compressive. Again, Eqs. (A-21) together with $\epsilon_2 = \epsilon_3$, and the initial conditions $\phi_2 = \phi_3 = 1$, lead to the result that $\phi_2 = \phi_3$ always. Similar to the case of simple tension, we find that

$$\phi_2\epsilon_2 = -\nu\phi_1\epsilon_1 \tag{A-28}$$

and

$$\sigma_1 = E\phi_1^2\epsilon_1 \tag{A-29}$$

The damage evolution in this case is, however, entirely different from that for simple tension. Since both $d\epsilon_1$ and ϵ_1 are compressive at all times, we find from Eq. (A-21) that $d\phi_1 = 0$ and thus $\phi_1 = 1$ always. However, in view of Eq. (A-28), ϵ_2 is now tensile and hence ϕ_2 (and ϕ_3) will increase with the consequence that damage will develop on planes which are parallel to the axis of compression, in accordance with experimental observation; this is the so-called axial splitting mode (Horii and Nemat-Nasser, 1985).

A-8

(a) Stress-strain relation in simple tension
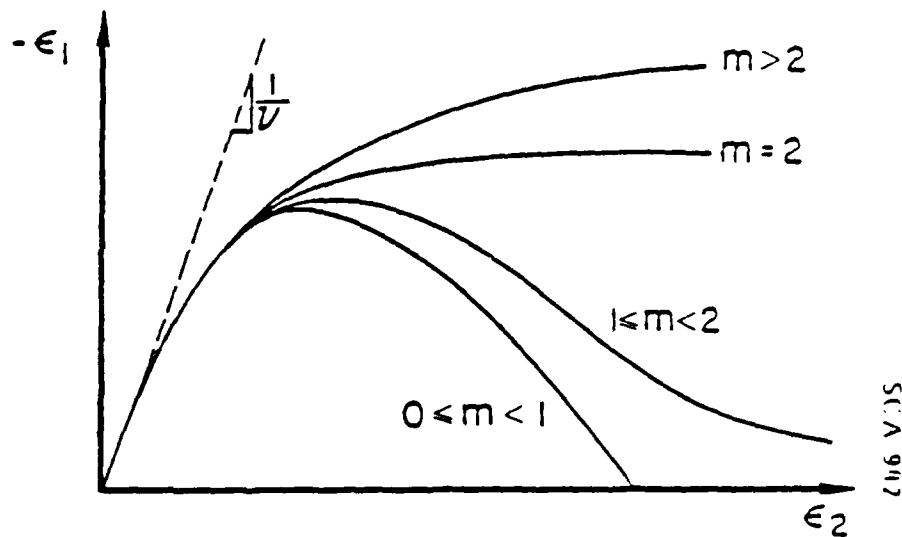
(b) Axial strain vs. lateral strain in simple compression

Figure A.1   Predicted responses for simple tension and simple compression, showing the effect of the parameters m on the resulting behavior.

From Eq. (A-21). we can write

$$d\phi_2 + \phi_2^m k \, d\epsilon_2 = 0 \quad , \tag{A-30}$$

the solution of which is

$$\phi_2 = \begin{cases} e^{-k\epsilon_2} & , \ m = 1 \\[3mm] \left\{ 1 - (1-m)k\epsilon_2 \right\}^{\frac{1}{1-m}} & , \ m \neq 1 \end{cases} \tag{A-31}$$

Thus, in view of Eq. (A-29) and the condition $\phi_1 = 1$, the axial stress strain relation is

$$\sigma_1 = E \, \epsilon_1 \quad , \tag{A-32}$$

so that the response in the axial direction is purely elastic.

To find the relation between the strains. we use Eqs. (A-28) and (A-31) together with the fact that $\phi_1 = 1$. It then follows that

$$- \nu\epsilon_1 = \begin{cases} \epsilon_2 e^{-k\epsilon_2} & , \ m = 1 \\[3mm] \epsilon_2 \left\{ 1 - (1-m)k\epsilon_2 \right\}^{\frac{1}{1-m}} & , \ m \neq 1 \end{cases} \tag{A-33}$$

Here. we may distinguish three different cases:

(a) $0 \leq m < 1$

The strain ϵ_1 is not a monotonic function of ϵ_2. It reaches a maximum absolute value and then goes to zero for a finite value of ϵ_2. Specifically.

$$|\epsilon_1|_{max} = \frac{1}{k\nu} \left(\frac{n}{n+1}\right)^{n+1} \tag{A-34}$$

where $n = 1/(1-m)$.

(b) $1 \leq m < 2$

Again, the strain ϵ_1 is not a monotonic function of ϵ_2. It reaches a maximum absolute value again given by Eq. (A-34) for $1 < m$ and then goes to zero for infinite ϵ_2. For $m = 1$

$$|\epsilon_1|_{max} = \frac{1}{\nu e k} ,$$

(A-35)

where e denotes the base of the natural logarithm.

(c) $2 \leq m < \infty$

In this case, ϵ_1 is a monotonic function of ϵ_2 and approaches the following limiting condition for increasing lateral strain:

$$\lim_{\epsilon_2 \to \infty} |\epsilon_1|_{max} = \begin{cases} \frac{1}{k} , & m = 2 \\ \infty , & m > 2 \end{cases}$$

(A-36)

The above cases are depicted graphically in Figure A.1(b).

A.4.4 Collapse of a Block Under Axial Compression.

It follows from the above discussion that a block consisting of elastic fracturing material will collapse under homogeneous axial compression if $0 \leq m \leq 2$, since ϵ_1 has an upper bound given by the expression:

$$|\epsilon_1|_{max} = \frac{1}{\nu k} \left(\frac{1}{2-m}\right)^{\frac{2-m}{1-m}}$$

(A-37)

The limiting cases are

$$|\epsilon_1|_{max} = \begin{cases} \frac{1}{\nu k e} , & m = 1 \\ \frac{1}{\nu k} , & m = 2 \end{cases}$$

(A-38)

The collapse stress may be calculated directly from Eq. (A-32), with the result:

$$|\sigma_1|_{max} = \frac{E}{\nu k} \left(\frac{1}{2-m}\right)^{\frac{2-m}{1-m}}$$

(A-39)

Thus, the theory predicts the collapse of a block under axial compression due to damage on planes parallel to the axis of compression. Again, this is the axial splitting mode.

A.4.5 Ratio of Collapse Stresses in Tension and Compression.

At this point, it is of interest to explore the rationality of the above results by comparing the ratio σ^c/σ^t, where σ^c and σ^t are collapse stresses in compression and tension, respectively, obtained analytically, with that observed experimentally for concrete, even though the end-grip conditions in the tests may not be ideal, as assumed in solutions obtained here. Restricting attention to the case $m = 1$, it follows from Eqs. (A-37) and (A-39) that

$$\frac{\sigma^c}{\sigma^t} = \frac{2}{\nu} \tag{A-40}$$

Since $\nu \approx 0.2$ for concrete, we have

$$\frac{\sigma^c}{\sigma^t} \approx 10 \quad , \tag{A-41}$$

which is close to experimental observation (Raphael, 1984).

A.4.6 Simple Shear.

Consider now the case of monotonically increasing shear strain under conditions of simple shear and small strain. The configuration of interest is depicted in Figure A.2. Inasmuch as the only non-zero strain component is ϵ_{12}, we can write

$$\phi_{k\ell}\epsilon_{k\ell} = 2\,\phi_{12}\epsilon_{12} \tag{A-42}$$

and

$$\phi_{ik}\phi_{j\ell}\epsilon_{k\ell} = \left(\phi_{i1}\phi_{j2} + \phi_{i2}\phi_{j1}\right)\epsilon_{12} \tag{A-43}$$

Therefore, in this case, the general constitutive relation

$$\sigma_{ij} = \lambda\,\phi_{ij}\phi_{k\ell}\epsilon_{k\ell} + 2\mu\,\phi_{ik}\phi_{j\ell}\epsilon_{k\ell} \tag{A-44}$$

reduces to the form

$$\sigma_{ij} = 2\left[\lambda\,\phi_{ij}\phi_{12} + \mu\left(\phi_{i1}\phi_{j2} + \phi_{i2}\phi_{j1}\right)\right]\epsilon_{12} \tag{A-45}$$
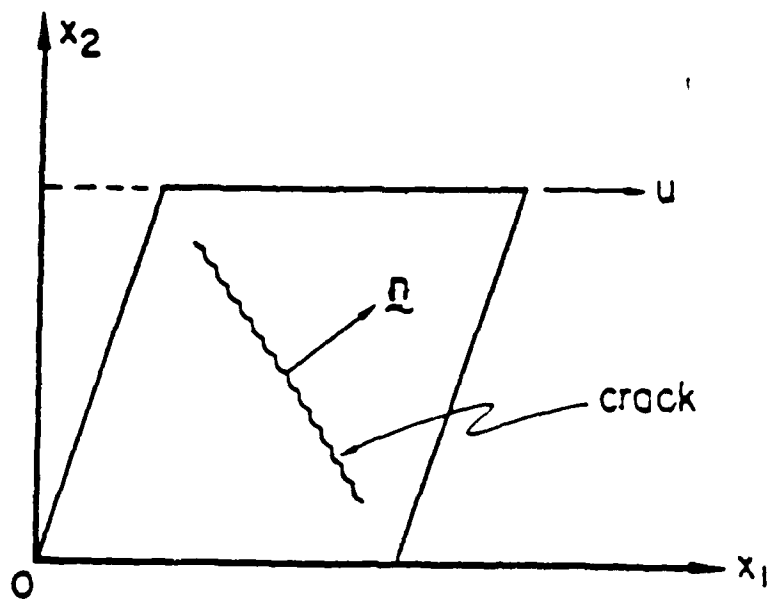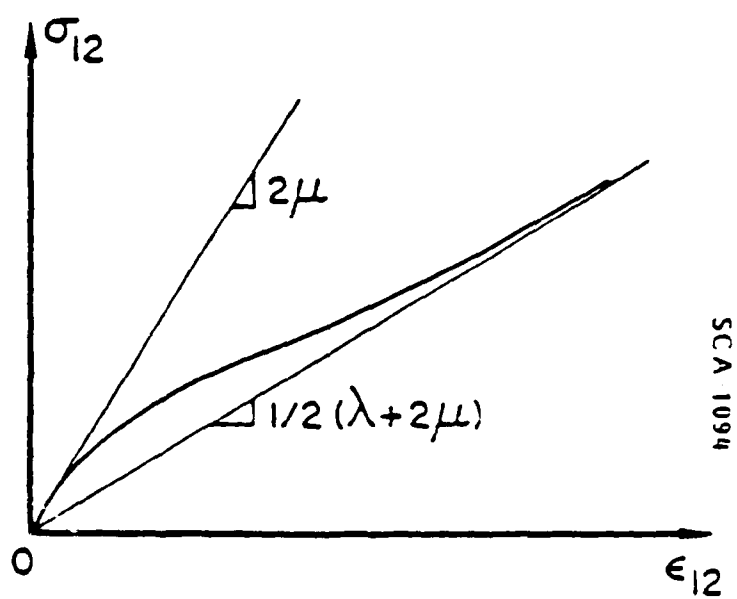
A-12

Figure A.2. Simple shear

Figure A.3. General relationship between σ_{12} and ϵ_{12} for the case in which $\lambda > 2\mu$.

Therefore, we can write

$$\sigma_{12} = 2\left[\lambda \, \phi_{12}^2 + \mu\left(\phi_{11}\phi_{22} + \phi_{12}^2\right)\right]\epsilon_{12} \qquad (A-46)$$

$$\sigma_{11} = 2\left(\lambda + 2\mu\right)\phi_{11}\phi_{12}\epsilon_{12} \qquad (A-47)$$

$$\sigma_{22} = 2\left(\lambda + 2\mu\right)\phi_{22}\phi_{12}\epsilon_{12} \qquad (A-48)$$

For a small shear strain. the maximum tensile strain will lie in a direction that makes a 45 degree angle with each of the coordinate axes. Consequently. cracks will develop in the material as shown in Figure A.2. The components of the unit normal $\underset{\sim}{n}$ to the crack are $n_1 = n_2 = 1/\sqrt{2}$.

Since there is only one cracking direction. we set $\alpha = 1$ in the evolutionary equation for $d\phi_{ij}$ and write

$$d\phi_{ij} = - k\left(\phi_n\right)^m d\epsilon \, n_i n_j \qquad (A-49)$$

where

$$\phi_n = \phi_{ij} n_i n_j$$
$$d\epsilon = d\epsilon_{12} \qquad (A-50)$$

Since $n_1 = n_2 = 1/\sqrt{2}$, it follows from Eq. (A-49) that

$$d\phi_{11} = d\phi_{22} = d\phi_{12} \qquad (A-51)$$

Hence

$$\int_1^{\phi_{11}} d\phi_{11} = \int_0^{\phi_{12}} d\phi_{12} , \qquad (A-52)$$

since $\phi_{ij} = \delta_{ij}$ initially. From Eq. (A-53) we find

$$\phi_{11} = 1 + \phi_{12} , \qquad (A-53)$$

and Eq. (A-50a) gives

$$\phi_n = \phi_{11} + \phi_{12} , \qquad (A-54)$$

A-14

since $\phi_{11} = \phi_{22}$ according to Eq. (A-51).

Substitution of Eq. (A-53) into Eq. (A-54) yields

$$\phi_n = 1 + 2 \phi_{12} \tag{A-55}$$

which, when combined with Eq. (A-49), leads to the result

$$d\phi_{ij} = - k\left(1 + 2\phi_{12}\right)^m d\epsilon_{12} n_i n_j \tag{A-56}$$

Therefore, since $n_1 = n_2 = 1/\sqrt{2}$, we can write

$$d\phi_{12} = - \frac{k}{2} \left(1 + 2 \phi_{12}\right)^m d\epsilon_{12} \tag{A-57}$$

which can be integrated to give, for m = 1:

$$\phi_{12} = \frac{1}{2} \left[e^{-k\epsilon_{12}} - 1\right] \tag{A-58}$$

and for $m \neq 1$:

$$\phi_{12} = \frac{1}{2} \left\{ \left[\frac{1}{k(m-1)\epsilon_{12}+1}\right]^{\frac{1}{m-1}} - 1 \right\} \tag{A-59}$$

Recalling Eq. (A-53) and the fact that $\phi_{22} = \phi_{11}$, Eq. (A-46) can be placed in the following form:

$$\sigma_{12} = 2\left[(\lambda + 2\mu)\phi_{12}^2 + 2\mu\phi_{12} + \mu\right]\epsilon_{12} \tag{A-60}$$

Therefore, Eqs. (A-58) to (A-60) describe the relationship between σ_{12} and ϵ_{12}.

From Eqs. (A-58) and (A-59) note that

$$\lim_{\epsilon_{12} \to \infty} \sigma_{12} = - \frac{1}{2} (\lambda + 2\mu)\epsilon \tag{A-61}$$

which in view of Eq. (A-60) leads to the result:

$$\lim_{\epsilon_{12} \to \infty} \sigma_{12} = \frac{1}{2} (\lambda + 2\mu)\epsilon_{12} \tag{A-62}$$

A-15

Hence, when $\lambda < 2\mu$, the ultimate slope given by Eq. (A-62) will be <u>less than</u> the initial slope, 2μ, as shown in Figure A.3. The case $\lambda > 2\mu$ on the other hand, leads to the ultimate slope being <u>greater than</u> the initial slope, i.e., a hardening, which is difficult to visualize from a physical standpoint. These limiting cases, however, fall outside of the assumption of small strains made here and therefore may not be physically meaningful.

## A.5 APPLICATION TO NON-HOMOGENEOUS STRAIN FIELDS.

In an effort to explore the capability of the continuous damage model to predict the proper trends for fracture problems involving non-homogeneous strain fields, we developed a computer program for the model and incorporated it into a finite element code. We then conducted a limited numerical study of a fracture problem, having a non-homogeneous strain field, for which a theoretical solution is available from linear elastic fracture mechanics (LEFM). The problem, depicted in Figure A.4(a), consists of a long flat plate of width w, which has a crack of length 2a and is acted upon by a uniform tensile stress σ. The problem is to find the magnitude of σ which causes the crack to grow catastrophically and thereby cause fracture of the plate.

The finite element grid used in the numerical study consisted of uniform, initially square zones of unit length. Because of symmetry, only the right half of the problem was considered. Vertically, there were 21 zones while 16 zones were used in the horizontal direction. Therefore, the width w had the value 32. The effect of an initial crack in the x-direction was introduced into the grid by simple setting $\phi_{yy} = 0$ in those zones through which the crack passed. In the study, three different values of initial crack length were considered, namely, a = 1, 3 and 6.

The results from the numerical study are shown in Figure A.4(b), where the stress σ_f to fracture the plate is plotted against the dimensionless ratio a/w. Also shown on this figure is the corresponding theoretical prediction from LEFM (see Knott, 1973), which is given by the expression:

$$\sigma_f = \frac{K_{IC}}{\left[w \tan\left(\frac{\pi a}{w}\right) \right]^{1/2}} , \qquad (A.63)$$

where K_{IC}, the mode I fracture toughness, was set to the value 7.07 so that the theoretical curve would pass through the central numerical point shown in the figure. As an inspection of the figure reveals, the continuous damage model predicts a decay
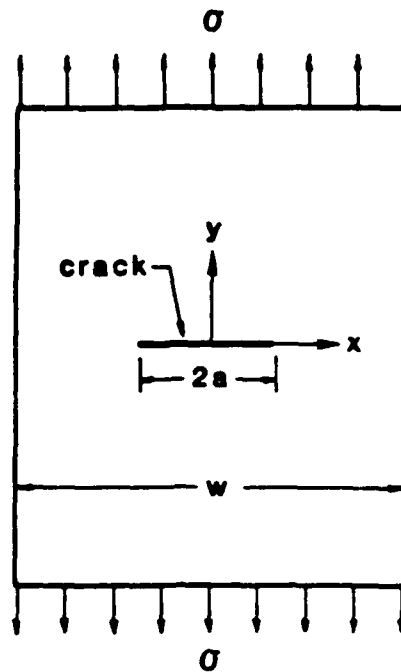
(a)   Geometric configuration of flat plate.
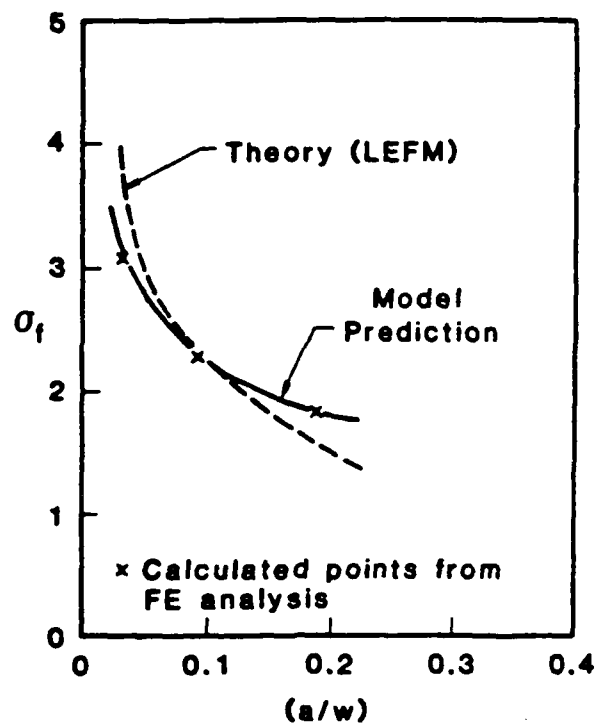
(b) Dependence of fracture stress σ_f on
the ratio a/w.

Figure A.4.   Response of a thin elastic plate with a crack to an applied
uniform tensile stress.

of σ_f with increasing a/w. which is qualitatively in agreement with the theoretical result from LEFM.

Exact agreement between the model prediction and LEFM is not to be expected. however, for several reasons. First, the model produces some damage in every zone of the grid from the onset of the tensile loading. while in LEFM theory it is assumed that the damage remains confined to the original crack until there is catastrophic crack extension. Secondly, for the material region just ahead of the crack. the two approaches lead to significantly different stress fields. In LEFM. the material ahead of the crack remains linearly elastic and undamaged until overall failure occurs. while. in the numerical simulation with the model. the zones ahead of the crack experience increasingly greater damage as σ grows. Thus. the stress fields in the material just ahead of the crack are very much different in the two cases. In view of these considerations. the differences between the two predictions shown in Figure A.4 are not surprising. The general trends. however. are similar and indicate that the present model. when used in conjunction with a finite element code. leads to realistic results. Closer agreement between the two predictions could probably be obtained by revising the evolution equation for ϕ.

A.6 POST-FAILURE BEHAVIOR AND CRACK CLOSURE.

It was shown in Section A.3 that if an eigenvalue ϕ^A of ϕ vanishes in a material element then the element cannot support stress on a plane normal to $\bar{N}^A$. the latter being the eigenvector of ϕ associated with ϕ^A. In a structural sense the element has developed damage equivalent to a crack on the plane normal to $\bar{N}^A$. It follows that the element has developed kinematic freedom in directions normal and tangential fo $\bar{N}^A$ in the following sense. Let $\Delta\bar{\epsilon}_{\alpha\beta}$ be the components of the strain increments $\Delta\epsilon$ defined relative to a system of coordinates x^α coincident with the eigenvectors $\bar{N}^\alpha$ of ϕ. Thus

$$\Delta\bar{\epsilon}_{\alpha\beta} = \begin{bmatrix} \Delta\bar{\epsilon}_{11} & \Delta\bar{\epsilon}_{12} & \Delta\bar{\epsilon}_{13} \\ \Delta\bar{\epsilon}_{21} & \Delta\bar{\epsilon}_{22} & \Delta\bar{\epsilon}_{23} \\ \Delta\bar{\epsilon}_{31} & \Delta\bar{\epsilon}_{32} & \Delta\bar{\epsilon}_{33} \end{bmatrix} \tag{A-64}$$

Let $\underline{A} = 1$. Perusal of Eqs. (A-18a,b,c) show that if $\phi^1 = \phi_{11} = 0$. then not only are $\bar{\sigma}_{11} = \bar{\sigma}_{12} = \bar{\sigma}_{13} = \bar{\sigma}_{31} = \bar{\sigma}_{21} = 0$ as discussed previously but the strains $\bar{\epsilon}_{11}$. $\bar{\epsilon}_{12} = \bar{\epsilon}_{21}$. $\bar{\epsilon}_{31} = \bar{\epsilon}_{13}$ become indeterminate from the constitutive properties of the element.

A.7 DIRECTED AND ISOTROPIC DAMAGE.

It has recently been observed (Diamond and Bentur. 1984) that. in multi-phase materials. such as plain concrete. the formation of directional cracks is usually accompanied by the presence of small cracks randomly oriented. which from a statistical viewpoint amount to isotropic damage. denoted here by Ω. In this sense Ω reduces the stress carrying capacity of a material by the same degree in all directions. Thus the integrity tensor. now denoted by ϕ_Ω must be reduced by the presence of Ω and hence it must be a state function of Ω. Thus. in symbolic form:

$$\phi_\Omega = \phi_\Omega\left(\Omega, \xi_\alpha\right) \tag{A-65}$$

subject to the following conditions which must always apply:

$$\phi_\Omega(0,0) = \delta$$

$$\tag{A-66}$$

$$\phi_\Omega\left(1, \xi_\alpha\right) = 0$$

where δ is the unit matrix.

To satisfy conditions (A-66) we adopt a relation of the multiplicative type. i.e.. we set

$$\phi_\Omega = \omega(\Omega)\phi\left(\xi_\alpha\right) \tag{A-67}$$

such that $\omega(0) = 1$. $\omega(1) = 0$. Furthermore ω must be a monotonically decreasing function of Ω. A suitable function that satisfies the above constraints is

$$\omega(\Omega) = (1 - \Omega)^a \tag{A-68}$$

where $a \geq 0$. Thus the integrity tensor ϕ. considered in the previous sections. is now modified by the presence of isotropic damage as specified by Eqs. (A-67) and (A-68).

The constitutive equation thus becomes

$$\phi = \frac{1}{2} \omega^2 \left\{ \lambda \left[\phi_{ij} \epsilon_{ij} \right]^2 + \mu \, \phi_{ik} \phi_{j\ell} \epsilon_{ij} \epsilon_{k\ell} \right\} \tag{A-69}$$

and

$$\sigma_{ij} = \omega^2 \left\{ \lambda \phi_{ij} \phi_{k\ell} \epsilon_{k\ell} + 2\mu \, \phi_{ik} \phi_{j\ell} \epsilon_{k\ell} \right\} \tag{A-70}$$

A.7.1 The Rate Equation for Ω.

Physical considerations suggest that isotropic damage in cementitious materials is caused mainly by shearing which gives rise to local decohesion (between the mortar and the aggregate, and/or the paste and the sand particles). Thus following similar reasoning that gave rise to Eq. (A-12) and noting that the ultimate value of Ω is unity, we set $d\Omega$ to be proportional to a positive monotonic function of the isotropic integrity $(1-\Omega)$, i.e.,

$$d\Omega = f(1 - \Omega) d\varsigma \quad , \tag{A-71}$$

where $d\varsigma$ is defined in terms of the increment in the deviatoric strain tensor de_{ij} as

$$d\varsigma^2 = c^2 \left(de_{ij} de_{ij} \right) \quad . \tag{A-72}$$

and $c > 0$ is a material parameter. A suitable form of the function f is as follows:

$$f(1 - \Omega) = (1 - \Omega)^b \tag{A-73}$$

where $b > 0$. Solution of Eq. (A-71) in the light of Eq. (A-73) gives rise to the expression

$$1 - \Omega = (1 - (1 - b)\varsigma)^{\frac{1}{1-b}} \quad , \tag{A-74}$$

which is of the same form as Eq. (A-26). Specifically, if $b = 1$ then

$$(1 - \Omega) = e^{-b\varsigma} \quad . \tag{A-75}$$

We note that c in Eq. (A-72) plays the role of an isotropic fracture toughness parameter which influences the rate of isotropic degradation.

A-20

A.7.2 Isotropic Damage in Homogeneous Triaxial Strain Fields.

In the presence of isotropic damage the counterparts of Eqs. (A-20) are:

$$\frac{\sigma_1}{\omega^2} = \lambda \phi_1 \sum \phi_k \epsilon_k + 2\mu \, \phi_1^2 \epsilon_1 \qquad \text{(A-76)}$$

$$\frac{\sigma_2}{\omega^2} = \lambda \phi_2 \sum \phi_k \epsilon_k + 2\mu \, \phi_2^2 \epsilon_2 \qquad \text{(A-77)}$$

$$\frac{\sigma_3}{\omega^2} = \lambda \phi_3 \sum \phi_k \epsilon_k + 2\mu \, \phi_3^2 \epsilon_3 \qquad \text{(A-78)}$$

In that which follows, we illustrate the application of the above equations to two special cases of interest, namely, simple tension and simple compression.

(A) SIMPLE TENSION

Here $\sigma_2 = \sigma_3 = 0$ and the analysis follows very closely that of Section A.4.2. Specifically, in view of Eqs. (A-78):

$$\phi_2 \epsilon_2 = - \nu \, \phi_1 \epsilon_1 \qquad \text{(A-79)}$$

$$\sigma_1 = \left(E \phi_1^2 \epsilon_1 \right) \omega^2 \qquad \text{(A-80)}$$

However, as opposed to the analysis in Section A.4.2 two functions ϕ_1 and ω are now necessary to determine the axial stress σ_1. In the absence of explicit coupling between directional and isotropic damage, ϕ_1 is still given by Eq. (A-26) in which case

$$\phi_1 = \left\{ 1 - (1 - m) k \epsilon_1 \right\}^{\frac{1}{1-m}} \qquad \text{(A-81)}$$

However, we expect that k in Eq. (A-81) will depend on Ω since clearly the material resistance to cracking will be greatly influenced by the presence of the isotropic damage. Specifically we expect that

A-21

$$k = k(\Omega) \tag{A-82}$$

where k is an increasing function of Ω. In this event Eq. (A-25) can no longer be integrated directly and Eq. (A-81) will not hold.

Evolution of Isotropic Damage.

In the presence of axial loading $(\sigma_2 = \sigma_3 = 0)$

$$d\varsigma = c\sqrt{\frac{3}{2}} \left| d\epsilon_1 - d\epsilon_2 \right| \tag{A-83}$$

which in the light of Eq. (A-79) becomes

$$d\varsigma = c\sqrt{\frac{3}{2}} \left| d\epsilon_1 + \nu\, d\left(\frac{\phi_1}{\phi_2}\,\epsilon_1\right) \right| \tag{A-84}$$

where use was made of Eq. (A-12). Thus, in general, we have the following <u>coupled</u> equations that govern simultaneously the evolution of directional and isotropic damage in simple tension:

$$d\phi_1 = -\phi_1^m\, k(\Omega)\, d\epsilon_1 \tag{A-85}$$

$$d\Omega = (1 - \Omega)^b\, c\sqrt{\frac{3}{2}}\left[1 + \nu\phi_1 - \nu k\phi_1^m\epsilon_1\right] d\epsilon_1 \tag{A-86}$$

Approximate Solution of Eqs. (A-85) and (A-86).

To obtain a qualitative understanding of the simultaneous effects of isotropic and directional damage we solve Eqs. (A-85) and (A-86) approximately. Specifically we uncouple the equations by setting $k(\Omega)$ equal to a constant k and setting equal to zero the terms on the righthand side of Eq. (A-86) that are multiplied by ν, since in the region of softening $\phi_1 < 1$ and the terms $\nu\phi_1$ and $k\phi_1^m$ are considerably less than unity. Then ϕ_1 is given by Eq. (A-81) while Ω is given by Eq. (A-87), i.e.,

$$1 - \Omega = \left\{1 - (1 - b)c\sqrt{\frac{3}{2}}\,\epsilon_1\right\}^{\frac{1}{1-b}} \tag{A-87}$$

in view of Eq. (A-74). Thus σ_1 may now be found upon use of Eqs. (A-80), (A-81) and (A-68) and is given below:

A-22

$$\sigma_1 = E\left[1 - (1 - m)k\epsilon_1\right]^{\frac{2}{1-m}} \epsilon_1 \left\{1 - (1 - b)c\sqrt{\frac{3}{2}}\,\epsilon_1\right\}^{\frac{2a}{1-b}} \tag{A-88}$$

In the very specific case where $m = b = 1$

$$\sigma_1 = E\epsilon_1 e^{-2\left[k + ac\sqrt{\frac{3}{2}}\right]\epsilon_1} \tag{A-89}$$

In other words, directional and isotropic degradation compound the effect of softening in simple tension. As we shall see this is not the case in compression. For comparison when isotropic damage is absent, see Eq. (A-27b).

(B) SIMPLE COMPRESSION

In this case Eqs. (A-79) and (A-80) apply but now $\phi_1 = 1$. Thus in this specific case

$$\phi_2\epsilon_2 = -\nu\,\epsilon_1 \tag{A-90}$$

$$\sigma_1 = E\epsilon_1\omega^2 \tag{A-91}$$

As opposed to tension, softening in compression is due entirely to volumetric damage. The appropriate rate equations in the presence of monotonic loading are:

$$d\phi_2 = -\phi_2^m\, k(\Omega)\, d\epsilon_2 \tag{A-92}$$

$$d\Omega = (1 - \Omega)^b c\sqrt{\frac{3}{2}}\left[1 + \frac{1}{\nu} - \frac{k(\Omega)}{\nu}\,\phi_2^m\epsilon_2\right]d\epsilon_2 \tag{A-93}$$

where Eqs. (A-71), (A-73), (A-90), and (A-92) were used. Eqs. (A-92) and (A-93) are coupled and cannot be integrated directly. We obtain, therefore, approximate solutions of these equations in order to study their qualitative trends. To that end we let $k(\Omega)$ be a constant k and define c^* by the relation

$$c\sqrt{\frac{3}{2}}\int_0^{\epsilon_2}\left[1 + \frac{1}{\nu} - \frac{k}{\nu}\,\phi_2^m\epsilon_2'\right]d\epsilon_2' = c^*\,\epsilon_2 \tag{A-94}$$

A-23

Equations (A-92) and (A-93) may now be integrated to give:

$$\phi_2 = \left\{ 1 - (1 - m)k\epsilon_2 \right\}^{\frac{1}{1-m}} \qquad \text{(A-95)}$$

$$1 - \Omega = \left\{ 1 - (1 - b)c^*\epsilon_2 \right\}^{\frac{1}{1-b}} \qquad \text{(A-96)}$$

$$-\nu\epsilon_1 = \epsilon_2\phi_2 = \epsilon_2\left\{ 1 - (1 - m)k\ \epsilon_2 \right\}^{\frac{1}{1-m}} \qquad \text{(A-97)}$$

$$\sigma_1 = E\epsilon_1\left\{ 1 - (1 - b)c^*\epsilon_2 \right\}^{\frac{2a}{1-b}} \qquad \text{(A-98)}$$

In Figure A.5 we show an experimental relation between the axial and transverse strains in the case of a concrete block under axial compression, according to Van Mier (1984), and the analytical relation according to Eq. (A-97) when $\nu = 0.35$, $k = 70$ and $m = 2.4$. Also shown is a compressive stress-strain relation for the same material and specimen. The approximate analytical axial stress-axial strain relation obtained on the basis of Eqs. (A-97) and (A-98) is shown in Figure A.6 when $2a/1-b = 1.5$ and $(1-b)c^* = 40$ (c^* assumed constant). For the same model, a comparison between the predicted and measured volume strain ϵ_{kk} as a function of the axial strain ϵ_1 is shown in Figure A.7. From this figure, it is evident that the model describes the observed dilatancy quite well.

A.7.3 Discussion.

The extensive and painstakingly precise investigations by Van Mier into the compressive deformation and fracture of concrete make it abundantly clear that the softening branch of the axial stress-strain curve represents the behavior of a geometric structure rather than that of a uniform material. The experiments in tension by Gopalaratnam and Shah (1985) lead to similar conclusions. There are therefore significant statistical variations in the behavior of concrete in the "softening regime."

The continuum damage theory which we have proposed in the previous sections captures, we believe, many of the essential features of the constitutive behavior of fracturing concrete. Further aspects of this approach shall be pursued in our future research.
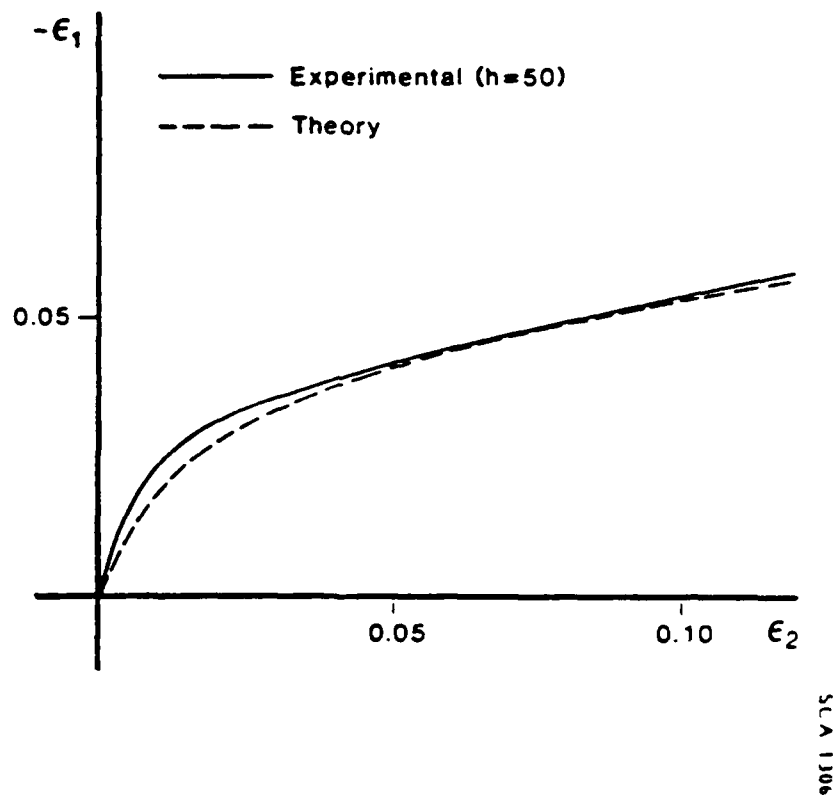
A-24

Figure A.5.   Relation between axial and transverse strains under conditions of simple compression.
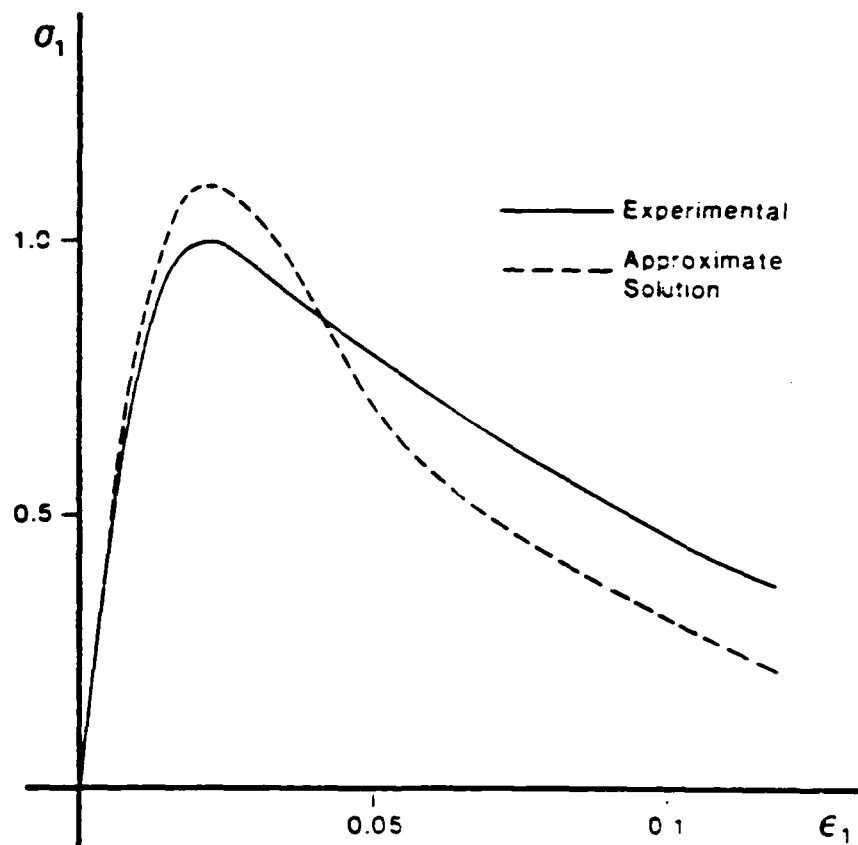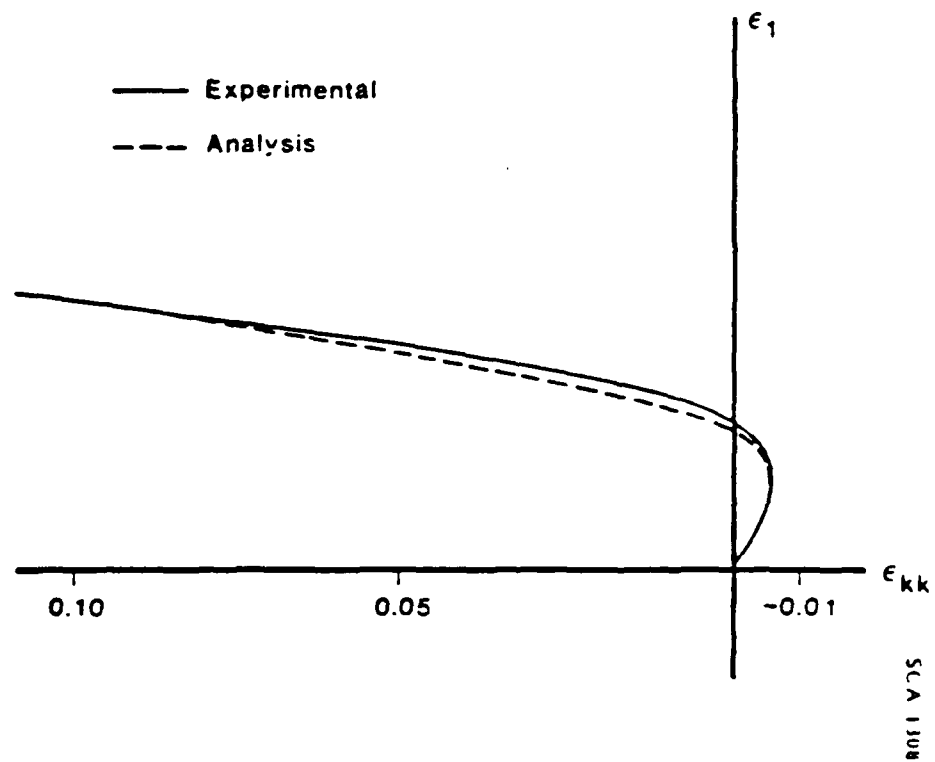
Figure A.6. Softening in compression.

Figure A.7. Dilatancy during simple compression.

A-27

A.8 REFERENCES FOR APPENDIX A.

1. Gopalaratnam, V. S., and S. P. Shah (1985). "Softening Response of Plain Concrete in Direct Tension." ACI Journal, May-June, 310.

2. Horii, H., and S. Nemat-Nasser (1985). "Compression-Induced Microcrack Growth in Brittle Solids: Axial Splitting and Shear Failure." J. Geophys. Research, 90, 3105.

3. Knott, J. F., (1973), Fundamentals of Fracture Mechanics, Butterworth and Co. (Publishers) Ltd., London, England.

4. Raphael, J. M., (1984), "Tensile Strength of Concrete", ACI Journal, March-April, 158.

5. Diamond, S., and Bentur, A., (1984), "On the Cracking in Concrete and Fiber-Reinforced Cements," in Application of Fracture Mechanics to Cementitious Composites, NATO Advanced Research Workshop, Ed. S. P. Shah, Northwestern University, September.

6. Valanis, K. C., (1985), "A Fracture Theory for Brittle Materials," S-CUBED, La Jolla, California, Informal Report.

7. Van Mier, J. G. M., (1984), "Strain Softening of Concrete Under Multi-Axial Loading Conditions," Doctoral Dissertation, Technische Hohenschule, Eindhoven, The Netherlands, November.

APPENDIX B

FINAL REPORT ON THE EXPERIMENTAL PART OF THE REASERCH PROJECT

Submitted by

Khalid H. Khan
University of Portland
Portland, Oregon

FINAL REPORT ON THE EXPERIMENTAL PART

OF THE AFOSR RESEARCH PROJECT

(July, 1989)

Submitted by: Khalid H. Khan, Ph.D.
University of Portland

This part describes briefly the experimental procedure, the
equipment used, and results of the tensile tests performed
on slotted gray cast iron specimens. It also describes the
same parameters for compression tests on concrete specimens
(slotted and unslotted). All of this experimental work is a
part of the ongoing research effort in the field of damage
modeling of brittle materials.

Materials:

Two different materials have been used for this study so far.
Gray cast iron of ASTM Class 35 and low to medium strength
concrete were chosen for this project based on their mechanical
properties. Results of tensile testing of gray cast iron and
compression testing of concrete will be described in separate
sections on the following pages.

TENSILE TESTING OF GRAY CAST IRON:

Specimen Geometry:

As described in the initial report under this research contract
(July, 1988), the "standard" specimen geometry had an hour-glass
shape with a reduced cross-section of 0.75x0.13 in. in the gauge
section of the specimen. Figure 1 shows schematically the specimen
geometry. Slots of various lengths and angles to the horizontal
axis were cut into these specimens using the EDM (Electrical
Discharge Machining) process. The width of these slots was kept
constant at 0.020 in., the minimum possible, given the available
technology. Multiple slots were also cut into some specimens to
determine their effect on fracture stress of this material. These
slotted specimens are shown schematically in Figs. 2 and 3.
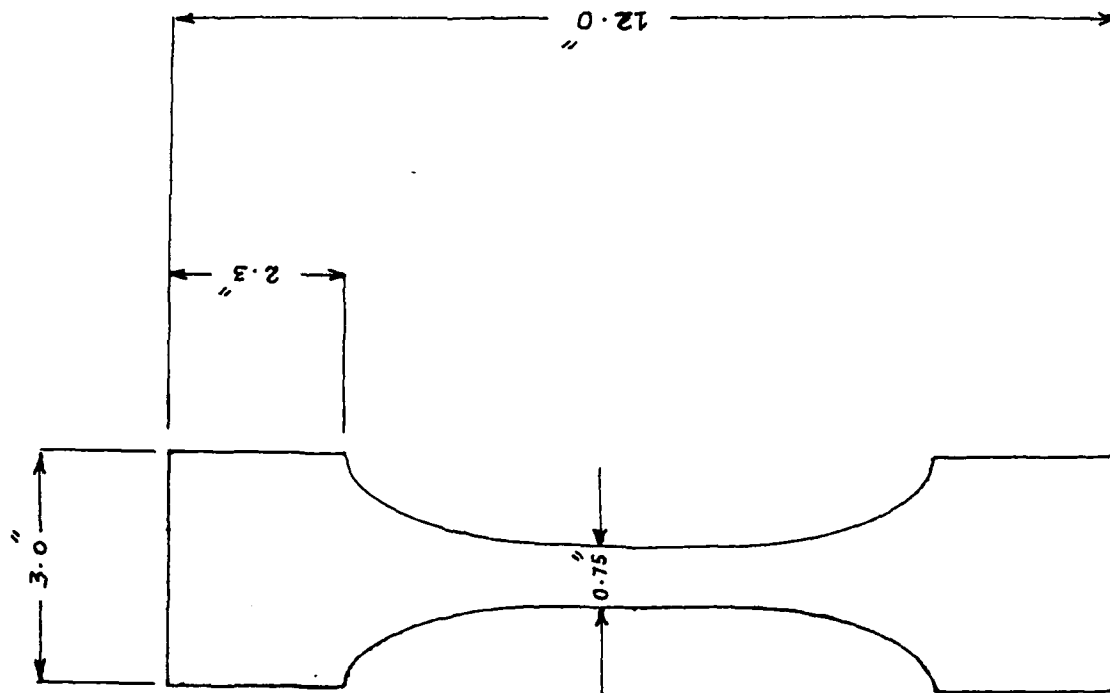Figs. 4 and 5 show pictures of typical specimens in the two
categories.

Fig. 1: Standard Specimen Geometry

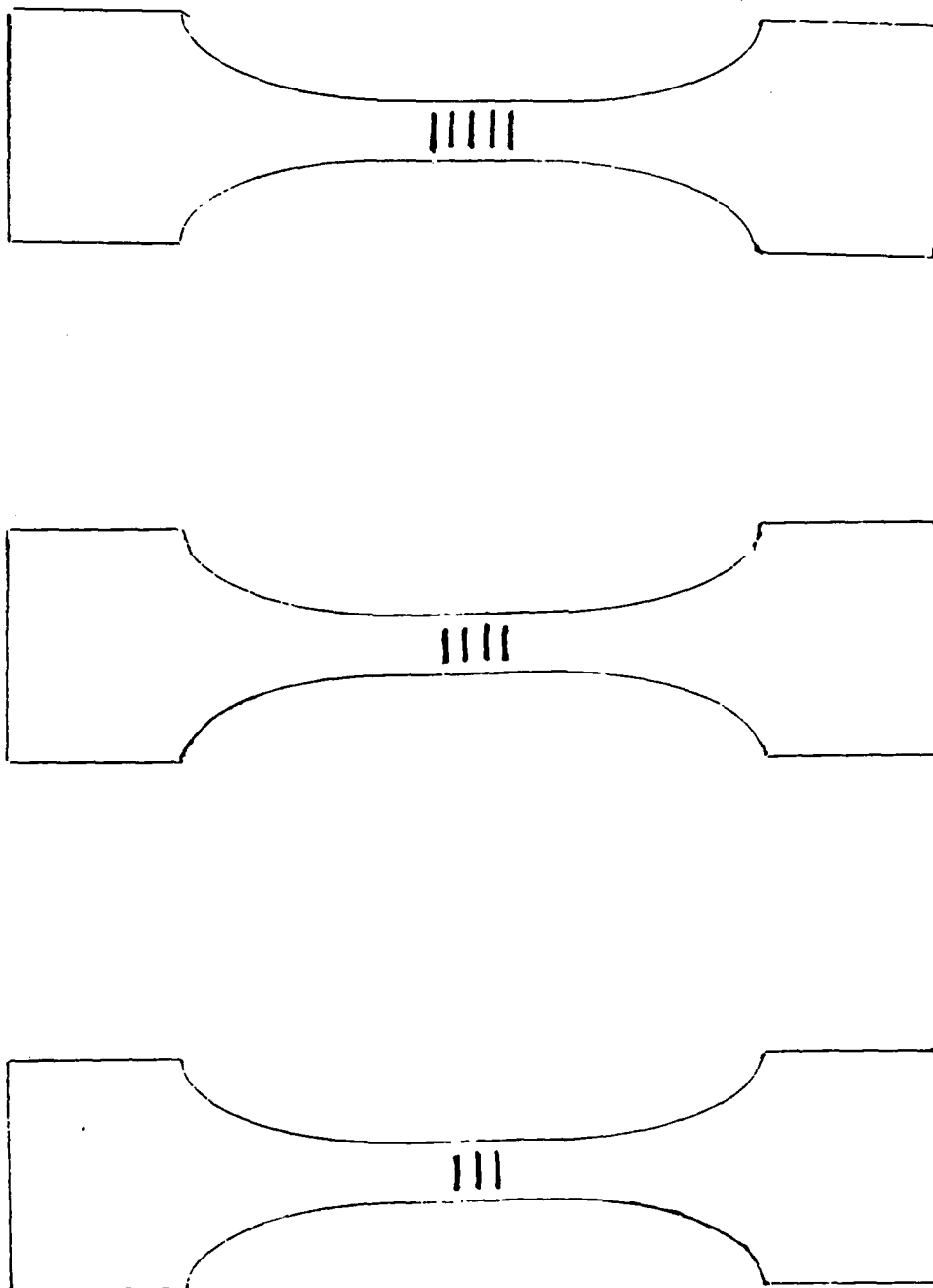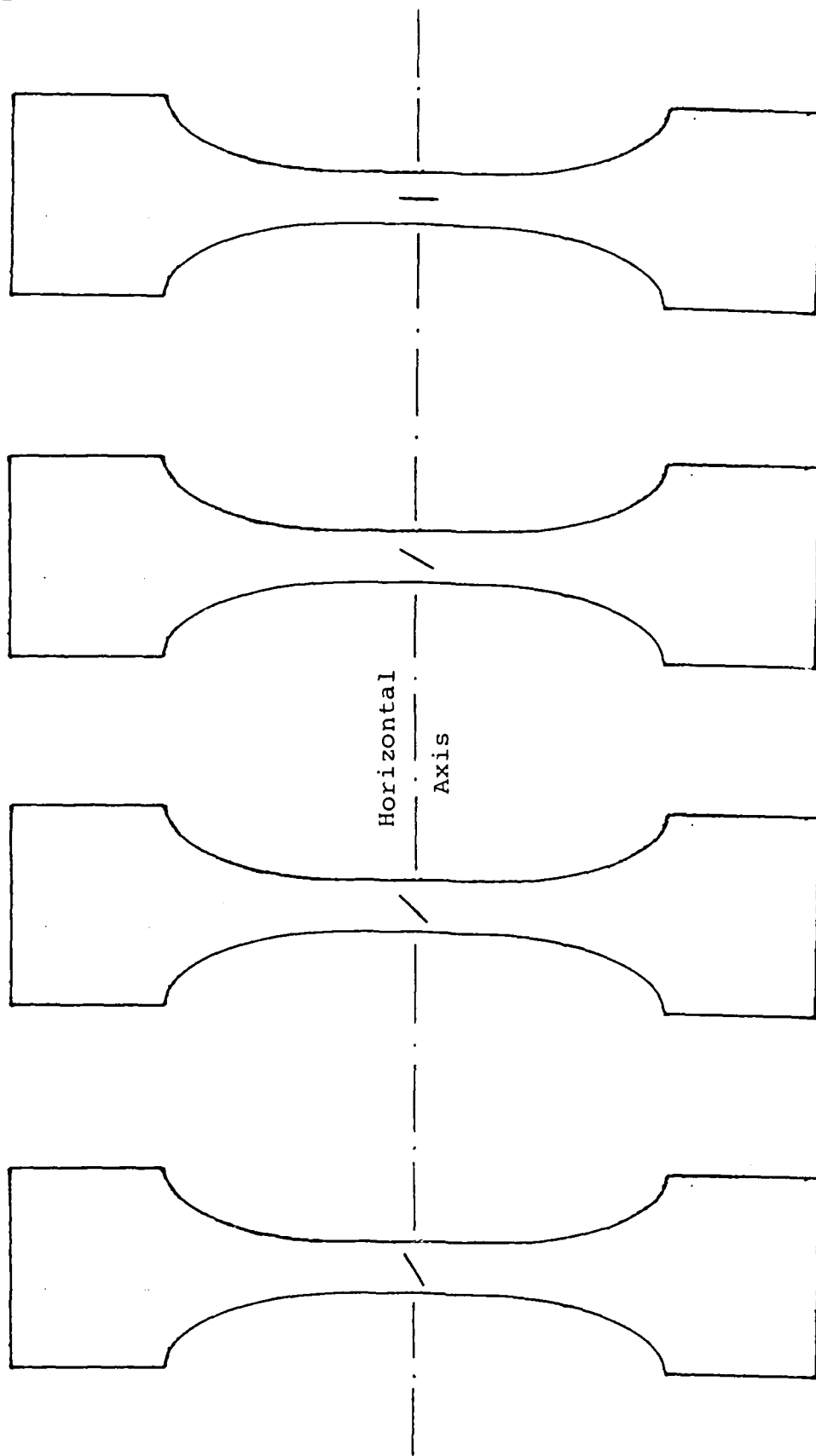Fig. 2: Slotted Specimens - Multiple Slots

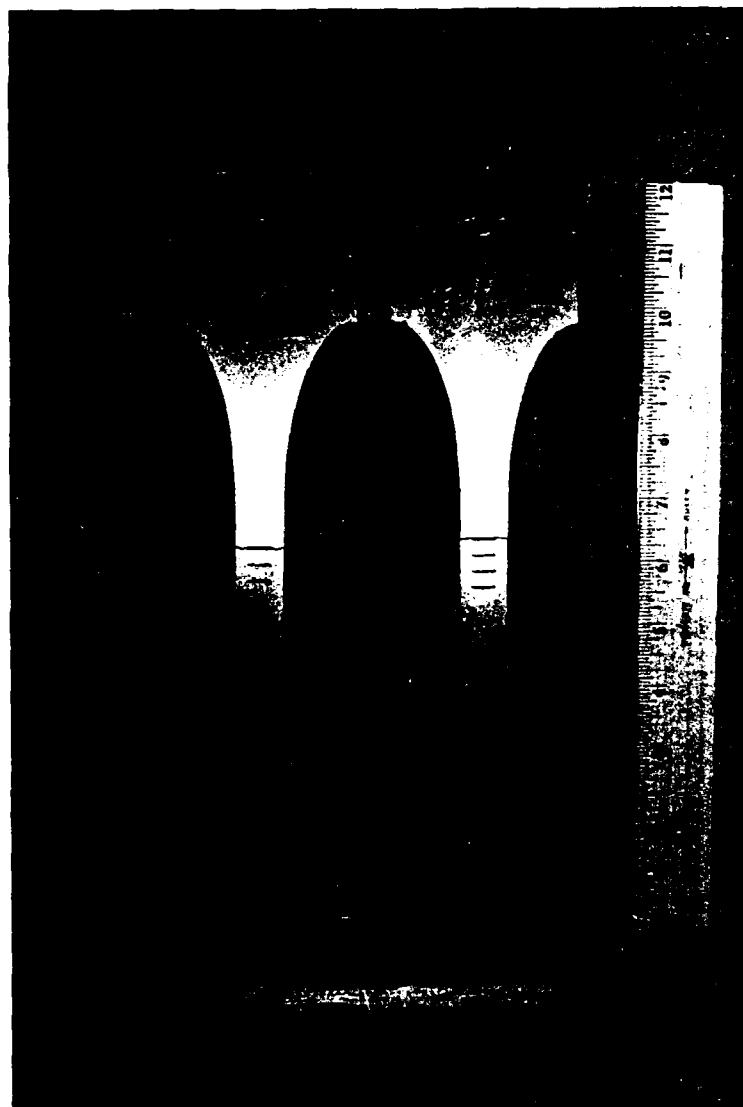Fig. 3: Slotted Specimens - Angled Slots

Horizontal Axis

Fig. 4: Photograph of typical slotted cast iron
specimens (Multiple Slots)

Fig. 5: Photograph of typical slotted cast iron
specimens (Angled Slots)

Experimental Procedure:

Tensile tests were performed on all the specimens using similar
test parameters. Loading and unloading sequences were employed
on some specimens while simple monotonic tensile loading was
used on others. Special, large gauge-length strain gauges were
applied to slotted specimens to obtain over-all (average) strains
rather than localized strains. These were "quality-control"
measurements and were not used in analytical calculations.

Results:

Table 1 below shows the experimental parameters and results of
testing performed on slotted specimens. In all cases, slots were
horizontal i.e; across the gauge section of the specimen.

Table 1: Test Results - Slotted Specimens
(Horizontal Slots)

Specimen #	Slot Size (& No. of Slots)	Fracture Strength (psi)
8	1/8 in.	20,833
9	3/16 in.	17,708
10	1/4 in.	17,708
11	3/8 in.	12,500
12	1/2 in.	8,542
13	3/8 in. (3 slots)	13,542
15	3/8 in. (5 slots)	12,292

Table 2 shows specimen parameters and fracture strength of
slotted specimens where slots were machined at an angle to the
horizontal axis as shown in Fig. 3. Slot size in all cases
was kept constant at 3/8 in.

Table 2: Test Results - Slotted Specimens
(Angled Slots)

Specimen #	Angle of Slot (degrees)	Fracture Strength (psi)
18	0	13,333
19	0	13,542
20	15	11,094 *
21	15	17,448 *
22	30	13,938
23	30	13,583
24	45	14,896
25	45	14,938
26	60	20,833 *
27	60	23,032 *
28	75	20,781
29	75	21,553
30	90	26,167
31	90	28,156
35	60	17,406 @

* - Experimental scatter

@ - Extra specimen to "double-check" the fracture strength
    of specimens with a 60 degree slot

Discussion:

As can be seen from Table 1, the fracture strength goes down
quite consistently as the slot size increases. This result is
very much as expected and there are no surprises here. What
is more interesting to note from Table 1 is the insensitivity
of the material to the extent of "damage" when one compares the
fracture strengths of specimens containing one, three, or five
slots of the same size. Note that the specimen failed at the
same location (top slot) in the case of multiple slots. This
is an aspect of fracture and damage modeling which should be
explored further in future work.

Table 2 shows the fracture strength increasing as the angle of
the slot with the horizontal axis increases. There is, however,
considerable scatter in the data for the 15 degree and 60 degree
specimens. One likely reason may be the material variability
although, so far, very consistent material behavior has been
observed in the course of this study. This material variability
may have arisen from different temperature histories experienced
by the different parts of the original plate material during
processing and heat treatment. So a certain amount of scatter
in the data was to be expected.

There is also a change in the fracture mode as one goes from
the zero to 45 degree slot group to 45 to 90 degree slot group.
In the first case, mode I fracture is the predominant one while
it is a "mixed-mode" or mode II fracture for the second group.
However, this change in fracture mode is continuous as the slot
angle changes and should not cause variations in the fracture
strength at a constant angle. Again, this is an extremely
interesting aspect of fracture which should be pursued further.
It becomes much more important for anisotropic and orthotropic
materials like the advanced composites where fracture is almost
always of a mixed-mode nature.

COMPRESSION TESTING OF CONCRETE:

Various concrete mixes were tried to see if an acceptable mix
could be arrived at for production in a small-batch environment
and would also give adequate mechanical properties. The final
choice of a typical concrete mix was as follows:

Cement:	3.0 lbs.
Sand (Fine):	7.26 lbs.
Sand (Coarse):	13.0 lbs.
Water:	1.23 - 1.45 lbs.
Water/Cement Ratio:	0.41 - 0.48

NOTE: A wet coarse sand was used in all cases. It was soaked
        for 15 minutes before use.

Specimen Geometry:

Straight, prism type concrete specimens were used for this study.
Both slotted and unslotted specimens were tested to see the
effect of "damage" on fracture strength of concrete. Slots were
"manufactured" into these specimens by an ingenious design of

the metal mold and pre-placing lubricated metal plates into the
concrete mix at the time of pouring. Molds were turned over and
these metal plates moved at regular intervals to make sure that
the gravel does not settle due to gravity at the bottom of the
mold and the plates do not get stuck in the specimen during the
curing process. The specimen dimensions were kept constant for
all tests whether these were slotted or unslotted specimens.
The specimen dimensions are given below:

      Cross-section: 3x3 in. square

         Height: 5 in.

Vertical slots of one, two, or three inch lengths were used in
the case of slotted specimens. The slot was parallel to the long
axis of the specimen as shown in Fig. 6.

Experimental Procedure:

Compression tests were performed on all the concrete specimens
using similar parameters. A loading rate of 2,000 lbs. force
per minute was employed in all cases.   recision mechanical dial
gauges were used to measure the overall contraction (axial strain)
and lateral expansion (transverse strain) of the specimens.
Specimen ends were ground in some cases to give flat faces which
would also be parallel to each other to ensure concentric loading.

Results:

Table 3 on the next page shows the mechanical properties of
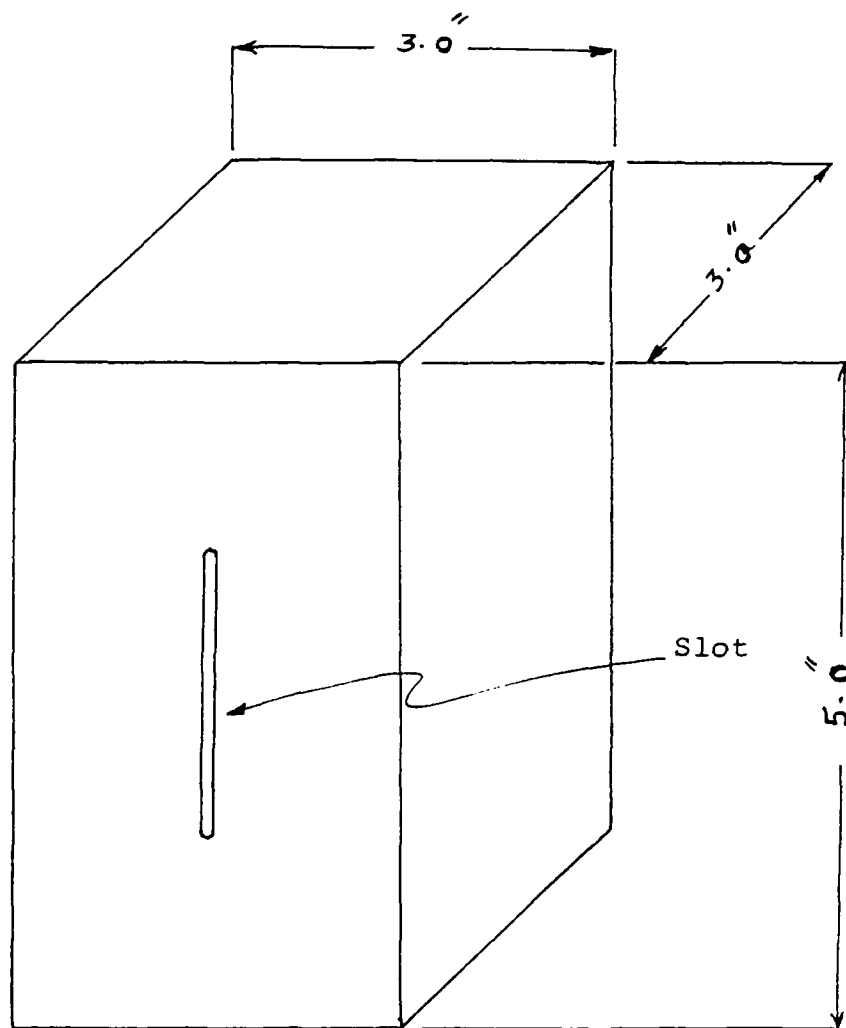typical slotted and unslotted specimens.

Fig. 6: Specimen Geometry of Slotted Concrete
          Samples

Table 3: Mechanical Properties of Concrete Specimens

Specimen #	Slotted?	Slot Size (in.)	Fracture Strength (psi)
H-1	No		1,600
H-2	No		1,800
I-1	Yes	1 in.	1,541
I-2	Yes	2 in.	1,618
I-3	Yes	2 in.	1,489
I-4	Yes	3 in.	1,718
H-3	Yes	3 in.	1,756

NOTE:

1. "Fracture Strength" here means the maximum stress level which the specimen attained before the onset of massive damage and crumbling.

2. Specimen batches H and I were identical in terms of their fabrication specifications and mechanical properties.

Discussion:

It is quite interesting to note from Table 3 that, in spite
of the fact that specimen batches H and I were two different
groups of specimens, the fracture strength in all cases stays
relatively constant. In other words, the material does not
see the slots, whether small or large, as "damage" and behaves
as if these slots were not even there! This point is discussed
at length in the main body of the report.

The micro-cracks which developed in all specimens had the same
pattern of development as the load increased. Most predominant
orientation of these cracks was along the loading axis i.e;
cracking due to lateral expansion of the specimen. This mode
of vertical splitting was seen in all cases and the presence
of vertical slots did not seem to affect it in any major way.
The damage did not, for example, start at the ends of these
slots. Fig. 7 shows this vertical splitting in some slotted
specimens.

All of the above observations are extremely interesting from
the point of view of the definition of "damage" in a given
material. When, for example, a crack, notch, or a geometrical
discontinuity becomes "damage" and is critical for the service
life of a material/structure? These questions should be looked
into very carefully through future work in the area of fracture
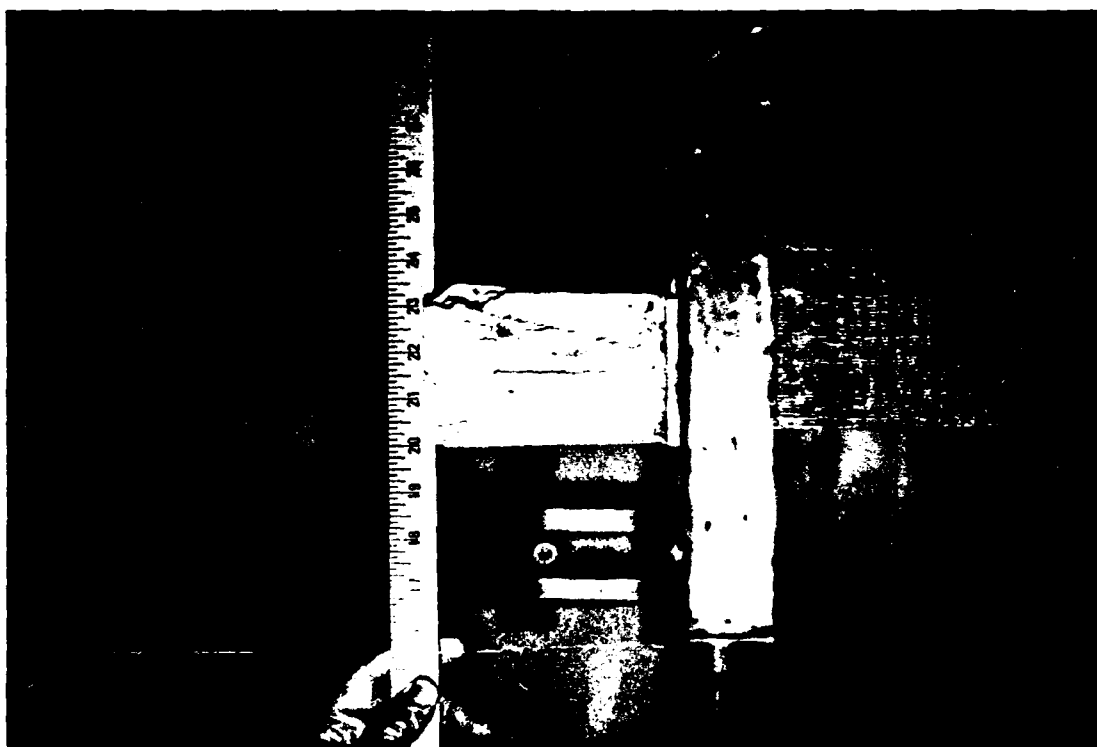control and damage tolerance.

Fig. 7: Photographs of Slotted Concrete Specimens showing Vertcal Splitting